Fatigue Life Predictions of Notched Members in Arabian Gulf Water

by

Zuhair Mattoug Gasem

A Thesis Presented to the

FACULTY OF THE COLLEGE OF GRADUATE STUDIES

KING FAHD UNIVERSITY OF PETROLEUM & MINERALS

DHAHRAN, SAUDI ARABIA

In Partial Fulfillment of the
Requirements for the Degree of

MASTER OF SCIENCE

In

MECHANICAL ENGINEERING

July, 1992

INFORMATION TO USERS

This manuscript has been reproduced from the microfilm master. UMI films the text directly from the original or copy submitted. Thus, some thesis and dissertation copies are in typewriter face, while others may be from any type of computer printer.

The quality of this reproduction is dependent upon the quality of the copy submitted. Broken or indistinct print, colored or poor quality illustrations and photographs, print bleedthrough, substandard margins, and improper alignment can adversely affect reproduction.

In the unlikely event that the author did not send UMI a complete manuscript and there are missing pages, these will be noted. Also, if unauthorized copyright material had to be removed, a note will indicate the deletion.

Oversize materials (e.g., maps, drawings, charts) are reproduced by sectioning the original, beginning at the upper left-hand corner and continuing from left to right in equal sections with small overlaps. Each original is also photographed in one exposure and is included in reduced form at the back of the book.

Photographs included in the original manuscript have been reproduced xerographically in this copy. Higher quality 6" x 9" black and white photographic prints are available for any photographs or illustrations appearing in this copy for an additional charge. Contact UMI directly to order.

University Microfilms International
A Bell & Howell Information Company
300 North Zeeb Road, Ann Arbor, MI 48106-1346 USA
313/761-4700 800/521-0600

Order Number 1354083

Fatigue life predictions of notched members in Arabian Gulf water

Gasem, Zuhair Mattoug, M.S.

King Fahd University of Petroleum and Minerals (Saudi Arabia), 1992

U·M·I
300 N. Zeeb Rd.
Ann Arbor, MI 48106

FATIGUE LIFE PREDICTIONS OF NOTCHED MEMBERS IN ARABIAN GULF WATER

BY

ZUHAIR MATTOUG GASEM

A Thesis Presented to the

FACULTY OF THE COLLEGE OF GRADUATE STUDIES

KING FAHD UNIVERSITY OF PETROLEUM & MINERALS

DHAHRAN, SAUDI ARABIA

In Partial Fulfillment of the
Requirements for the Degree of

MASTER OF SCIENCE
In

MECHANICAL ENGINEERING

JULY, 1992

KING FAHD UNIVERSITY OF PETROLEUM & MINERALS

DHAHRAN, SAUDI ARABIA

This thesis, written by

ZUHAIR MATTOUG GASEM

under the direction of his thesis committee, and approved by all the members, has been presented to and accepted by the Dean, College of Graduate Studies, in partial fulfillment of the requirements for the degree of

MASTER OF SCIENCE IN MECHANICAL ENGINEERING

Thesis Committee

Chairman (Dr. Zafarulla Khan)

Member (Dr. Zaki Ahmad)

Member (Dr. Anwar K. Sheikh)

Dr. M. U. Budair
Department Chairman

Dr. Ala H. Rabeh
Dean College of Graduate Studies

Date : 12-7-92

بسم الله الرحمن الرحيم

اللهم علمنا ماينفعنا وأنفعنا بما علمتنا
إنك أنت العليم الحكيم

Dedicated to

my beloved parents,

my wife and daughter

ACKNOWLEDGEMENTS

Praise be to Allah, Lord of the worlds who taught man that which he knew not. Acknowledgement is due to King Fahd University of Petroleum and Minerals for providing unlimited facilities with which this work was possible to be accomplished.

I would like to express my deep gratitude to my major thesis advisor Dr. Zafarulla Khan for his valuable guidance, remarkable assistance, and generous support. His dedication, attention, and patience is greatly appreciated. Thanks also are given to committee members: Dr. Anwar Sheikh and Dr. Zaki Ahmad for their useful advice.

I wish to acknowledge Dr. Zaki Ahmad for supplying the experimental material. I must also thank M.E. workshop staff for their cooperation.

I owe sincere thanks to Dr. Mohammad Benten and Dr. Habib Abualhamayel who enriched me with moral support, inspiration, and valuable help. Thanks also are given to Dr. Mohammad Budair Chairman of M.E. department.

It is my pleasure to express my gratitude for the many useful comments, assistance, and moral support provided by my colleagues Asad Asghar and Ebal Ahmad.

Most importantly, my parents, uncle Ahmad, and Dr. Mahmoud Zaini and their family members deserve the highest appreciation for their encouragement, support, and prayers which illuminated my path right from the beginning.

Finally, this work could not have been attempted or completed without the understanding and patience of my wife. Her sacrifice was great; my gratitude is profound.

TABLE OF CONTENTS

LIST OF TABLES

LIST OF FIGURES

NOMENCLATURE

a	= crack length (mm)
a_i ,a_f	= initial, final crack length (mm)
b	= fatigue strength exponent
c	= fatigue ductility exponent
C	= Paris crack growth coefficient
da/dN	= fatigue crack growth rate (mm/cycle)
e	= nominal strain (mm/mm)
Δe	= nominal strain range (mm/mm)
E	= modulus of elasticity (MPa)
K	= stress intensity factor (MPa$\sqrt{m}$)
ΔK	= stress intensity factor range (MPa$\sqrt{m}$)
K′	= cyclic strength coefficient (MPa)
K_c	= fracture toughness (MPa$\sqrt{m}$)
ΔK_{eff}	= effective stress intensity factor range (MPa$\sqrt{m}$)
K_t	= theoretical stress concentration factor
ΔK	= threshold stress intensity factor range (MPa$\sqrt{m}$)
K_ε	= actual strain concentration factor
K_σ	= actual stress concentration factor
n′	= cyclic strength exponent
N	= number of cycles to failure
2N	= number of reversals to failur (1 cycle = 2 reversals)
N_i,N_p,N_t	= initiation, propagation, and total fatigue life estimates (cycles)
ΔP	= load range (KN)
R	= stress ratio ($\sigma_{min}/\sigma_{max}$)

S	= nominal stress (MPa)
S_{max}	= maximum nominal stress (MPa)
ΔS	= nominal stress range (MPa)
t	= specimen thickness (mm)
W	= specimen width (mm)

Greek Symbols

$\Delta\varepsilon/2$	= total strain amplitude
$\Delta\varepsilon_e/2, \Delta\varepsilon_p/2$	= elastic , plastic strain amplitude
ε'_f	= fatigue ductility coefficient
σ	= local stress (MPa)
$\Delta\sigma$	= local stress range (MPa)
$\Delta\sigma/2$	= local stress amplitude (MPa)
σ_o	= mean stress (MPa)
σ_y	= yield strength (MPa)
σ'_f	= fatigue strength coefficient (MPa)
$\sigma_{max}, \sigma_{min}$	= maximum , minimum local stress (MPa)

THESIS ABSTRACT

NAME OF STUDENT : **Zuhair M. Gasem**

TITLE OF STUDY : **Fatigue Life Predictions of Notched Members in Arabian Gulf Water**

MAJOR FIELD : **Mechanical Engineering**

DATE OF DEGREE : **July, 1992**

The use of empirically developed procedures in fatigue life predictions is current practice for notched members under the joint action of mechanical loads and a corrosive environment. A simple model has been investigated where the total fatigue life of a notched member is considered to be the sum of: crack initiation, and crack propagation lives.

The local strain approach has been employed for the crack initiation life estimates. LEFM concept using Paris relationship was used for fatigue crack propagation life estimates. It is shown that the influence of the corrosive environment on fatigue life can be incorporated by determining the relevant material properties in the environment and at the frequency of interest.

An experimental program was performed in an attempt to determine the fatigue properties of a modified Al- 2.5 Mg aluminum alloy under constant amplitude cyclic loading. Testing environments include laboratory conditions and Arabian Gulf water. Fatigue life predictions were compared with experimental data of central notched specimens. Good correlation between the analytical predictions and experimental data was observed.

MASTER OF SCIENCE DEGREE

KING FAHD UNIVERSITY OF PETROLEUM AND MINERALS

Dhahran, Saudi Arabia

July, 1992

ملخص الرسالة

إسم الطالـــب : زهير معتوق قاسم .

عنوان الرسالـة : تقدير عُمر الكلال للأجزاء المحززه الواقعة في مياه الخليج العربي.

التخصص العلمي : الهندسة الميكانيكية .

تاريخ الرسالـة : يوليو ١٩٩٢م .

استخدام الطرق المستحدثة تجريبياً لتقدير عُمر الكلال للأجزاء المحززه الواقعة تحت كُلاً من حمولة ميكانيكية ووسط حات ، ممارسة قائمة حديثاً . تمت دراسة أنموذج بسيط لتقدير عُمر الكلال لعضو محزز مع الإعتبار بأن العُمر الكلي ينقسم إلى : عُمر شق إبتدائي وعُمر شق إمتدادي .

تم تقدير عُمر الشق الإبتدائي بطريقة التوتر الموضعية . أما بالنسبة لعمر الشق الإمتدادي فقد قُدِّر بإستخدام ميكانيكية الإنكسار الخطي المرن متمثلة في علاقة باريز . أوضحت الدراسة بأن تأثير الوسط الحات على عُمر شقوق الكلال يمكن إدراجه بتحديد الخواص المعنيه للمادة في الوسط المعين وعند التردد المطلوب .

نُفِّذ برنامج تجريبي لتحديد خواص الكلال لسبائك الومنيوم معدلة خاضعة لحمل دوري ثابت السعة . اشتملت الأوساط التجريبية على الظروف المحيطه في المعمل ومياه الخليج العربي . وُجد من هذه الدراسة بأن هنالك ترابطاً وثيقاً بين التقادير التحليلية والنتائج المعملية .

درجة الماجستير في العلوم

جامعة الملك فهد للبترول والمعادن

الظهران - المملكة العربية السعودية

يوليو ١٩٩٢م

CHAPTER 1

INTRODUCTION

Most engineering structures and components, subjected to cyclic loading, contain some form of stress raisers that result from geometrical or metallurgical discontinuities. These notches are usually responsible for providing the origin of fatigue crack formation and thus reduce the fatigue resistance of otherwise smooth members. Hence, considerable attention has been given to fatigue properties and fatigue life prediction of notched members.

Most of the earlier approaches were performed on smooth specimens where the effects of notches is accounted for by the fatigue notch factor. However, as the fracture mechanics gained engineering significance, the total fatigue life of a notched member is considered to consist of two portions: crack initiation life, which is consumed in developing and propagating short cracks, and crack propagation life, which is spent in growing an engineering size crack to unstable length.

The local strain approach is conventionally employed for the estimation procedure of crack initiation life [1]. The basic assumption of this method is that equivalent fatigue damage will occur at the critical location of the component and a smooth specimen if both are undergoing the same stress and strain histories. By means of this technique, fatigue initiation estimates are deduced from data presented in the form of strain amplitudes versus reversals to failure of small unnotched axial specimen subjected to completely reversed constant amplitude cyclic loading.

Linear elastic fracture mechanics has been used to estimate fatigue crack propagation lives of engineering components and structures [2] . In this approach, the growth of a fatigue crack under constant-amplitude cyclic loading is principally controlled by the stress intensity factor, K, which defines the elastic stress field around the crack tip. For a certain material, the crack extension per cycle versus the stress intensity factor range is a typical presentation of fatigue crack propagation data. The results of constant amplitude fatigue crack growth rates are usually correlated using Paris power law [3].

A simple approach for combining the initiation life and propagation life of notched members has been developed by Socie et al [4]. In this model, the local strain concepts is used to compute the initiation life. Paris equation is employed in

the estimates of propagation life assuming an initial crack length equal to the notch depth.

Environment interactions have been observed to reduce fatigue resistance of metallic materials when operating under corrosive environment [5]. The deleterious effects of the conjoint action of mechanical loading and chemical attack are more significant than would be predicted by considering fatigue and corrosion damage processes separately. This unique failure mode,termed corrosion fatigue, has been recognized as a serious problem in many industries such as aerospace, nuclear power plants, chemical systems and naval structures [6].

The difficulty of fatigue life prediction under a corrosive environment becomes evident when considering the numerous mechanical, metallurgical and environmental variables that contribute to the process [7]. However, from an engineering point of view, it is often assumed that the adverse effects of the environment can be included in fatigue life estimation procedures by determining the material fatigue properties in the same environment and frequency of interest [8].

The objective of the present study is to investigate the applicability of the initiation-propagation model for fatigue life estimation of notched members in Arabian Gulf water environment. Two types of the modified Al- 2.5 Mg alloy are

chosen for the study. Two notched geometries will be investigated, one with a low stress concentration factor ($K_t = 2.4$) and the other with higher value ($K_t = 4.2$). Initiation, propagation, and total life will be compared with experimental fatigue life data conducted in air as well as in Arabian Gulf water environments.

CHAPTER 2

LITERATURE REVIEW

In recent years, considerable effort has been given to the development and application of quantitative procedures to correlate and estimate crack initiation and propagation response of engineering structures under the conjoint action of mechanical loading and aggressive environment. Although, most service loading can not be characterized as constant amplitude, it is believed that assuming constant amplitude loading can reveal valuable characteristic information about the behavior of the material under investigation.

Fatigue lives of notched structures subjected to constant amplitude loadings are assessed by a variety of analytical methods including stress-life curves, local stresses and strains, and linear elastic fracture mechanics [9]. Nominal stress combined with fatigue strength reduction factor approach fails to account for plastic behavior at the notch region and does not consider the propagation life regime which

may be of great significance to the total fatigue life. Therefore, stress-life analysis is considered as very conservative and hence inappropriate for total fatigue life evaluation of notched members [10].

It is well established that fatigue is essentially a two stages process: initiation, controlled by notch plasticity, and propagation, controlled by nominal stress and crack length. Initiation life is considered to be the number of cycles consumed in the nucleation and growth of a small crack to a length where it becomes a dominant fatigue crack. Propagation life concerns with the growth of the dominant fatigue crack to final fracture.

Local-strain and fracture mechanics approaches have been involved extensively in fatigue life analysis. For crack initiation, local strain is the most widely employed technique whereas fracture mechanics has found wide acceptance for crack propagation.

2.1 Fatigue Crack Initiation

Various models have been suggested to estimate the number of cycles to initiate a detectable crack. The definition of the initial crack is quite arbitrary and depends upon the viewpoint of the analyst as well as to the technique involved to

observe and measure the crack at the notch root. Because the maximum local strain at the notch root is thought to be the controlling parameter during initiation process, consideration of local strains at the highly strained regions are essential for fatigue initiation life assessments. The most widely used method for initiation life estimates is known as the local-strain method. In this approach, it is assumed that: (1) a given notch strain will result in the same fatigue life, and (2) equal fatigue life damage and hence fatigue life is considered to occur in both notched member and smooth specimen if they experience identical strain histories [1].

The total strain amplitude is the sum of the elastic and plastic strain amplitudes,

$$\frac{\Delta\varepsilon_T}{2}=\frac{\Delta\varepsilon_e}{2}+\frac{\Delta\varepsilon_p}{2} \tag{2.1}$$

using Basquin stress-life relation [11] and Coffin-Manson plastic strain-life equation [12], Equation (2.1) can be rewritten as:

$$\frac{\Delta\varepsilon_T}{2}=\frac{\grave{\sigma}_f}{E}(2N)^b+\grave{\varepsilon}_f(2N)^c \tag{2.2}$$

where,

b = Fatigue strength exponent

σ'_f = Fatigue strength coefficient

c = Fatigue ductility exponent

ε'_f = Fatigue ductility coefficient

2N = Number of strain reversals to failure (one cycle is two reversals)

Equation (2.2) requires four materials constants which can be determined by low-cycle fatigue testing of smooth specimens. To include the mean stress effects, both elastic and plastic strain terms in Equation (2.2) should be modified [13],

$$\frac{\Delta\varepsilon_T}{2}=\frac{\grave{\sigma}_f-\sigma_o}{E}(2N)^b+\grave{\varepsilon}_f\left(\frac{\grave{\sigma}_f-\sigma_o}{\grave{\sigma}_f}\right)^{\frac{c}{b}}(2N)^c \qquad (2.3)$$

where σ_o is the mean stress.

Hence, by knowing the local strain at the notch root and strain life data for a smooth specimen of the same material, fatigue initiation life of notched components can be evaluated. A variety of methods have been involved to determine local strains at the notch : direct measurements , empirically relating nominal stresses and strains to local values, and finite element analysis. The most widely used empirical relation is Neuber's rule which states that the product of the local stress and strain concentration factors is constant and equal to the square of the theoretical stress concentration factor [14] . For any loading conditions , Neuber's relation can be expressed as:

$$K_t^2 = \frac{\Delta\sigma\ \Delta\varepsilon}{\Delta S\ \Delta e} \qquad (2.4)$$

where ΔS and Δe are the nominal range values of stress and strain, and $\Delta\sigma$ and $\Delta\varepsilon$ are local stress and strain ranges, respectively. This relation, in conjunction with the cyclic stress-strain response of the metal of interest, characterize the cyclic behavior at the critical location for any loading conditions.

Sato and Shimada proposed a new procedure to estimate fatigue crack initiation life for notched members of different materials using low-cycle fatigue tests [15]. Under constant amplitude fatigue testing, they observed that the maximum strain value at the notch decreases rapidly reaching a minimum value and then increases gradually as the number of elapsed cycles increases. One of the main results of their experiments was that the maximum local strain value at the first cycle coincided with the local maximum strain value at crack initiation. Crack initiation life was determined experimentally by microscopic observation of small crack propagation having a length of 10-15 μm.

Figure 2.1 shows the relationship of ε_{max} versus N for a steel alloy at two different initial stress intensity factor ranges, where N_c is the crack initiation life ascertained experimentally. Though the physical interpretation of this relation is not established, it has been verified independently of material, notch radius and length,

prestrained conditions, and initial applied stress intensity factor ranges. However, initial applied stress intensity factor values do affect the number of cycles for initiation life.

Furthermore, a method to determine the crack initiation life was proposed [15]. Three measurements or estimates of local maximum strain are plotted versus the corresponding values of the cyclic number. Then, if a line is drawn parallel to the N axis passing through the maximum strain value at the first cycle, the point of intersection of the horizontal line with the curve will yield approximate initiation life. The results of this method for two different materials are displayed in Figure 2.2 .

A mechanical model for fatigue crack initiation prediction has been developed by Zheng [16]. It is assumed that no fatigue damage is produced and a fatigue crack will not initiate if the local strain at the notch is below a critical value which is referred to as the endurance strain range limit $\Delta\varepsilon_e$. A formula relating initiation life to tensile properties, loading conditions, and notch geometry was derived:

$$N_i = C\left[(\Delta\sigma_{eqv})^{\frac{2}{(1+n)}} - (\Delta\sigma_{eqv})_{th}^{\frac{2}{(1+n)}}\right]^{-2} \qquad (2.5)$$

where $\Delta\sigma_{eqv}$ is an equivalent stress range which induces an equal strain range at the notch tip regardless of notch acuity and stress ratio, it is expressed as:

$$\Delta\sigma_{eqv}=\sqrt{\frac{1}{2(1-R)}}K_t\Delta S \tag{2.6}$$

the threshold value of the equivalent stress range can be obtained by the following equation:

$$(\Delta\sigma_{eqv})_{th}=\sqrt{E\sigma_f\varepsilon_f}(\frac{\Delta\varepsilon_e}{2\varepsilon_f})^{(1+n)/2} \tag{2.7}$$

the constant C in Equation (2.5) can be approximated by:

$$C=1/4(\sqrt{E\sigma_f\varepsilon_f})^{4/(1+n)} \tag{2.8}$$

Thus,initiation life can be estimated solely with tensile properties, strain endurance limit, and strain hardening exponent. Furthermore,the constants in Equation (2.5) can be obtained by linear regression analysis of the equivalent stress range versus cycles to initiation data as shown in Figure 2.3 for an aluminum alloy. The fatigue crack initiation threshold obtained numerically agrees well with that obtained using Equation (2.7). Comparison between predicted fatigue crack initiation life and test results is depicted in Figure 2.4 for 2024-T3 Aluminum Alloy.

2.2 Corrosion Fatigue Crack Initiation

For any given material, general degradation of fatigue properties will take place as a result of the presence of a corrosive environment. Various gaseous and liquid mediums are considered to have serious effects on fatigue life but aqueous solutions at ambient temperature is the most frequently encountered in engineering applications.

Bernstein and Loeby [17] have conducted low-cycle fatigue tests under strain control in salt water to study the life dependence upon environment and cyclic frequency. All the materials that were studied have shown a significant reduction in life ranging from 60% to 35% of the experimentally determined life in lab air. However, time dependence has been found to vary with materials. Both elastic and plastic strain ranges versus life equations were modified by a frequency term to estimate the corrosion fatigue life. Hence, Equation (2.2) is rewritten as,

$$\Delta\varepsilon_t = A\,(2N)^{\alpha}\ \nu^{(-\alpha\gamma_e)} + B\,(2N)^{\beta}\ \nu^{(-\beta\gamma_p)} \qquad (2.9)$$

where A, α, B, β, γ_e, and γ_p are materials constants, which can be determined experimentally, and ν represents the frequency of the tension loading. Equation (2.9) provides good correlation to experimental data for the air and salt water

environments as can be seen in Figure 2.5 through 2.7 . The correlation coefficients for the salt water data were between 0.93 to 0.96 .

Quantitative evaluation of pitting growth can be involved to predict the corrosion fatigue crack initiation life for materials exhibiting excessive pitting corrosion [18]. It has been observed that corrosion fatigue of such materials consists of three stages: pit growth, crack formation emanating from a critical pit, and corrosion fatigue crack growth. It is assumed that the critical pit size at which transition into a crack can be determined by the intersection between pit growth rate and small fatigue crack propagation rate. A corrosion pit growth law was suggested as:

$$\frac{dc}{dN} = \frac{1}{3f} C_p^3 \alpha^2 \pi^2 Q^{-2} (2.24\sigma)^4 \Delta K^{-4} \qquad (2.10)$$

where,

C_p = a material coefficient

f = frequency

α = aspect ratio (pit depth/pit radius)

Q = shape factor

Thus, by means of Equation (2.10) the stress intensity factor at the critical pit size can be obtained.

For the case where crack initiation is controlled by pitting, the author [18] proposed a procedure to determine the number of cycles taken to form a small crack as follows. First, the maximum pit size in the critical area is measured or estimated. Then, using the pit growth law, it is possible to determine the number of cycles needed to attain the calculated critical pit size which corresponds to the residual life. Finally, initiation life is the sum of the number of cycles at the maximum pit size measurement and the residual life.

Linear Elastic Fracture Mechanics (LEFM) has been used in the evaluation of crack initiation for both inert and corrosive environment [19,20]. Data has been presented in terms of the stress intensity factor divided by the square root of notch radius ,$\Delta K/\sqrt{\rho}$, versus N_i . The maximum cyclic stress range at the notch tip can be obtained in terms of the elastic stress concentration factor and remote stress as,

$$\Delta\sigma_{max}=K_t\Delta\sigma_{nom} \tag{2.11}$$

On the basis of LEFM, however, it can be related to the stress intensity factor:

$$\Delta\sigma_{max}=\frac{2}{\sqrt{\pi}}\left(\frac{\Delta K}{\sqrt{\rho}}\right) \tag{2.12}$$

combining Equation (2.11) and (2.12), it can be shown that the $\Delta K/\sqrt{\rho}$ parameter is nothing more than fracture mechanics approach to determine stress concentration factors.

Novak [20] has investigated the long-life corrosion fatigue crack initiation of typical construction steels in 3.5% NaCl solution using the above parameter. It was found that a linear relationship can correlate $\Delta K/\sqrt{\rho}$ and the logarithm of initiation life cycles for all steels as shown in Figure 2.8 . It was concluded that prediction of corrosion fatigue strength (initiation life) for relatively short life (high load) would yield conservative characteristics information for steels. Thus if similar data is available, it is possible to estimate the initiation life with reasonable accuracy.

2.3 Fatigue Crack Propagation

Significant portion of fatigue life may be spent in the propagation of cracks inherently present in engineering components and structures. Such cracks can be the result of manufacturing defects, welds, surface flaws, or excessive plastic deformation at notched regions. LEFM presently offers the most powerful applicable analytical technique in predicting the remaining life of such members. In this approach, pre-cracked panels are subjected to constant-amplitude cyclic loading. Fatigue crack growth rate is measured and plotted against stress intensity factor range.

Numerous fatigue crack propagation laws have been proposed [2]. Perhaps the most commonly used law which relates crack growth rate to stress intensity range (ΔK) in the linear region is the paris law [3]. By means of this law:

$$\frac{da}{dN}=C(\Delta K)^m \qquad (2.13)$$

where C and m are materials constants that characterize materials resistance to crack propagation and can be determined by the best fit to tests data. Fatigue propagation life (N_p) can be calculated by integrating Equation (2.13) from initial (a_i) to critical crack size (a_f) :

$$N_p=\int_{a_i}^{a_f}\frac{da}{C(\Delta K)^m} \qquad (2.14)$$

Modifications of Equation (2.13) are usually utilized to include mean stress effects. Forman equation [21] is the most frequently employed,

$$\frac{da}{dN}=\frac{C(\Delta K)^m}{(1-R)K_c-\Delta K} \qquad (2.15)$$

where K_c is the fracture toughness of the materials. To account for crack closure phenomenon, ΔK is replaced by ΔK_{eff} in Equation (2.13) as suggested by Elber [22] where ΔK_{eff} is the difference between K_{max} and the crack opening stress intensity factor K_{open} .

An attempt has been made by Krausz [23] to describe the entire crack growth curve:

$$\frac{da}{dN} = C\left[\frac{\Delta K-\Delta K_{th}}{K_c-\Delta K}\right]^m \qquad (2.16)$$

here, K_{th} denotes the threshold stress intensity factor. Based on a simple physical model, another equation that can be fitted to the entire curve was proposed [24],

$$\frac{da}{dN} = C(\Delta K-\Delta K_{th})^2\left[1+\frac{\Delta K}{K_c-K_{max}}\right] \qquad (2.17)$$

The materials constants in the above equations are not necessarily having the same values.

Scanning Electron Microscopy of fracture surface reveal the existence of patches of finely spaced parallel marks, called fatigue striations. Many investigators [15,25] have assumed that each striation spacing corresponds to one loading cycle and sought to use striation count to relate the fracture surface analysis to crack growth per cycle (da/dN) . Based on this correlation, fatigue crack propagation can be obtained by the following relation:

$$\frac{da}{dN} = \frac{1}{magnification} \frac{distant\ on\ fractograph}{(striation / unit\ distant\ on\ fractograph)} \quad (2.18)$$

This correlation is recognized for a wide range of ΔK especially for Aluminum Alloys [26]. It was noticed, however, that this assumption holds only for limited range of ΔK for both a high strength aluminum alloy as well as for a steel alloy [27].

2.4 Corrosion Fatigue Crack Propagation

Fatigue crack growth rate in corrosive environment is much more complicated than in laboratory air environment due to the numerous variables involved. Chemical reactions at the crack tip vicinity as well as the predominant crack assisting mechanisms have great influence and at the same time they are not likely to be predicted. However, experimental data for fatigue crack propagation under service conditions have been correlated quite successfully for many alloys in terms of da/dN versus ΔK .

For life prediction purposes, Paris's law or one of its modifications are still capable to represent corrosion fatigue data provided that a number of assumptions are made regarding some physically significant parameters in favor of simplicity. In the absence of susceptibility to stress corrosion cracking, it has been observed that

an aggressive environment merely causes a shift of the da/dN versus ΔK curve of the reference environment . From the above observation it can be argued that corrosion fatigue crack growth still can be described by Paris's equation . In fact, many investigators have used the Paris's equation to describe corrosion fatigue crack growth data [28-30].

In general, fatigue crack growth behavior in a certain environment involves a dependance upon cyclic frequency , which reflects the effects of time, and the level of stress ratio R which accounts for wedging effects of corrosion-products at the tip of cracks. Frequency effects can be simulated by choosing the frequency of interest in the experimental stage. On the other hand, two analytical models have been proposed for determining effective stress intensity factors that incorporate the effects of stress ratio and crack closure phenomenon using Elber's analysis [31]. In this analysis, Paris's equation is written as

$$\frac{da}{dN} = C\,(\Delta K_{eff})^m \qquad (2.19)$$

where ΔK_{eff} is a function of R and ΔK values. Bamfold [32] has presented a number of forms that the ΔK_{eff} parameter may have in corrosion fatigue applications.

Endo et al [33] found that the corrosion-products induced wedge effect can be eliminated if the crack growth rate is presented in terms of ΔK_{eff}. Furthermore,

they proposed a model for corrosion fatigue crack propagation for materials exhibiting stress-assisted dissolution mechanism at the crack tip :

$$(\frac{da}{dN})_{CF} = (\frac{da}{dN})_F + \frac{1}{f}(\frac{da}{dt})_D \qquad (2.20)$$

where $(da/dn)_{CF}$ and $(da/dn)_F$ are crack growth rates in a corrosive environment and in air,respectively, where the crack growth rate in air is given by Equation (19) and $(da/dt)_D$,which represents the contribution of stress-assisted dissolution crack growth, was derived as

$$(\frac{da}{dt})_D = A f^{\alpha} (1-R)^{\beta} (\Delta K_{eff})^m \qquad (2.21)$$

where f is the frequency and C, m, A, α, and β are materials constants.

Chu and Macco [34] have employed the following equations to characterize the crack growth data in air and saltwater environments for a high strength aluminum alloy

$$\frac{da}{dN} = \frac{c(\Delta K - \Delta K_{th})^n}{[(1-R)K_c - \Delta K]^m} \qquad (2.22)$$

or

$$\frac{da}{dN} = \frac{c(\Delta K^a - \Delta K_{th}^a)}{[(1-R)K_c - \Delta K]^m} \qquad (2.23)$$

Figure 2.9 delineates the applicability of Equation (2.22) to describe the crack growth behavior from fatigue threshold to critical crack length for different R values in saltwater environment.

2.5 I-P Model for Fatigue Life Estimation

The total fatigue life can be separated into two portions: initiation and propagation lives. The transition from initiation to propagation is still the basic problem that researchers face when attempting to estimate the total fatigue life by summing the two portions. Furthermore, it has been observed that crack initiation is controlled by notch root plasticity, whereas crack growth rate is controlled by crack tip stress field. This observation has led to the introduction of the nonarbitrary definition of crack initiation length.

Socie et al [35] suggested a model to estimate the total fatigue life of notched members, where the initiation life is calculated using local strain approach and the propagation life is computed by fracture mechanics approach. They assumed that a fatigue crack is initiated when the fatigue damage due to crack propagation mechanisms outstrips that due to strain cycle fatigue mechanisms at some distance along the crack path ,a_i , from the notch root. Subsequently, crack initiation life is based on the strain range occurring at a_i from the notch root and crack propagation

life is then calculated using a_i as the initial crack size. Figure 2.10 compares experimental and predicted fatigue lives of circular notched plates for a high and low strength steel and a high strength aluminum alloy.

Another method, numerically equivalent to the above analysis, have been postulated by Chen and Lawrence [36]. The total fatigue life (N_T) of a number of micro-elements along the crack path were determined using local strain and fracture mechanics approaches to calculate initiation and propagation lives, respectively. The minimum value of N_T was taken as the total fatigue life and the corresponding distant was considered as the initiation length (a_i). Although this approach is numerically equivalent to Socie et al 'model, it is simpler and it can show the effects of arbitrary assumed initiation crack on the total fatigue life.

A much more simpler procedure to estimate the total fatigue life of cracked ligaments has been suggested [4]. This method uses the local strain approach to estimate the initiation life. The crack propagation life is computed by simply collapsing the notch to become an initial crack of the same width as the notch. The total life is then the sum of the two portions.

2.6 I-P Model for Corrosion Fatigue Life Estimation

For Fatigue life prediction under corrosive environment, The above model has been applied by Khan et al [8] for notched specimens. It was assumed that the environmental effects can be included in fatigue life assessment models by determining the material fatigue properties in the environment and frequency of interest. Estimates were obtained without involvement of the growth of small cracks in the notch region or the electrochemical issues. Good life estimates were obtained by this procedure in the high cycle region as can be inferred from Figure 2.11 and 2.12 for two different notch geometries having different stress concentration factors.

CHAPTER 3

ANALYTICAL MODEL

Fatigue life prediction of notched members is conveniently separated into two portions: crack initiation and crack propagation until final fracture. Crack initiation life is the number of cycles spent in forming and growing short cracks at the highly strained region. Crack propagation constitutes the portion of life spent in growing a predominant crack size to unstable length where fracture takes place. The difficulty arises when defining the crack size at which the crack characteristics change from the initiation process to the propagation regime. Furthermore, fatigue crack growth rates are often difficult to predict for short cracks growing near stress concentrations.

To circumvent this problem, a simple model has been used successfully to estimate fatigue lives of notched members using constant amplitude fatigue data obtained on laboratory specimens [4]. In this approach, local strain concepts is utilized to calculate the initiation life. The crack propagation life is computed by the application of LEFM concepts with the notch width taken as the initial crack size.

Figure 3.1 represents this approach schematically. The same approach has been used for fatigue life prediction of notched members in corrosive environments. It was assumed that the effects of the aggressive conditions can be included by determining the fatigue properties in the environment and at the frequency of interests [8].

3.1 Initiation Life Calculation

Fatigue crack initiation life calculation of notched members depends on the relationship between the nominal stresses , S, and strains , e, to the local notch stresses and strains, σ and ε . For the current analysis, the local strain-stress response will be approximated using Neuber's relation. Neuber's rule postulates that beyond yielding the geometric mean of the stress and strain concentration factor K_σ and K_ε remains equal to the concentration factor K_t :

$$K_t = \sqrt{K_\sigma K_\varepsilon} \tag{3.1}$$

where,

K_σ = actual stress concentration = $\Delta\sigma/\Delta S$

$\Delta\sigma$ = local stress range

ΔS = nominal stress range

K_ε = actual strain concentration = $\Delta\varepsilon/\Delta e$

$\Delta\varepsilon$ = local strain range

Δe = nominal strain range

Using the definition of K_σ and K_ε, Equation (3.1) becomes :

$$K_t^2 = \frac{\Delta\sigma\,\Delta\varepsilon}{\Delta S\,\Delta e} \tag{3.2}$$

If the remote stresses and strains are assumed to be elastic, then Equation (3.2) can be expanded to show

$$\frac{(\Delta S\,K_t)^2}{E} = \Delta\sigma\,\Delta\varepsilon \tag{3.3}$$

Equation (3.3) relates the stress and strain response at the notch to the nominal stress and strain. The expression for the cyclic stress - strain curve may be represented in the form:

$$\frac{\Delta\varepsilon}{2} = \frac{\Delta\sigma}{2E} + \left(\frac{\Delta\sigma}{2K'}\right)^{\frac{1}{n'}} \tag{3.4}$$

where,

$\Delta\varepsilon$ = cyclically stable strain range

$\Delta\sigma$ = cyclically stable stress range

K′ = cyclic strength coefficient

n′ = cyclic strain hardening exponent

E = modulus of elasticity

combining Equation (3.3) and (3.4) gives

$$\frac{\Delta\sigma^2}{2E} + \Delta\sigma\left(\frac{\Delta\sigma}{2K'}\right)^{\frac{1}{n'}} = \frac{(K_t\,\Delta S)^2}{2E} \tag{3.5}$$

Thus the local stress can be determined by solving Equation (3.5) using iterative technique. The local strain can be then computed from Equation (3.4).

Once the local stress and strain response has been determined the strain life equation with the appropriate set of material properties can be solved for number of reversals to failure, 2N, where N is the number of cycles to initiation. Material properties are determined by low cycle fatigue concepts in the environment of interests at zero mean stress. To account for the presence of mean stress effects, the strain-life equation is modified as,

$$\frac{\Delta\varepsilon}{2} = \frac{\grave{\sigma}_f - \sigma_o}{E} (2N)^b + \grave{\varepsilon}_f (2N)^c \qquad (3.6)$$

where,

σ_o = mean stress

σ'_f = fatigue strength coefficient

b = fatigue strength exponent

ε'_f = fatigue ductility coefficient

c = fatigue ductility exponent

2N = number of strain reversals to failure (N = number of cycles to failure)

A computer program has been developed for the initiation life calculation is given in Appendix I.

3.2 Propagation Life Calculation

Linear elastic fracture mechanics (LEFM) concepts are employed for fatigue crack propagation life calculations. The concept utilizes the crack growth rate data from cracked specimens. Paris's power law is the most commonly used correlation between constant amplitude fatigue crack growth rates (da/dN) and the crack tip cyclic stress intensity factor range (ΔK). In this formulation:

$$\frac{da}{dN} = C(\Delta K)^m \tag{3.7}$$

The material constants, C and m, can be found experimentally from constant amplitude fatigue crack growth data at the environment of interests. The crack growth life, in terms of cycles to failure, may be estimated by integrating Equation (3.5) as follows:

$$N_p = \int_{a_i}^{a_f} \frac{da}{C(\Delta K)^m} \tag{3.8}$$

where, a_i is the initial crack length and, a_f is the critical crack length. The stress intensity factor range, ΔK, for center cracked tension specimen is [37]:

$$\Delta K = \frac{\Delta P \sqrt{\pi a}}{W t} \sqrt{\sec\left(\frac{\pi a}{W}\right)} \tag{3.9}$$

where,

ΔP = load range

t = specimen thickness

W = width of specimen

Because ΔK is a function of the crack length, the integration above must be solved using a numerical procedure. For the current analysis, a_i, is equal to the notch dimension perpendicular to the maximum nominal stress. This simple definition of the initial crack size eliminates the need to find a nonarbitrary initial crack length through sophisticated procedures. The final crack size , a_f, is calculated from the limiting load capability of the cracked member based on the yield strength of the material under investigation [8] :

$$a_f = \frac{W}{2} - \frac{S_{max}}{2 t \sigma_y} \qquad (3.10)$$

where t is the thickness of the specimen and σ_y is the 0.2% offset yield. Appendix II is a computer program listing for integrating Equation (3.6) numerically.

CHAPTER 4

EXPERIMENTAL PROGRAM

4.1 Material Selection and Experimental Setup

The experimental program of this study consists of three parts: strain controlled fatigue tests, fatigue crack propagation tests, and stress-life tests. The material used in this investigation were two different compositions of Al-2.5 Mg alloy. The temper designation of this material is H34. The weight percent of the alloying elements in the experimental aluminum alloys are given in Table 4.1 . All specimens were machined from 1000 x 80 x 2 mm sheets parallel to the rolling direction. All fatigue tests were carried out in both laboratory air and in Arabian Gulf water under constant amplitude loading. Analysis of the Arabian Gulf water shows the composition given in Table 4.2 . Special plexiglass chambers have been fabricated for the purpose of testing under the corrosive conditions. A small pump was employed to circulate the water inside the chamber.

4.2 Testing Apparatus

Cyclic loading was provided by an Instron 8051 closed-loop servohydraulic testing system. This system is suitable for testing materials under static and dynamic loading conditions. The system is fully digital controlled. The major parts of this system consists of the following: a closed load frame with movable crosshead, a digital control console, an actuator with a capacity of 100 KN in dynamic phase, servohydraulic grips with 400 bar maximum gripping pressure, a load cell which measures the actual applied force, and a hydraulic power supply. Figure 4.1 is a front view of the system.

The digital control console provides facilities for control and monitoring of the overall testing machine through an interactive front panel. The front panel houses all the controls and indicators necessary for operation. Load, displacement, and strain may be selected as the controlling mode. Different waveforms can be generated: ramps, sine, triangle, square, haversine, havertriangle, and haversquare. Depending on the load level, loading frequency may be vary from 0 to 100 HZ.

A digital Phillips oscilloscope was used to monitor the applied load. A horizontally travelling microscope was employed in the measurement of the crack length. A digital readout system, connected to the microscope, provided crack length measurements with an accuracy of 0.001 mm.

4.3 Strain-Controlled Fatigue Test

Results of strain-controlled fatigue testing are used in the formulation of the strain-life equation (Equation (2.2)) . Four fatigue parameters are to be determined using empirical relations between stress and plastic strain versus reversals to failure. The American Society of Testing and Materials (ASTM) has a standard recommended practice ASTM E606-88 for conducting strain-controlled testing using uniaxially push and pull loaded specimens [38]. The general guidelines of this practice will be followed. However, the specimen design of this procedure is suitable for either round specimens with minimum diameter of 6.35 mm (0.25 in) in the test section or sheet specimens as thin as 2.54 mm (0.1 in).

Both of these specimen designs could not be used since the experimental alloy was 2 mm in thickness and round bars of the same material were not available. The major problem was to determine an appropriate specimen geometry that will produce valid results.

Miller [39] has suggested a specimen design for performing strain-controlled fatigue tests on high strength steels having thickness < 0.1 in . No alternative specimen geometry for thin aluminum sheets was found in the literature. Thus, an attempt has been made in this study to use the specimen suggested by Miller although it was expected that results may not be reliable. The validity of the results will be judged through comparison

of the fatigue properties obtained using this specimen with values in the literature for similar aluminum alloy. The specimen configuration is shown in Figure 4.2 .

Fully reversed cyclic strain amplitudes were maintained by means of Instron extensometer with 10 mm gauge length. The strain function exhibited a sine waveform where the mean strain was kept at zero. Frequency of loading was varied from 10 Hz , at low strain ranges, to 0.5 Hz at high values. For nominally elastic strain range, the test was conducted under load control.

The stress-strain hysteresis loops were recorded by an X-Y recorder. The stress range , $\Delta\sigma$, and the plastic strain range , $\Delta\varepsilon_p$, were determined from the height and the width of the stable hysteresis loops, respectively. Failure was defined either as the total separation of the specimen at the gauge length or sudden change of the controlled strain exceeding the physical limits of the extensometer. Failures outside the gauge length have been discarded.

Despite of very careful testing, the values of the required fatigue properties obtained from these tests were found to be in conflict when compared to the values found in literature for similar alloy. Thus the values obtained from our tests were discarded and the values from the literature [8] were used for fatigue life estimation.

4.4 Fatigue Crack Growth Test

The main purpose of this test is to assess the crack propagation resistance of the material under investigation in order to predict fatigue crack propagation life of a pre-cracked member. These tests were carried out under constant amplitude loading in accordance to the general guidelines of the ASTM E647-88a [40]. The loading was sinusoidal with the stress ratio kept at a value of 0.1 . Central notched specimens 38 mm wide and 2 mm thick were used to determine the long crack growth rates. Specimens were polished using 400 grit emery papers perpendicular and parallel to the crack direction. This was followed by final polishing with 600 grit emery paper perpendicular to the crack direction. Fatigue precracking was performed at higher stress amplitudes to produce a predominant fatigue crack. The crack length , a, was measured visually by a travelling microscope to within 0.001 mm and displayed on a digital display.

4.5 Stress-Life Curves

Stress -life fatigue data were obtained to verify the prediction model. Fatigue tests were performed under load controlled conditions at a stress ratio of R = 0.1 and testing frequency at 20 Hz with a sine waveform. The specimen configuration and notch geometries are presented in Figure 4.3 .

CHAPTER 5

EXPERIMENTAL RESULTS

5.1 Strain Cycle Fatigue Results

Figure 5.1 and 5.2 are plots of elastic strain ($\Delta\varepsilon_e/2$) and plastic strain ($\Delta\varepsilon_p/2$) amplitudes versus reversals to failure on log-log scale for alloy type 1, respectively. Similar plots for alloy type 2 are shown in Figure 5.3 and 5.4 . Fatigue properties, which have been derived from these plots using least square fitting technique, are presented in Table 5.1 .

Comparing strain-controlled fatigue properties obtained from this work with properties of similar aluminum alloys found in the literature, it was observed that these results were not comparable and could not be used. It is deemed that the major source of error is attributed to the specimen design. Although the same specimen design gave comparable results for high strength sheet steels with the same thickness [39], the problem here may be due to the lower buckling resistance of aluminum alloys when compared to steels in general. The number of specimens failures outside the gage length (more than 50%) , even at relatively very low strain amplitudes, support this reasoning.

Excessive bending at the gage length may also affect the data which then can not be interpreted as fatigue data. Attempts to use small strain amplitudes to avoid buckling proved to be of little help because strain amplitudes for which valid results can be obtained would be limited [37,39] . Because of the above reasons, the required fatigue parameters were obtained from literature for a similar aluminum alloy [8]. Strain-controlled fatigue properties for lab air as well as corrosive environment are given in Table 5.2 .

The completely reversed stabilized cyclic true stress versus true plastic strain relation has been approximated by a power law function as shown in Figure 5.5 and 5.6 for both alloy types. The relation may be expressed as:

$$\sigma = \dot{K}(\varepsilon_p)^{\dot{n}} \qquad (5.1)$$

where,

σ = cyclically stable stress amplitude

ε = cyclically stable plastic strain amplitude

K' = cyclic strength coefficient

n' = cyclic strain hardening exponent

The cyclic strength coefficient and exponent were derived from these plots using least square fitting and presented in Table 5.3 for both alloys. It is assumed that these values will not be largely affected by the presence of a corrosive environment.

5.2 Fatigue Crack Growth Results

Figure 5.7 and 5.8 show graphical representation of crack length , a, versus number of load cycles for both alloy types. This in turn is used along with a computer program to calculate crack growth rate , da/dN, and stress intensity factor , ΔK . The program is based on the seventh incremental polynomial method as was recommended by the ASTM practice. The program listing is given in Appendix III . Fatigue crack growth rates as a function of stress intensity factor ranges in both environments are depicted in Figure 5.9 and 5.10 for alloy type 1 and type 2, respectively. A linear regression analysis, using the least square technique, was performed on each set of data to obtain the fatigue crack growth parameters from Paris power law regime. Table 5.4 presents values of C and m for both alloys in air as well as in Gulf seawater.

5.3 S-N Curves

Figure 5.11 and 5.18 represent high cycle fatigue data for both alloys in the environment of interests. The loading ratio and frequency were kept at a value of 0.1 and 20, respectively. As for most aluminum alloys, these alloys do not tend to show fatigue limit. When testing in corrosive environment, the flow rate of the seawater was

kept constant for all tests. Laboratory condition is considered as the air environment. Table 5.5 to Table 5.12 give fatigue life data in tabular form.

CHAPTER 6

DISCUSSION

6.1 Fatigue and Corrosion Fatigue Resistance of the Experimental Alloys

Figure 6.1 to Figure 6.12 compare the experimental stress-life data of alloy type 1 and alloy type 2 for circular and elliptical notches in air and seawater environments. Figure 6.1 shows that alloy type 1 specimens have longer lives than alloy type 2 when compared at the same stress level for almost the entire range of life considered. For the case of the elliptical notch, the opposite behavior is displayed in Figure 6.2 .

This observation can be explained in view of the lower fatigue crack growth resistance associated with alloy type 1 in contrast to alloy type 2 (Fig. 5.9 and 5.10). Thus, for sharp notches, where significant contribution to total life may be due to fatigue crack propagation, alloy type 2 show higher fatigue resistance whereas for blunt notches, where the total life is initiation dominant, alloy type 1 exhibit higher fatigue resistance. Essentially the same trends are depicted in the corrosive environment (Fig. 6.3 and 6.4) but with less manifestation which may be attributed to the fact that corrosive environment decreases the relative susceptibility to notch effects as will be discussed below.

The influence of stress concentrators on the fatigue resistance of alloy type 1 and 2 in the two environments are shown in Figure 6.5 through 6.8 . Figure 6.5 and 6.7 show the effect of the circular notch on alloy type 1 in air and in the corrosive media, respectively. By comparing these two figures, it is obvious that notch effects on fatigue strength in the aggressive environment is less sever than in air. This behavior is exhibited in general by aluminum alloys and alloy steels [41]. Figure 6.6 and 6.8 demonstrate principally the same observation for alloy type 2 . This behavior can be explained by the fact that multiple crack initiation take place at the notch root under corrosive environment which reduces the severity of the notch and thus lowering the stress concentration factor [41].

Typical effects of corrosive environment can be seen in Figure 6.9 to 6.12 , where a reduction in fatigue resistance at all stress levels is observed for both alloys. Direct comparison of the air and the seawater data show that, the deleterious effect of the corrosive environment is more pronounced in the high cycle region and this effect diminishes in the low cycle region (Fig. 6.9 , 6.11 and 6.12). Crack propagation rate data, where only a modest effect of environment was observed, confirms the latter observation. This means that the environmental influence on fatigue life should be considered seriously in the long life regime where a large percentage of life is spent in crack initiation.

This observation reflects the effects of the exposure time to the corrosive environment which increases the interactions between the material and the environment, thus resulting in shorter lives when compared to air data. Moreover, these figures conform well with the fact that the presence of corrosive environment eliminates the possible existence of an endurance limit [42].

6.2 Fatigue Life Predictions

Comparisons of the experimental data and fatigue life estimates for circular notched specimens in both environments are displayed in Figure 6.13 through 6.16 . Similar plots for the elliptical notch are shown in Figure 6.17 to 6.20 . In these figures, initiation and propagation, and total life estimates were computed by the prediction model presented in this study. For the case of circular notch in laboratory air (Fig. 6.13), the model provides good estimates for the total life of alloy type 1 for the range of life considered. However, for alloy type 2 the good estimates are limited in the region of intermediate life (Fig. 6.14) which may be attributed to the higher chromium content of alloy type 2 when compared to the alloy of which the fatigue properties were used. However, excellent fatigue life estimates have been obtained for circular notched members in corrosive environment as can be seen in Figure 6.15 and 6.16 for alloy type 1 and 2 , respectively.

For bluntly notched members, an initiation dominant behavior is expected in both air and seawater environments. The model should be able to confirm this expectation. A comparison of the predicted and experimental results of the circular notched specimens indeed show that the model properly predicts this trend for alloy type 1 in both air and seawater environments and for alloy type 2 in the seawater environment. From the above figures, it is apparent that fatigue life estimates in the long life region is initiation-dominant process whereas in the short life regime fatigue crack propagation contribution becomes evident.

Figure 6.17 and 6.18 provide comparisons between experimental results and fatigue life estimates for elliptically notched members in laboratory air. Good life estimates were obtained in the life range considered. For elliptical notched specimens, Figure 6.19 and 6.20 show that fatigue life estimates agree well with the experimental results observed for both environments. From the above figures it is obvious that all fatigue life estimates lie in the safe side.

For sharply notched members, a relatively large contribution of crack propagation is expected to the total fatigue life. This must be especially true in the low to intermediate life regions, where higher stress levels and higher K_t values cause a combined effect. Comparison of observed and estimated lives for elliptical notched members illustrate that the model was able to adequately exhibit this trend as can be inferred from Figure 6.17 to 6.20 .

A survey [43] of the different assessments of fatigue life prediction methodologies postulates that the ratio of actual life to the predicted value is the relevant criterion by which prediction models can be evaluated. Thus, a perfect model will deliver a ratio of unity and a standard deviation of zero. However perfect predictions is neither achievable nor of engineering significance in view of the inherent scatter associated with fatigue data. Furthermore, according to Bush [44], a model works sufficiently well if the ratio for all prediction lies within the range of 0.5 to 2.0 . Figure 6.21 through 6.28 are comparisons between predicted versus actual lives for various combinations of notch types and environments for both alloys. These comparisons show that good estimates have been obtained especially in the seawater environment.

CHAPTER 7

CONCLUSIONS

The conclusions of this study are summarized as follows:

1. High-cycle fatigue curves show that fatigue resistance of the modified Al-2.5 Mg alloys is reduced by the presence of seawater.

2. The effect of the aggressive environment should be considered seriously in the long life regime whereas this effect diminishes at the short life regime.

3. Alloy type 2 show better fatigue crack growth resistance than alloy type 1 for data in air as well as in corrosive environments.

4. Reliable constant amplitude fatigue life estimates for notched members of Al-2.5 Mg type 1 and 2 alloys exposed to Arabian Gulf water can be obtained from the initiation-propagation model presented in this investigation.

5. Good fatigue life estimates have been obtained without detailed considerations of the environmental issues or the difficulties encountered when attempting to define a non-arbitrary initial crack length.

6 For the purpose of fatigue life calculation using the initiation-propagation model, the effects of an aggressive environment on fatigue life can be included by determining the materials properties in the environment and at the frequency of interest.

7. For the stress concentration factors considered, fatigue life estimates exhibit initiation dominant behavior in the long life region for air and seawater environments.

8. As the stress concentration increases (from 2.4 to 4.2), contributions from fatigue crack propagation life to the total life increases.

9. Both type 1 and 2 of the modified Al-2.5 Mg alloys exhibit low notch sensitivity in corrosive environment.

Recommendations for Future Work

The extension of this work can study the effects of other notch geometries and a number of other engineering materials. The model may also be examined when the process is primarily propagation dominant. Since this study was concerned with free corrosion conditions, it is valuable to evaluate the model predictions under controlled corrosion variables such as potential, oxygen concentration, pH etc. Another important consideration is to assess the model under variable amplitude loading conditions to evaluate its applicability to real life engineering situations.

REFERENCES

[1] Morrow,J.,and Socie,D.F., "The Evolution of Fatigue Crack Initiation Life Prediction Methods," Materials, Experimentation and Design in Fatigue, Sherratt,F., and Sturgeon,Eds., Westbury House, Warwick, England,1981,pp.3-21.

[2] Hoeppner,D.W., and Krupp,W.E., "Prediction of Component Life by Application of Fatigue Crack Growth Knowledge," Engng. Fracture. Mech.,Vol. 6,1974,pp. 47-70.

[3] Smith,R.A., Fatigue Crack Growth 30 Years of Progress, Pergamon Press,1986.

[4] Socie,D.F., Dowling,N.E., and Kurath,P., "Fatigue Life Estimation of Notched Members," Fifteenth National Symp. on Fracture Mechanics, ASTM STP 833,Sanford,R.J.,Ed., ASTM,1984,pp.284-299.

[5] Congleton,J.,and Parkins,R.N., "Degradation of Mechanical Properties by Corrosion Fatigue," J. of Mech. Engng. Science Part C, Proc. Insm. Mech. Engrs., Vol. 203,1989.pp.73-84.

[6] Devereux,O., McEvily, A.J., and Staehle,R.W.,Eds., Corrosion Fatigue: Chemistry, Mechanics, and Microstructure, conference proceedings, University of Connecticut,June 14-18,1971, National Association of Corrosion Engineers, Houston.

[7] Sudarshan,T.S., Srivatsan,T.s., and Harvey, D.P., "Fatigue Processes in Metals-Role of Aqueous Environments." Engng. Fracture Mech.,Vol. 36,No. 6, 1990,pp. 827-852.

[8] Kurath,P., Khan,Z., and Socie,D.F., "Fatigue Life Estimates for a Notched Member in a Corrosive Environment," J. Press. Vessel. Tech.,Vol. 109,Feb. 1987, pp.135-141.

[9] Dowling,N.E., "A Review of Fatigue Life Prediction Methods," Society ofAutomotive Engineers TPS 871966.

[10] Hunt,W.A., "Fatigue of Commercially Aluminum Alloy" A PhD. Dissertation,Birmingham University,1986.

[11] Basquin,O.H., " The Exponential Law of Endurance Tests," ASTM Proc.,Vol. 10,1910, pp.625-630.

[12] Coffin,L.F., " A Study of the Effects of Cyclic Thermal Stresses on a Ductile Metal," Trans. ASME, Vol.76,1954, pp. 931-950.

[13] Bannantine,J.A., Comer,J.J.,and Handrock J.L., Fundamentals of Metal Fatigue Analysis,Prentice-Hall ,1990.

[14] Neuber,H., "Theory of Stress Concentration for Shear Strained Prismatic Bodies with Arbitrary Nonlinear Stress-Strain Law," ASME Journal of Applied Mechanics, Vol. 28,1961, pp. 544-560.

[15] Sato,T., and Shimada,H., "Evaluation of Fatigue Crack Initiation Life From a Notch," Int. Journal Fatigue, Vol.10,No.4,Oct. 1988,pp. 243-247.

[16] Zheng,X., "A Further Study on Fatigue Crack Initiation Life-Mechanical Model for Fatigue Crack Initiation" Int. Journal Fatigue,Vol. 8,No. 9,1986.pp. 17-21.

[17] Bernstein,H., and Loeby,C., "Low-Cycle Corrosion Fatigue of Three Engineering Alloys in Salt Water" Journal of Eng. Mat. Tech.,Trans. of the ASME,Vol. 110,July 1988, pp. 234-239.

[18] Kondo,Y., "Prediction of Fatigue Crack Initiation Life Based on Pit Growth" Corrosion,Vol. 45,No. 1,Jan. 1989, pp. 7-11.

[19] Rolfe,S.T., and Barsom,J.M., Fracture and Fatigue Control in Structures,2nd ed.,Prentice-Hall,1987.

[20] Novak,S.R., "Corrosion-Fatigue Crack Initiation Behavior of Four Structural Steels," Corrosion Fatigue: Mechanics , Metallurgy, Electrochemistry, and Engineering, ASTM STP 801,Crooker,T.W., and Leis,B.N.,Adduce., ASTM, Philadelphia, 1983,pp. 26-63.

[21] Forman,R.G., Keary,V.E., and Engle,R.M., "Numerical Analysis of Crack Propagation in Cyclic-Loaded Structures." ASME Journal of Basic Engineering,Vol. 89,Sept. 1967,pp. 459-464.

[22] Elber, W., "The Significance of Fatigue Crack Closure," Damage Tolerance in Air Craft Structures, ASTM STP 486, ASTM, Philadelphia,1971,pp. 230-242.

[23] Krausz,K.,and Krausz,A.S.,"On the Physical Meaning of the Power-Function Type Fatigue Equations," Int. Journ. of Fracture,Vol. 47,1991,pp. R37-R42.

[24] McEvily,A.J., "On Closure in Fatigue Crack Growth," ASTM STP 982,ASTM,Philadelphia,1988,pp. 35-43.

[25] Antolovich,S.D., and Saxena,A., Fatigue Failures, in Metals Handbook,Vol. 10,9th ed.,ASM,1983,pp.102-135.

[26] Georgiev,M.N., and Mezhova,N.Ya., " Determination of the Fatigue Crack Growth Rate By the Electron Fractographic Method." Sov. Materials Science, March-April,1985,pp. 161-163.

[27] Yokobori,T., and Sato,K., "The Effect of Frequency on Fatigue Crack Propagation Rate and Striation Spacing in 2024-T3 Aluminum Alloy" Engng. Fracture Mechanics,1976 ,Vol. 8,pp. 81-88.

[28] Alawi,H.,Ragab,A., and Shaban,M., "Corrosion Fatigue Crack Growth of Steels in Various Environments." Journal of Eng. Mat. and Tech.,Trans. of ASME,Vol. 111,Jan. 1989, pp. 40-45.

[29] Bolton,J.D., and Redington,M.L., "The Effects of Saline Aqueous Corrosion on Fatigue Crack Growth Rates in 316 Grade Stainless Steels." Int. J. Fatigue,Vol. 5,No. 3,July 1983, pp. 155-163.

[30] McEvily, A.J., Atlas of Stress-Corrosion and Corrosion Fatigue Curves. ASM International, Materials Park, 1990.

[31] Ewalds,H.L., van Door,F.C., and Sloof,W.G., "Influence of Environment and specimen Thickness on Fatigue Crack Growth Data Correlation by Means of Elber-Type Equations," Corrosion Fatigue:Mechanics, Metallurgy, Electrochemistry, and Engineering, ASTM STP 801,Crooker T.W., and Leis,B.N.,Adduce.,ASTM,Philadelphia,1983,pp. 115-134.

[32] Bamfold,W.H., "Implementing Corrosion-Fatigue Crack Growth Rate Data for Engineering Applications," Corrosion Fatigue:Mechanics, Metallurgy, Electrochemistry, and Engineering, ASTM STP 801,Crooker T.W., and Leis,B.N., Adduce.,ASTM,Philadelphia,1983,pp. 405-422.

[33] Endo,K., Komai,K., and Shikida,T., "Crack Growth by Stress-Assisted Dissolution and Threshold Characteristics in Corrosion Fatigue of a Steel," Corrosion Fatigue : Mechanics Metallurgy, Electrochemistry, and Engineering, ASTM STP 801,Crooker T.W., and Leis B.N., Adduce., ASTM, Philadelphia,1983,pp. 81-95.

[34] Chu,H.P., and Macco,J.G., "Corrosion Fatigue of 5456- H117 Aluminum Alloy in Saltwater," Corrosion Fatigue Technology,ASTM STP 642,1976,pp.

[35] Socie,D.F., Morrow,J., and Chen,W., "A Procedure for Estimating The Total Fatigue Life of Notched and Cracked Members" Engng.Fracture. Mech.,Vol. 11,1979,pp. 851-859.

[36] Lawrence,J., and Chen,W., "A Model for Joining the Fatigue Crack Initiation and Propagation Analyses" Fracture Control Program,University of Illinois at Urbana-Champaign,Report No. 32,Nov. 1979.

[37] Hertzberg,R.W., Deformation and Fracture Mechanics of Engineering Materials,3rd ed.,John Wiley & Sons,1989.

[38] ASTM E606-80, Annual Book of ASTM Standards, ASTM, Philadelphia,1991.

[39] Miller,G.A, "Strain-Cycle Fatigue of Sheet and Plate Steel I:Test Method Development and Data Presentation," Society of Automotive Engineers TPS 830175.

[40] ASTM E647-88a, Annual Book of ASTM Standards, ASTM, Philadelphia,1991.

[41] Karlashov,A.V., Gnatyouk,A.D. and Kardash,A.B., "Corrosion Fatigue Strength of Aluminum Alloys," Corrosion Fatigue, Proceedings of the 1st USSR-UK Seminar on Corrosion Fatigue of Metals, Parkins,R.N., and Kolotyrkin,M.Ya.,Adduce.,The Metals Society,May 1980,pp. 101-111

[42] Pokhmurskii,V.I., " General Aspects of Corrosion Fatigue in Metals and Alloys," Corrosion Fatigue, Proceedings of the 1st USSR-UK Seminar on Corrosion Fatigue of Metals, Parkins,R.N., and Kolotyrkin,M.Ya.,Adduce.,The Metals Society,May 1980,pp. 47-53.

[43] Heuler,P.,and Schultz,Z., "Assessment of Concepts for Fatigue Crack Initiation and Propagation Life Prediction," Z. Werkstofftech.,17,1986,pp.397-456.

[44] Bush,A., "Verification of Fatigue Crack Initiation Life Prediction Results." Techn. Israel Inst. of Techn., Haifa,TAE No. 400,1980.

[45] AbdulAleem,B.J., "The Effects of Suspended Solids on Flow Dependent Corrosion of Tube Materials for Desalination," Master Thesis, KFUPM,March 1989.

TABLE 4.1

Composition of the modified Al- 2.5 Mg alloys (H34) (Weight Percent)

Type	Fe	Si	Cu	Mn	Mg	Cr	Zn	Ti
1	0.05	0.05	<0.01	<0.01	2.47	0.1	0.02	0.003
2	0.05	0.04	<0.01	<0.01	2.48	0.29	0.01	0.003

TABLE 4.2

Analysis of Arabian Gulf Water (in milligrams/liter) [45]

ions	Na^+	Ca^{++}	Mg^{++}	So^{-4}	Cl^-	Co^{-3}	HCo^{-3}	total
	19186	704	2400	4894	34080	18	189	61471

TABLE 5.1

Fatigue properties of the modified Al- 2.5 Mg alloys

Type	Environment	σ_f(MPa)	b	ε_f	c
1	air	699	-0.15	0.379	-0.64
	seawater	324	-0.103	0.379	-0.64
2	air	832	-0.16	0.79	-0.74
	seawater	924	-0.2004	0.79	-0.74

TABLE 5.2

Fatigue properties of 5454-H32 aluminum alloy [8]

	σ_f (MPa)	b	ε_f	c
Air	348	-0.044	0.82	-0.628
Seawater	1648	-0.2001	0.82	-0.628

TABLE 5.3

Cyclic strength coefficients and exponents for the modified Al-2.5 Mg alloys

Type	K'(MPa)	n'
1	889	0.248
2	653	0.179

TABLE 5.4

Fatigue crack propagation parameters for the modified Al-2.5 Mg alloys

Type	Environment	C	m
1	Air	7.527E-11	3.144
1	Seawater	4.156E-10	2.584
2	Air	7.943E-12	3.873
2	Seawater	8.106E-10	2.232

Table 5.5

Constant amplitude fatigue life data of circular notch, alloy type 1 in lab. air.

Sp#	S_{max} (MPa)	Life (cycle)	Remark
xca1	142.8	145652	
xca2	125	360434	
xca3	107.1	1.5E6	Run out
xca4	178.6	34850	
xca5	142.8	86317	

Table 5.6

Constant amplitude fatigue life data of elliptical notch, alloy type 1 in lab. air.

Sp#	S_{max} (MPa)	Life (cycle)	Remark
xea1	107.1	79124	
xea2	71.4	405724	
xea3	142.8	15670	
xea4	142.8	15029	

Table 5.7

Constant amplitude fatigue life data of circular notch, alloy type 1 in seawater.

Sp#	S_{max} (MPa)	Life (cycle)	Remark
xcc1	107.1	304887	
xcc2	89.3	886964	
xcc3	125	144362	
xcc4	71.4	1.5E6	Run out

Table 5.8

Constant amplitude fatigue life data of elliptical notch, alloy type 1 in seawater.

Sp#	S_{max} (MPa)	Life (cycle)	Remark
xec1	89.3	134454	
xec2	71.4	299776	
xec3	107.1	51653	
xec4	107.1	45244	

Table 5.9

Constant amplitude fatigue life data of circular notch, alloy type 2 in lab. air.

Sp#	S_{max} (MPa)	Life (cycle)	Remark
yca1	125	164841	
yca2	142.8	141767	
yca3	89.3	2E6	Run out
yca4	107.1	447986	
yca5	178.6	26553	
yca6	142.8	71214	

Table 5.10

Constant amplitude fatigue life data of elliptical notch, alloy type 2 in lab. air.

Sp#	S_{max} (MPa)	Life (cycle)	Remark
yea1	142.8	32615	
yea2	125	53819	
yea3	107.1	129570	
yea4	89.3	924577	
yea5	98.2	135054	
yea6	92.8	1368348	
yea7	178.6	11220	
yea8	142.8	16966	
yea9	142.8	20519	

Table 5.11

Constant amplitude fatigue life data of circular notch, alloy type 2 in seawater.

Sp#	S_{max} (MPa)	Life (cycle)	Remark
ycc1	125	108815	
ycc2	107.1	76598	
ycc3	89.3	415693	
ycc4	71.4	1.5E6	Run out

Table 5.12

Constant amplitude fatigue life data of elliptical notch, alloy type 2 in seawater.

Sp#	S_{max} (MPa)	Life (cycle)	Remark
yec1	142.8	19466	
yec2	125	32161	
yec3	107.1	54507	
yec4	89.3	190404	
yec5	71.4	188419	

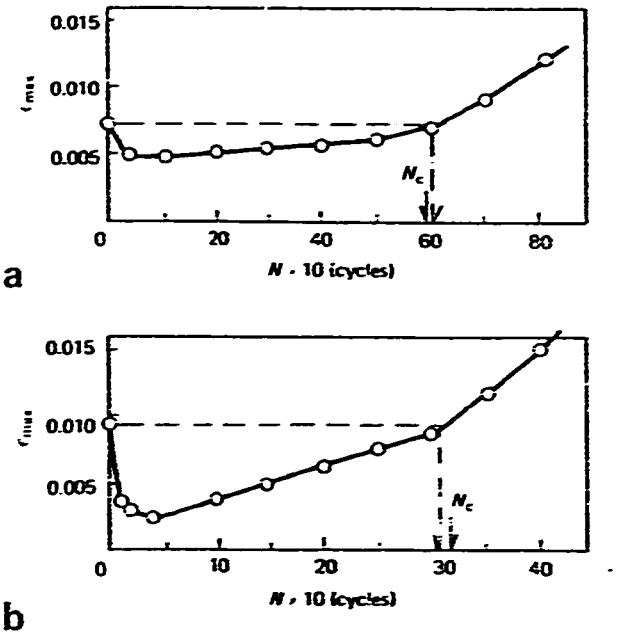

Fig. 2.1 The relation between maximum strain and cyclic number for SUS304 stainless steel at initial stress intensity factor ranges (a) 22 and (b) 23.8 MPa $\sqrt{m}$ [15]

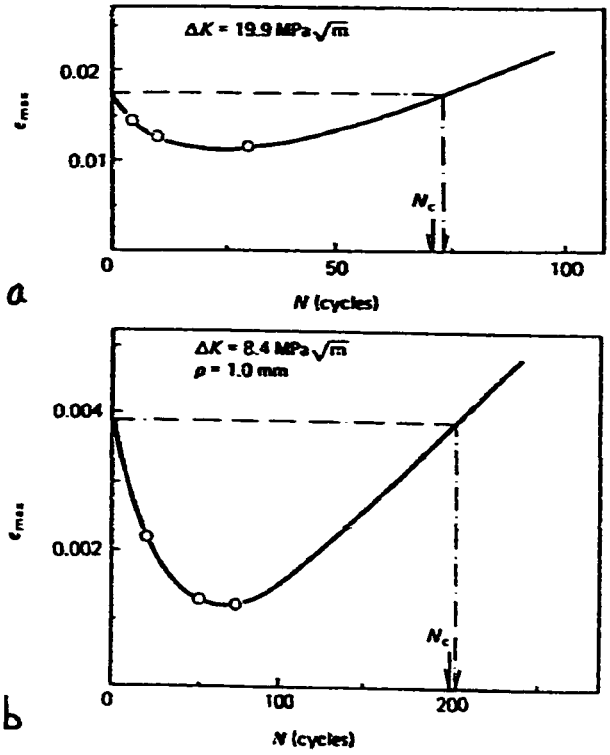

Fig. 2.2 The relation between maximum strain and cyclic number estimated by the proposed method for (a) brass (b) 5052 aluminum alloy [15]

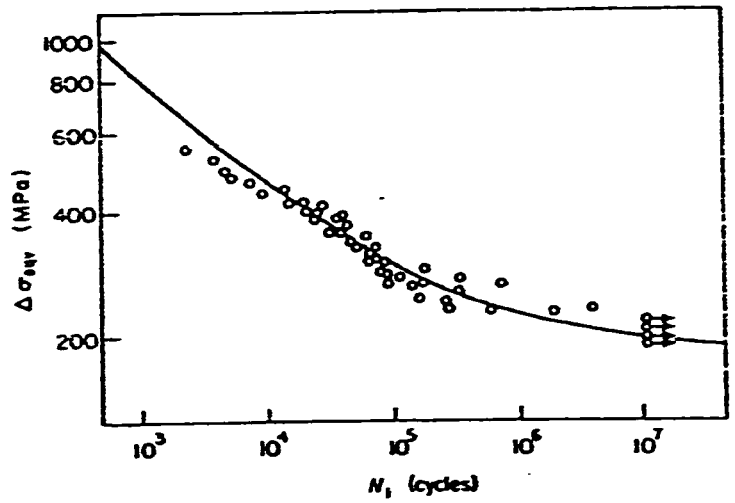

Fig. 2.3 Regression analysis for Equation (2.5) [16]

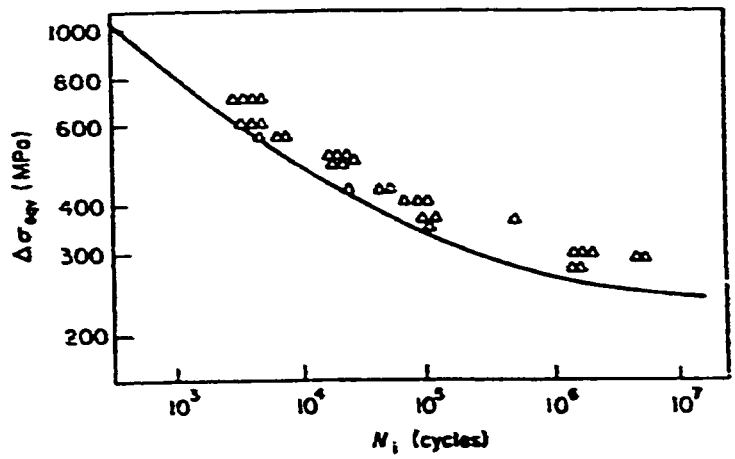

Fig. 2.4 Comparison between test results and predictions using Equation (2.5) for 2024-T3 aluminum alloy [16]

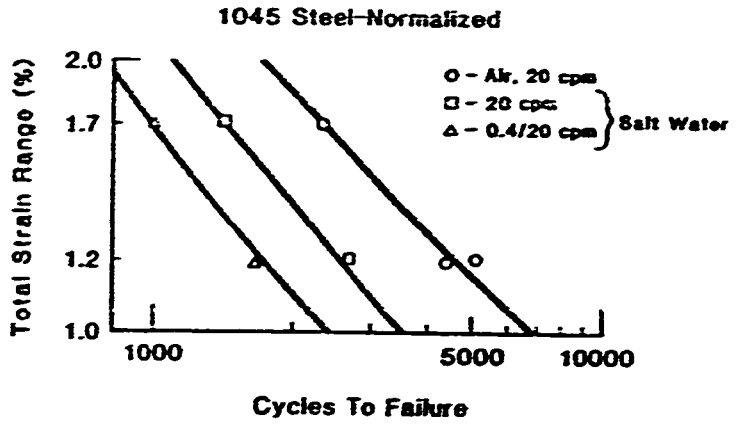

Fig. 2.5 Stress vs. cycles to failure: 1045 steel [17]

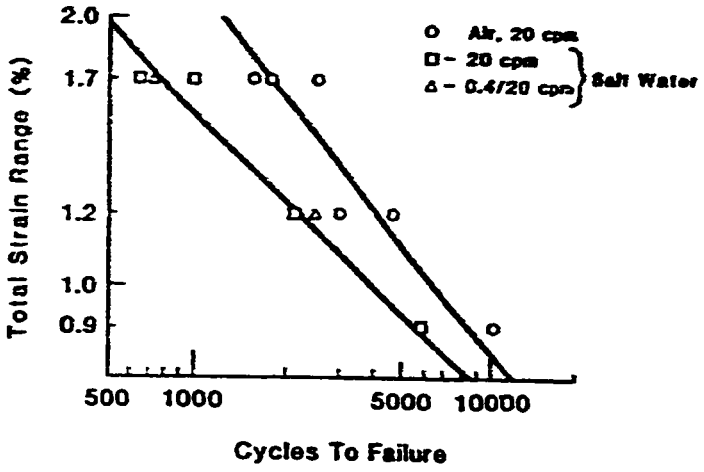

Fig. 2.6 Stress vs. cycles to failure: 304 stainless steel [17]

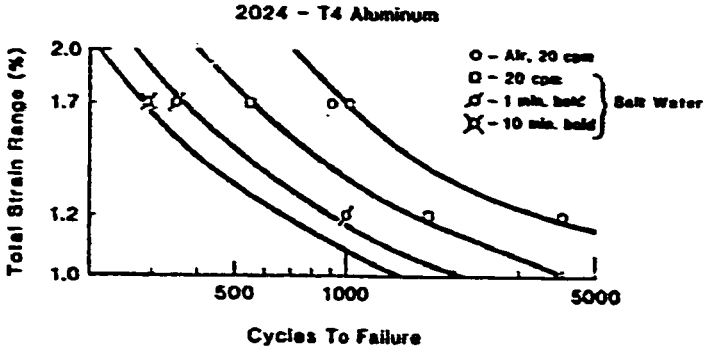

Fig. 2.7 Stress vs. cycles to failure: 2024-T4 [17]

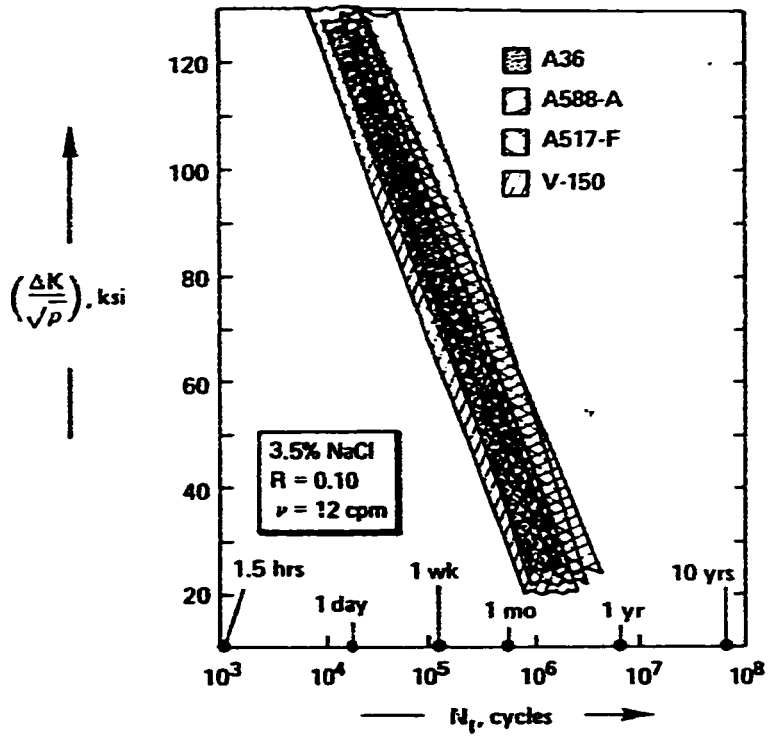

Fig. 2.8 Comparison of scatterbands for corrosion fatigue crack initiation results of four steels [20]

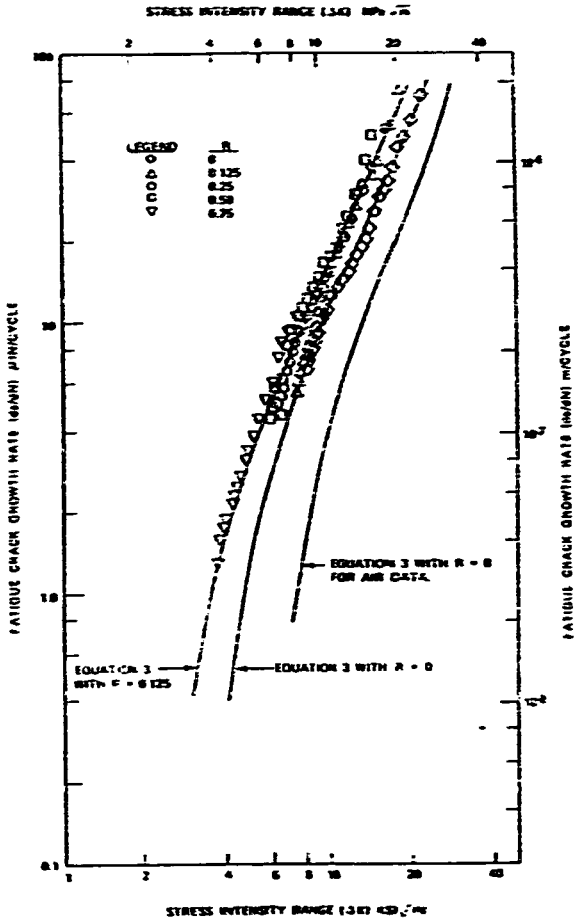

Fig. 2.9 Comparison between test results and predictions using Equation (2.22) [34]

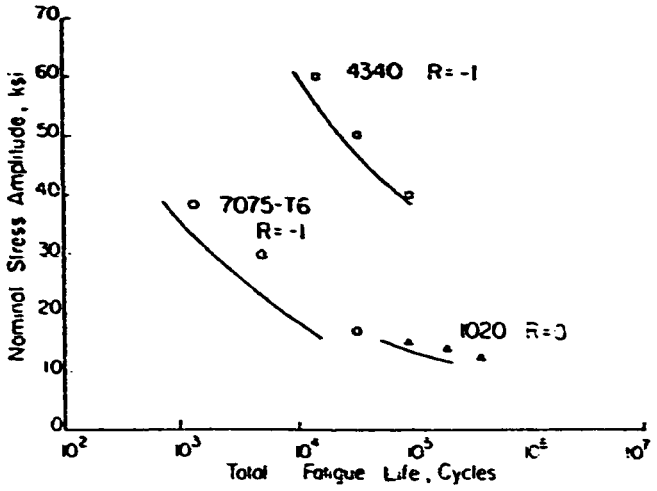

Fig. 2.10 Comparison between predicted and experimental results [35]

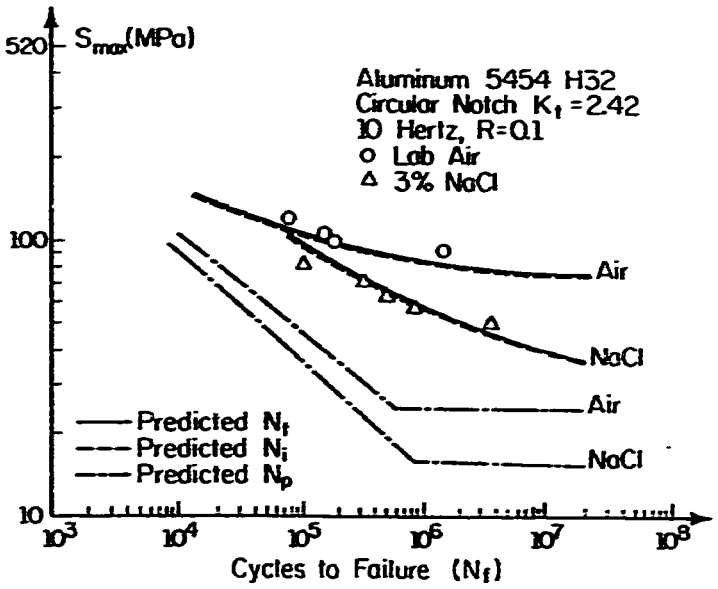

Fig. 2.11 Fatigue life estimates for circular notch [8]

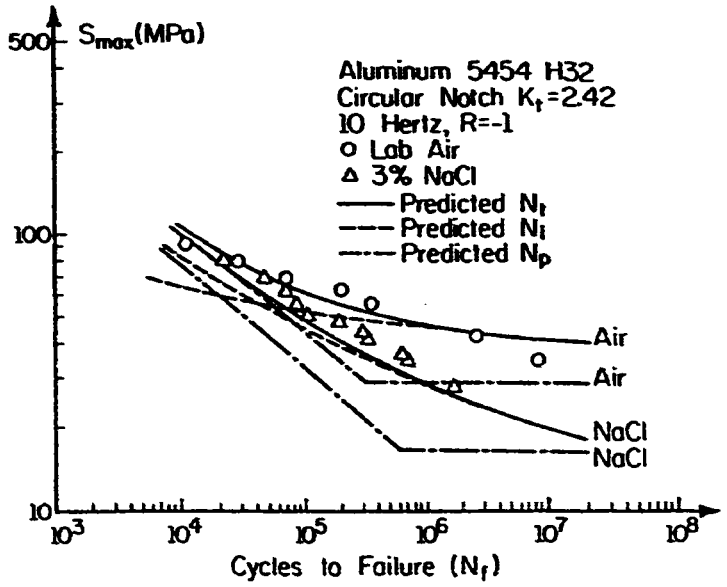

Fig. 2.12 Fatigue life estimates for elliptical notch [8]

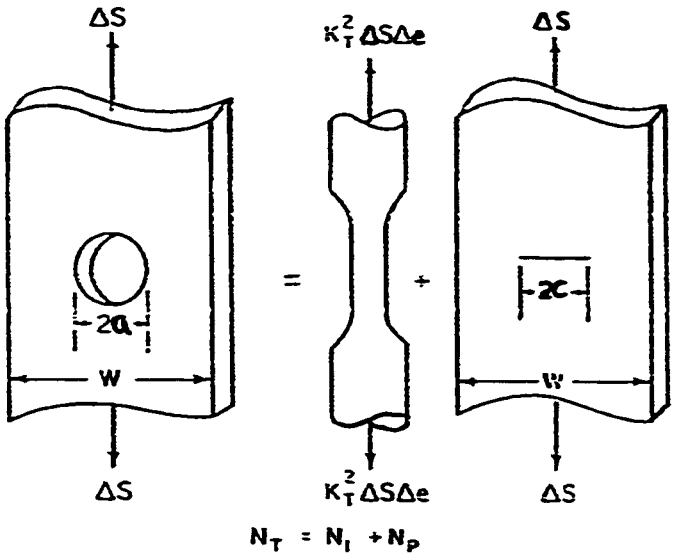

Fig. 3.1 Schematic fatigue life initiation-propagation model

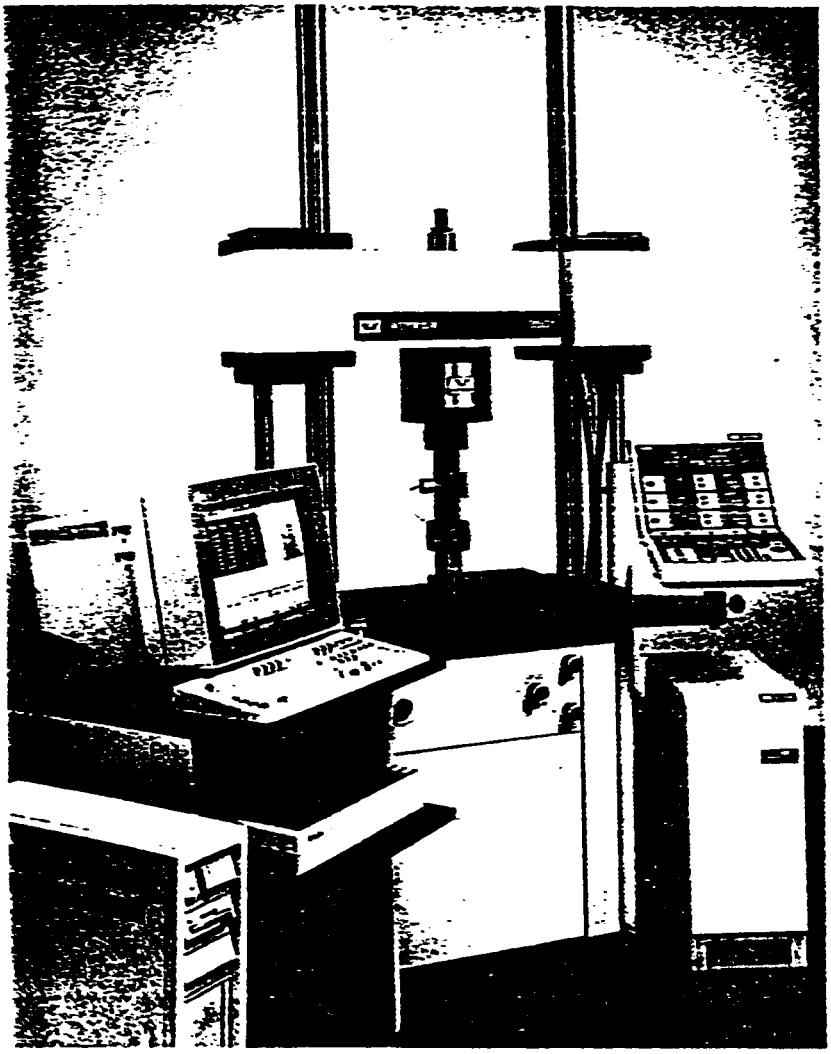

Fig. 4.1 Front view of the Instron testing system

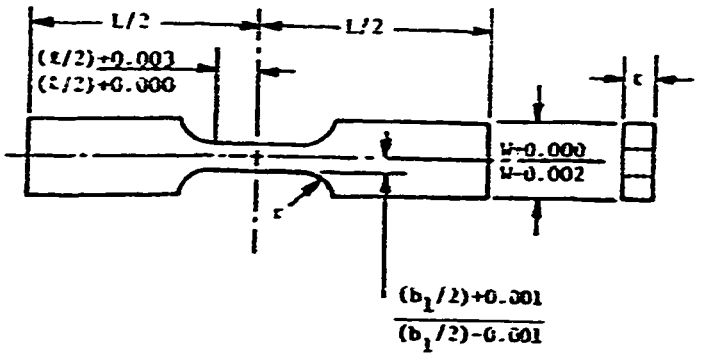

L = 2.75
ℓ = 0.35
W = 0.5
b_1 =0.25
r = 0.188

Figure 4.2 Strain-Controlled Specimen Design
(Note: All dimensions in in.)

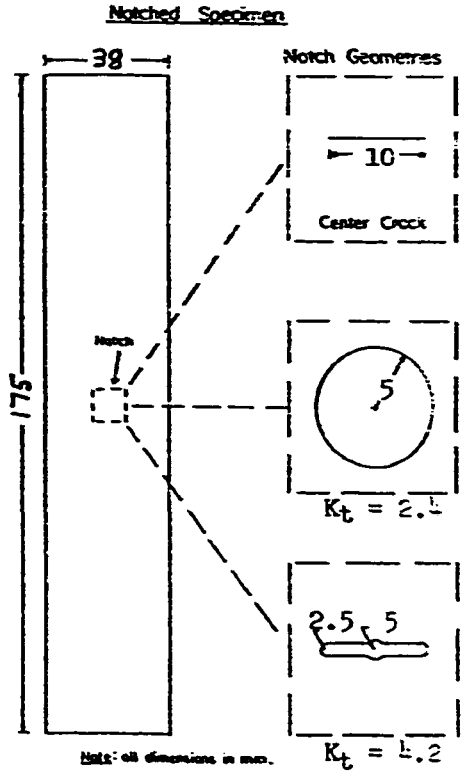

Figure 4.3 Notched Fatigue Specimen Design

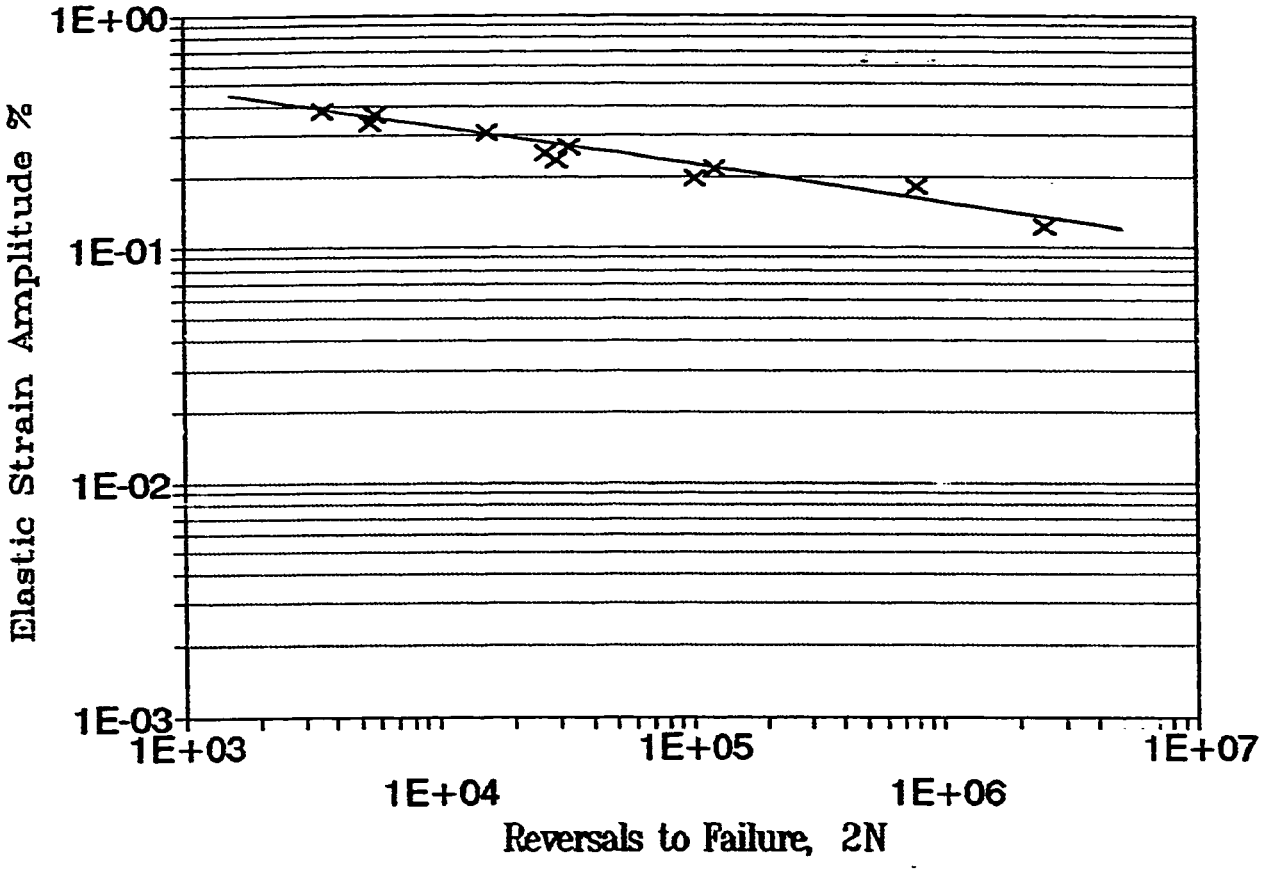

Fig. 5.1 Elastic strain amplitude vs. reversals to failure, alloy type 1 in lab. air

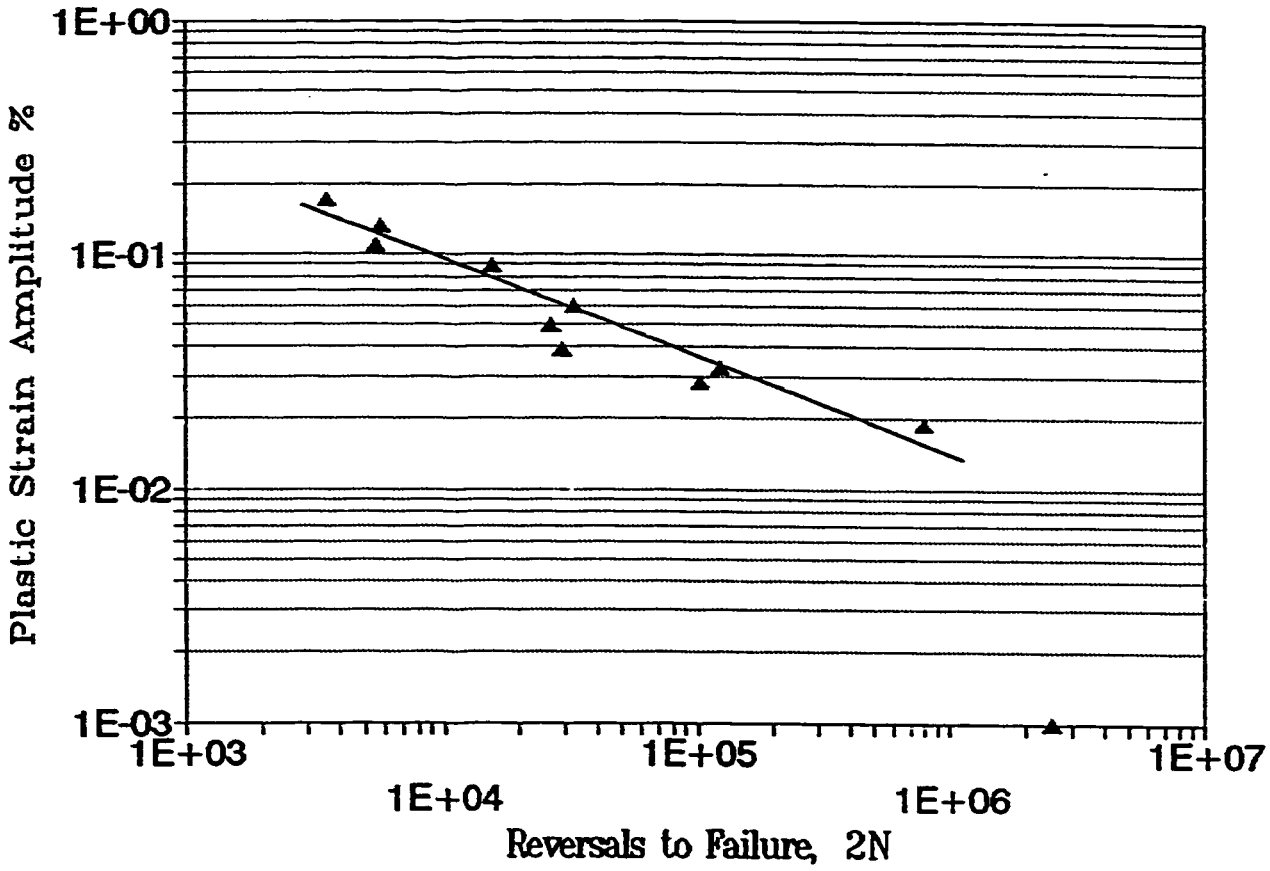

Fig. 5.2 Plastic strain amplitude vs. reversals to failure, alloy type 1 in lab. air

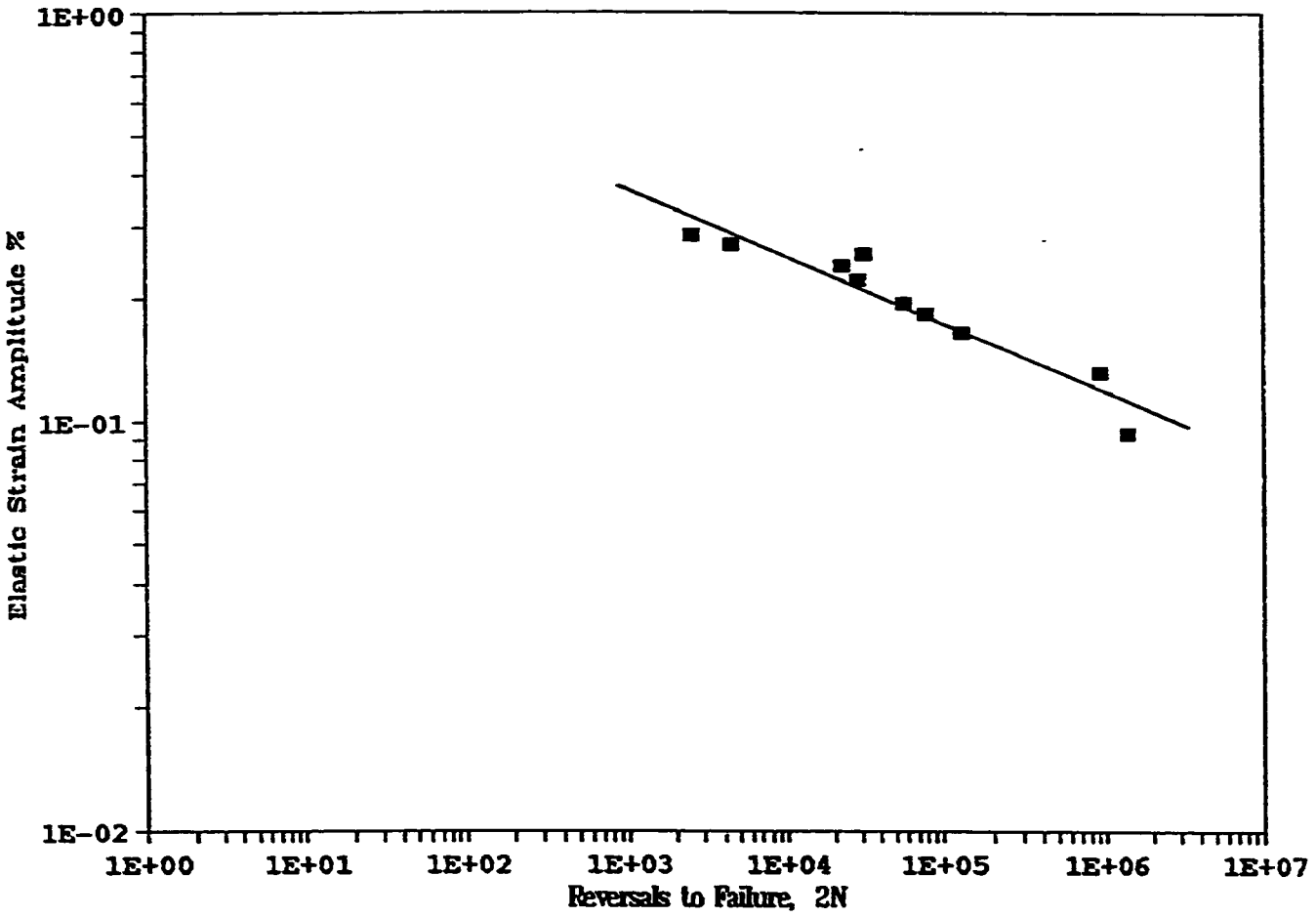

Fig. 5.3 Elastic strain amplitude vs. reversals to failure, alloy type 2 in lab. air

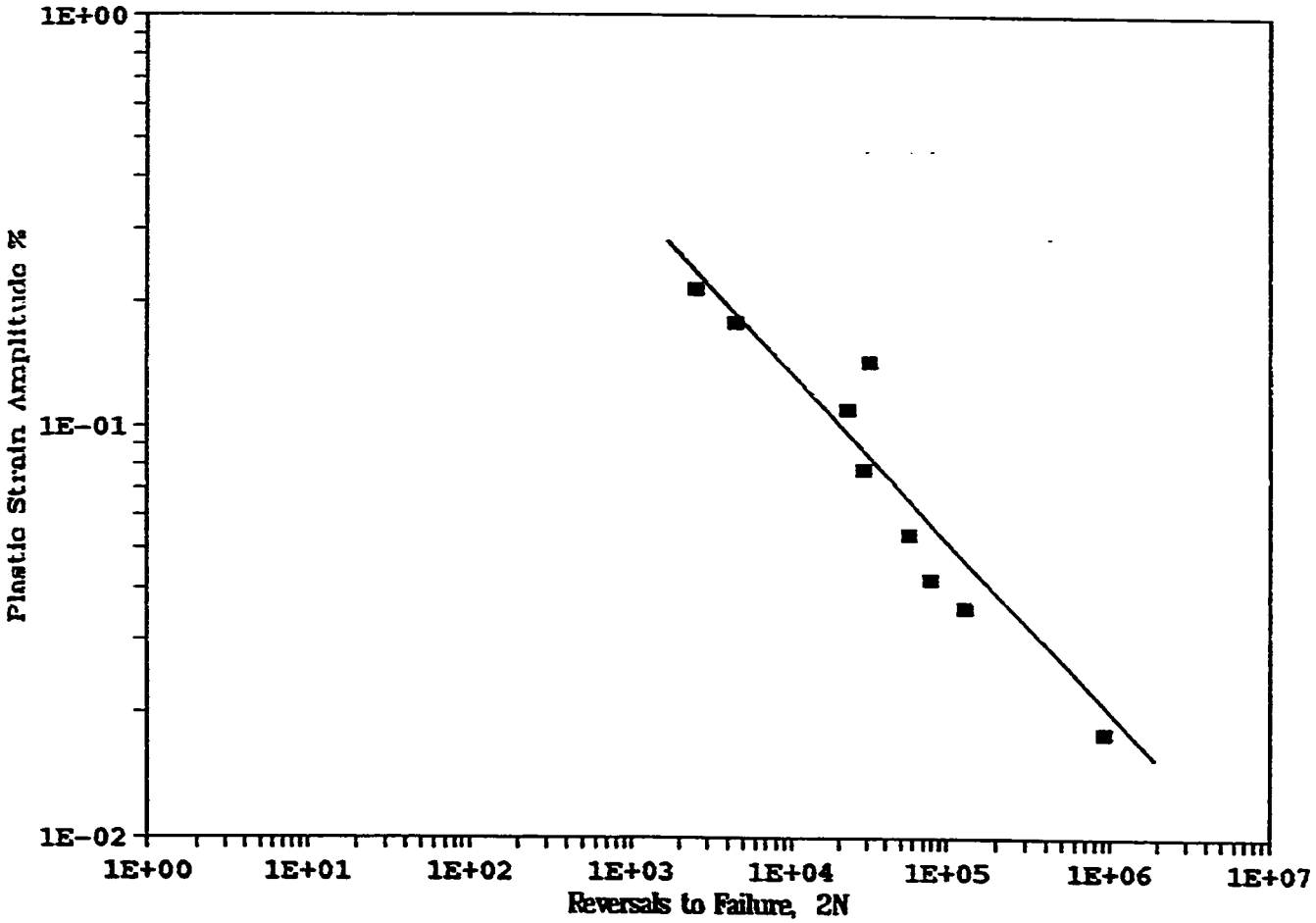

Fig. 5.4 Plastic strain amplitude vs. reversals to failure, alloy type 2 in lab. air

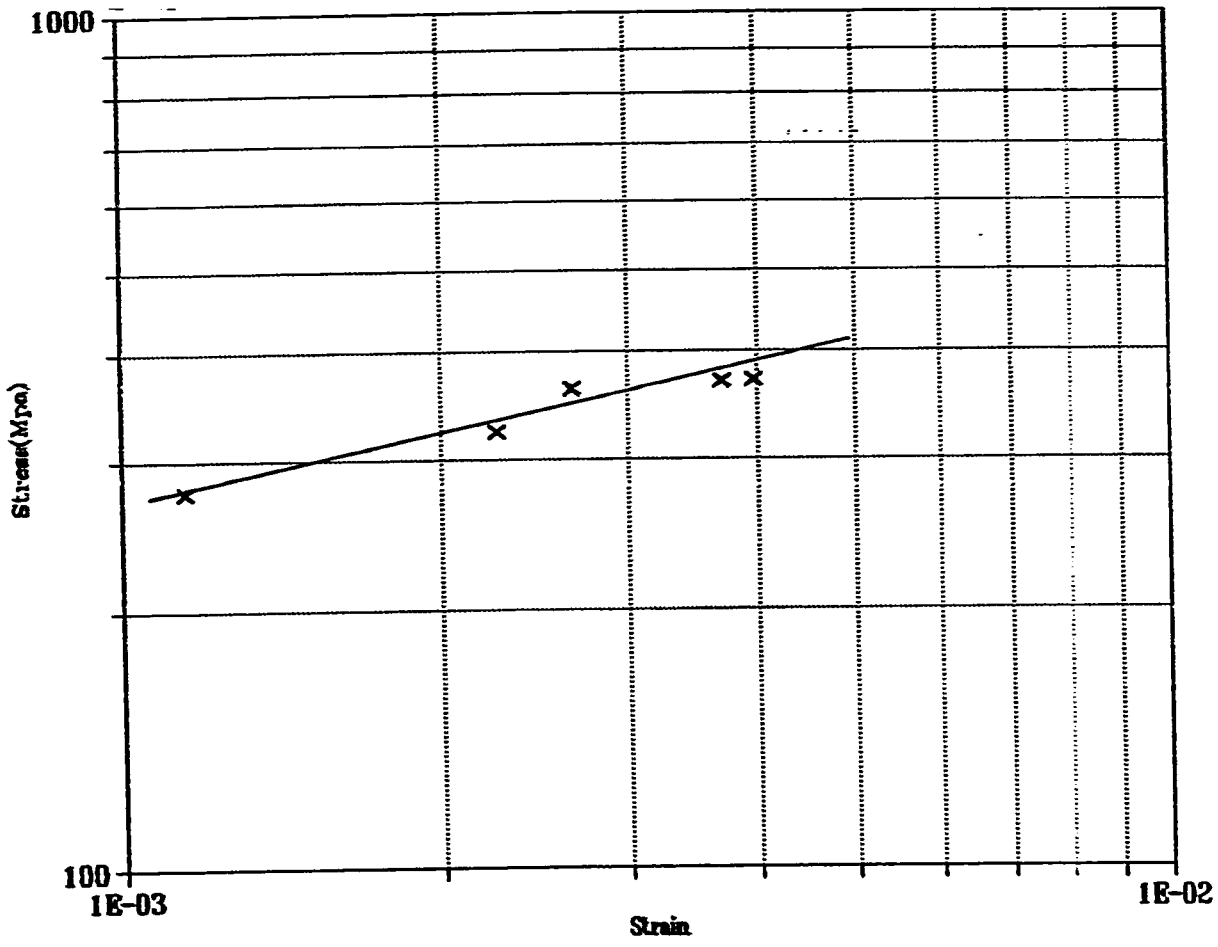

Fig. 5.5 Stress vs. plastic strain amplitude, alloy type 1 in lab. air

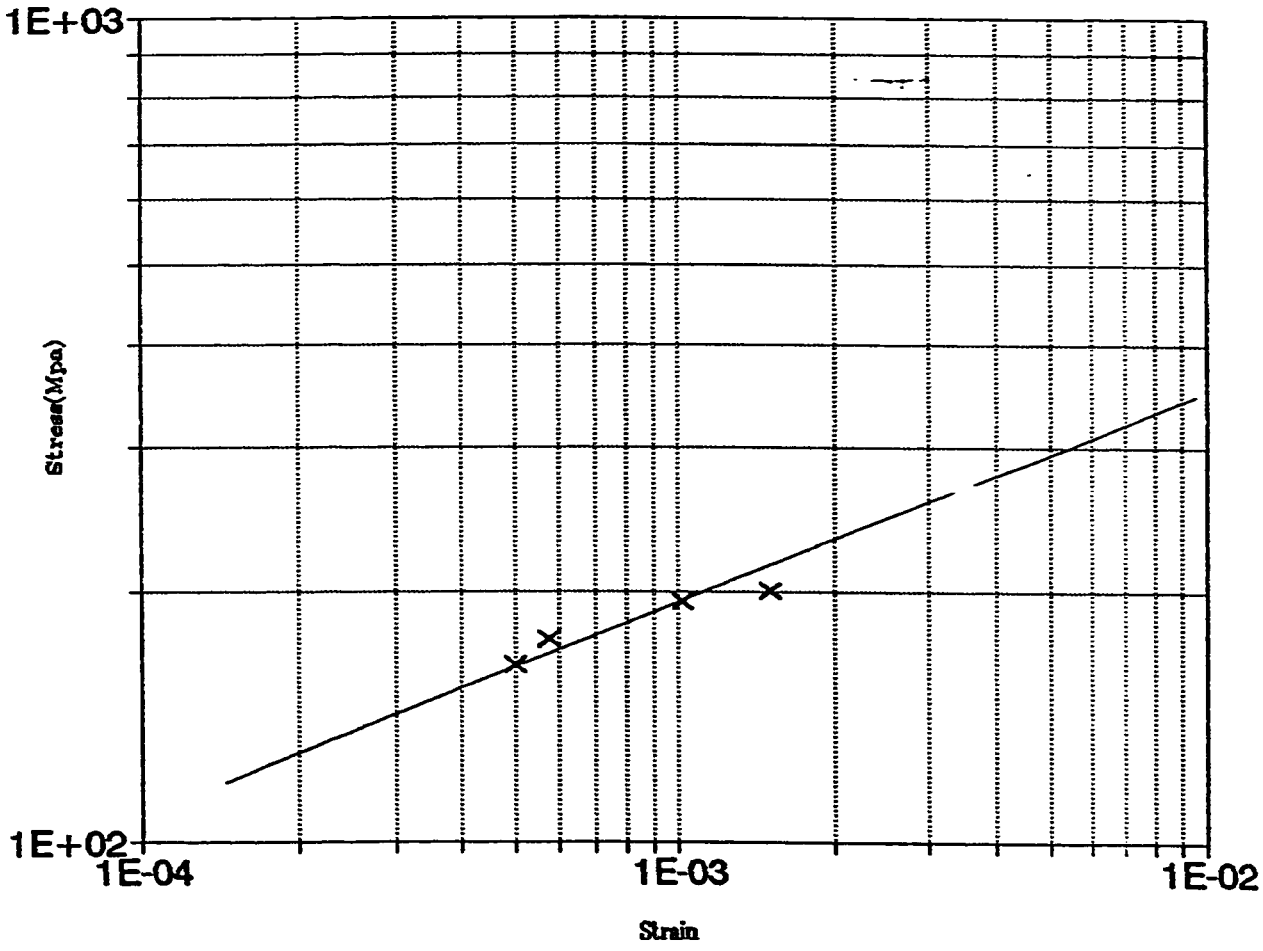

Fig. 5.6 Stress vs. plastic strain amplitude, alloy type 1 in lab. air

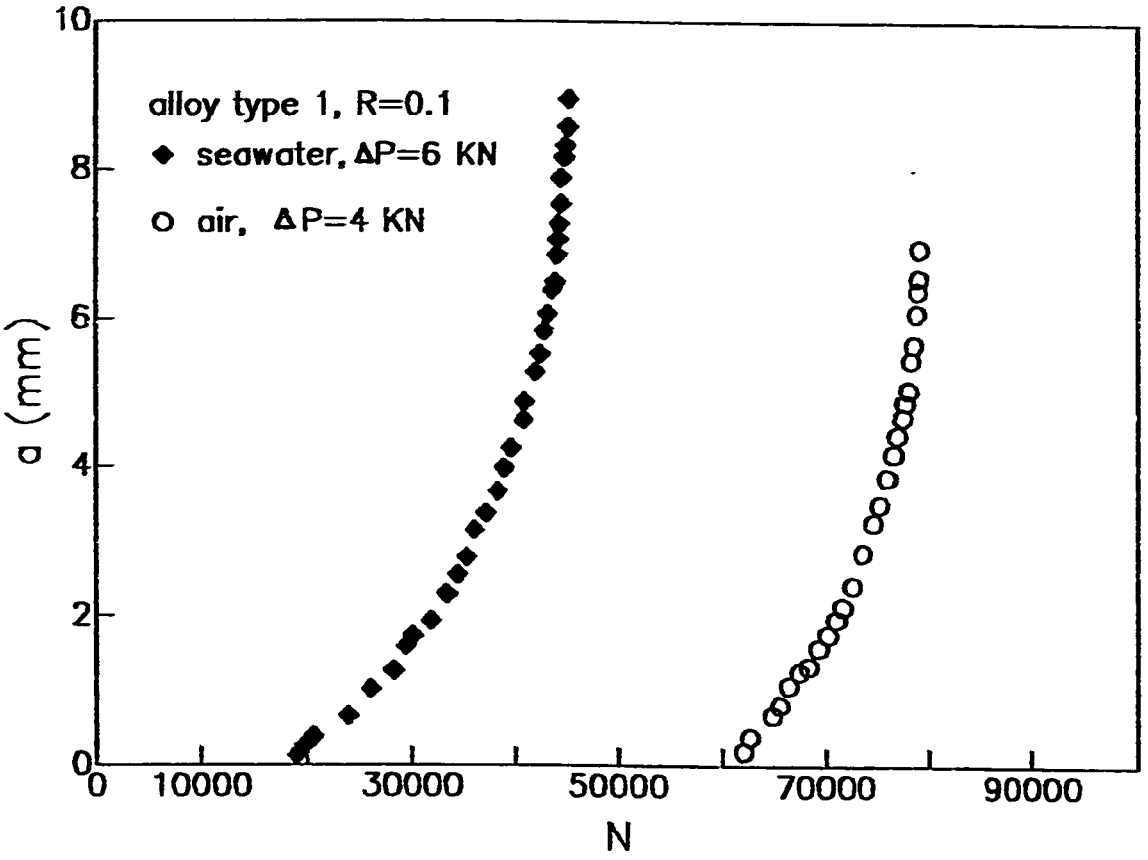

Fig. 5.7 Crack length versus number of cylces for alloy type 2

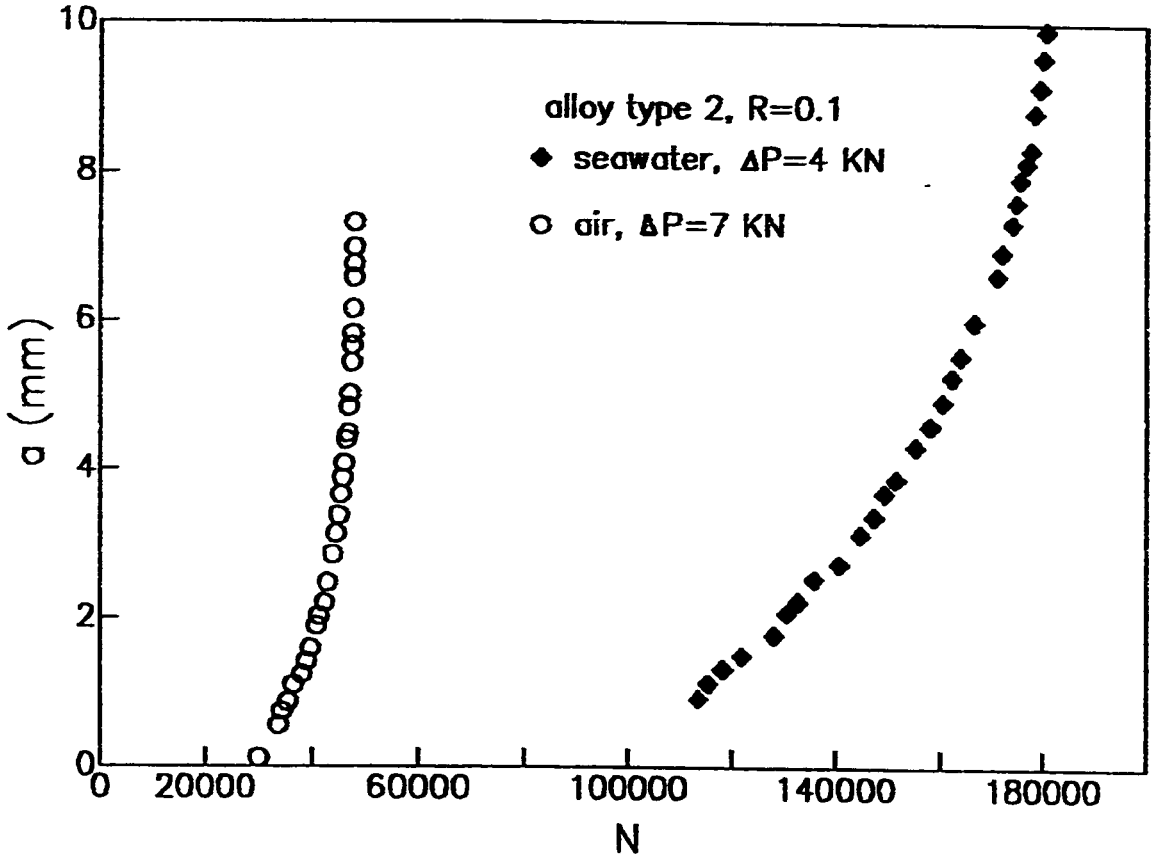

Fig. 5.8 Crack length versus number of cycles for alloy type 2

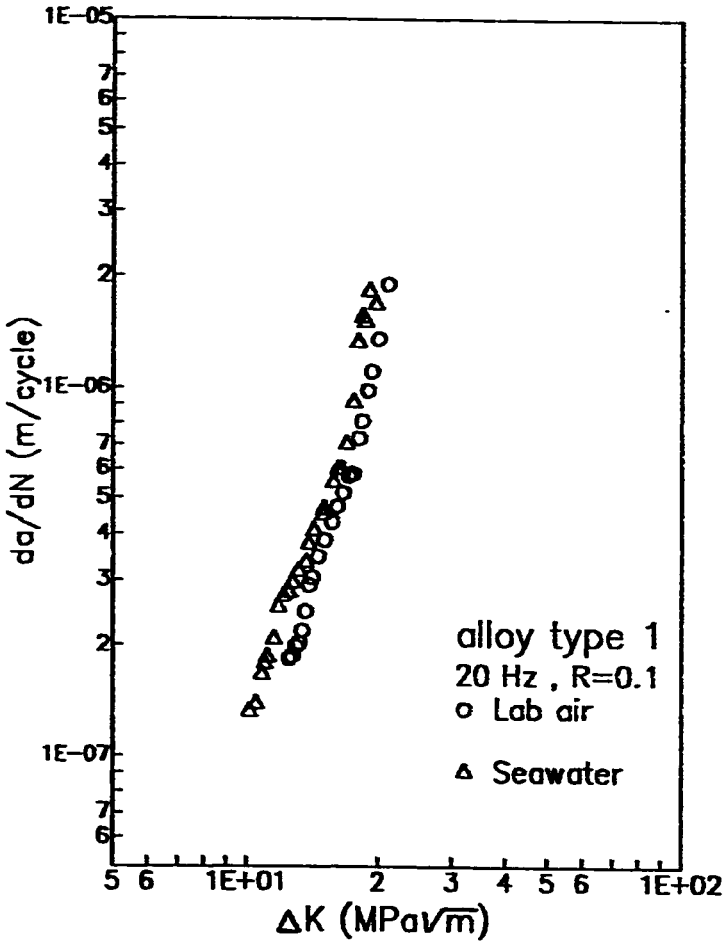

Fig. 5.9 Fatigue crack growth rate vs. stress intensity factor range for alloy type 1

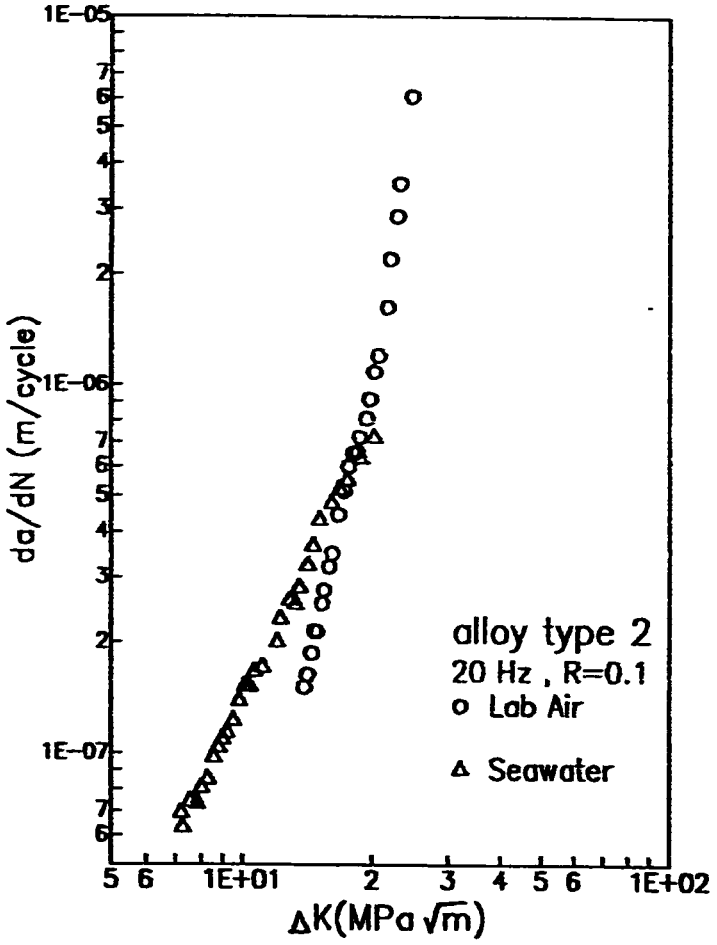

Fig. 5.10 Fatigue crack growth rate vs. stress intensity factor range for alloy type 2

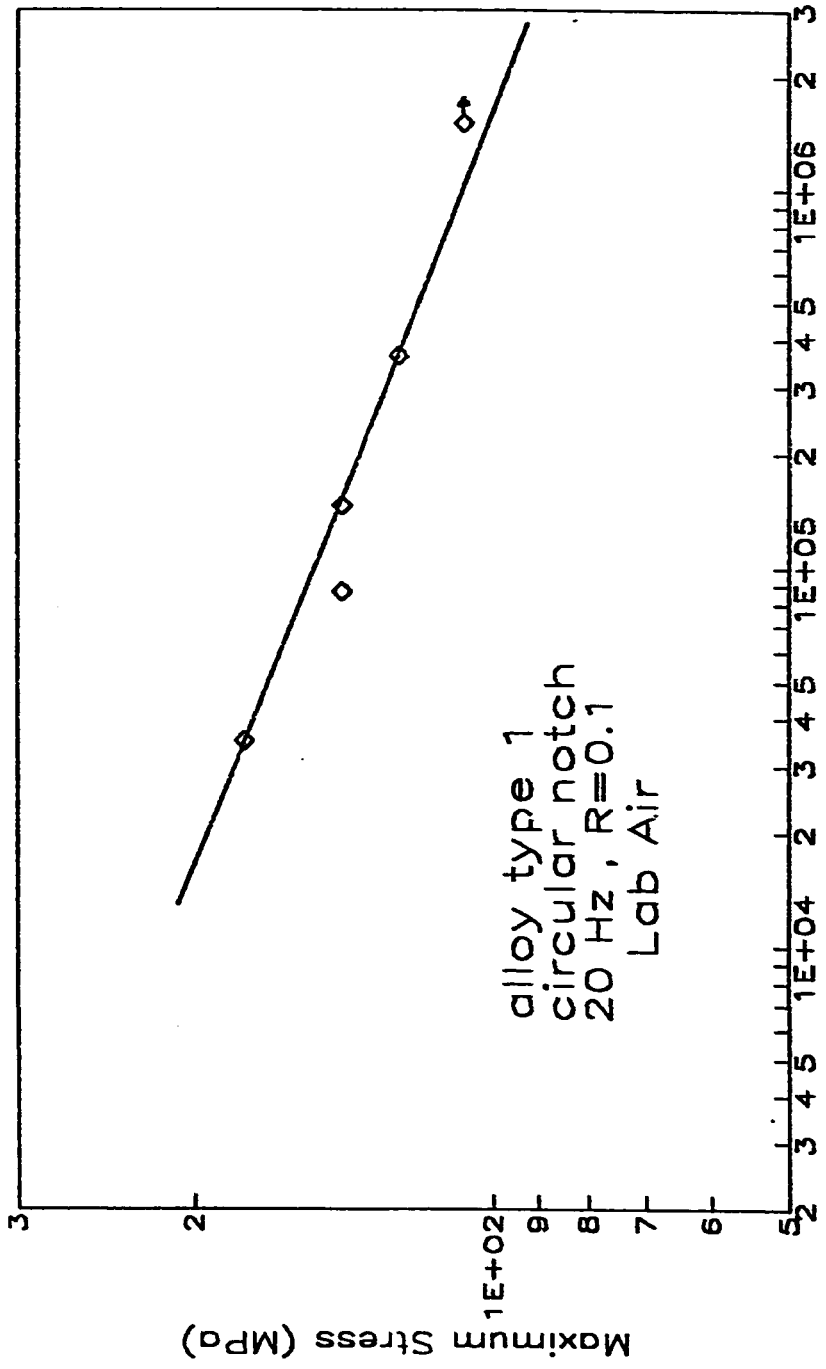

Fig. 5.11 Constant amplitude circular notched specimen experimental results

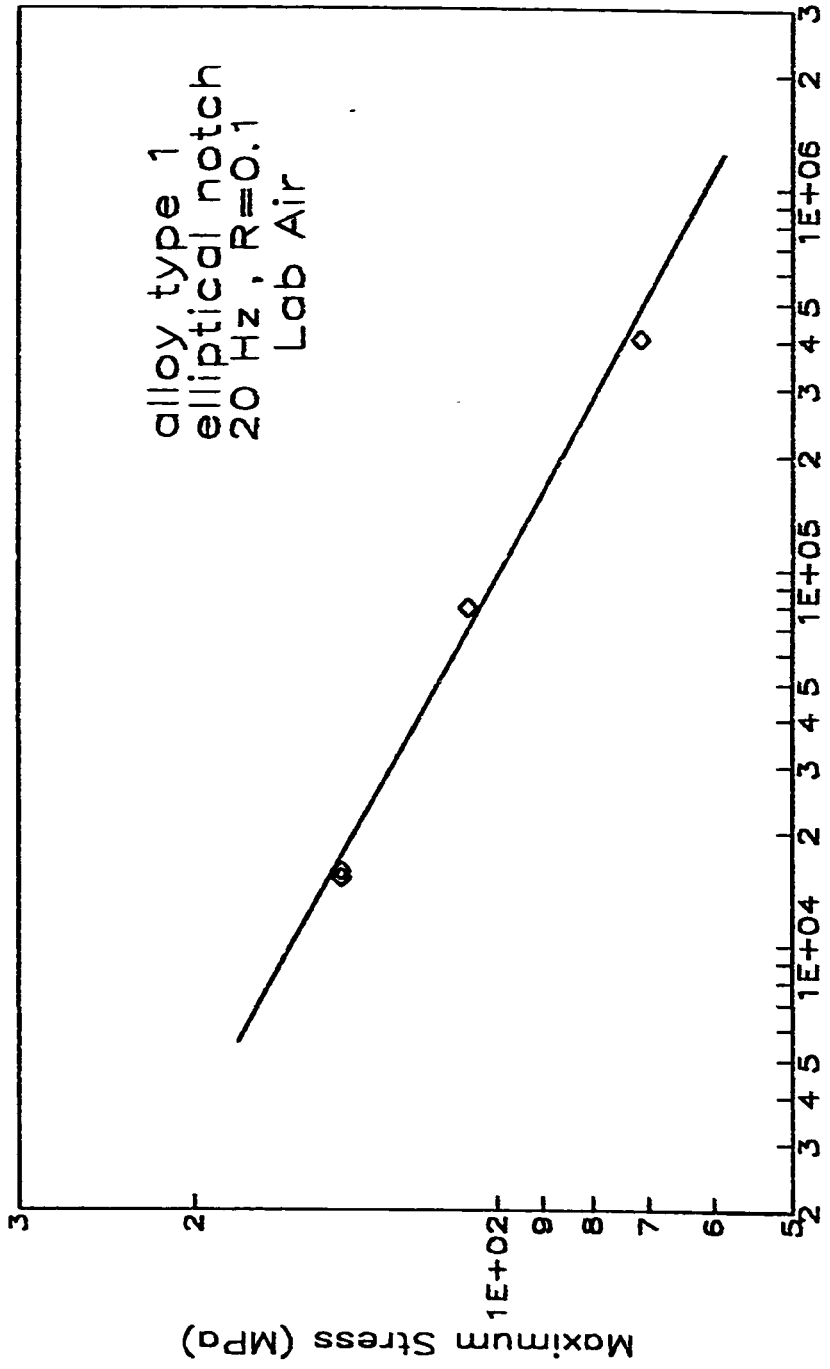

Fig. 5.12 Constant amplitude elliptical notched specimen experimental results

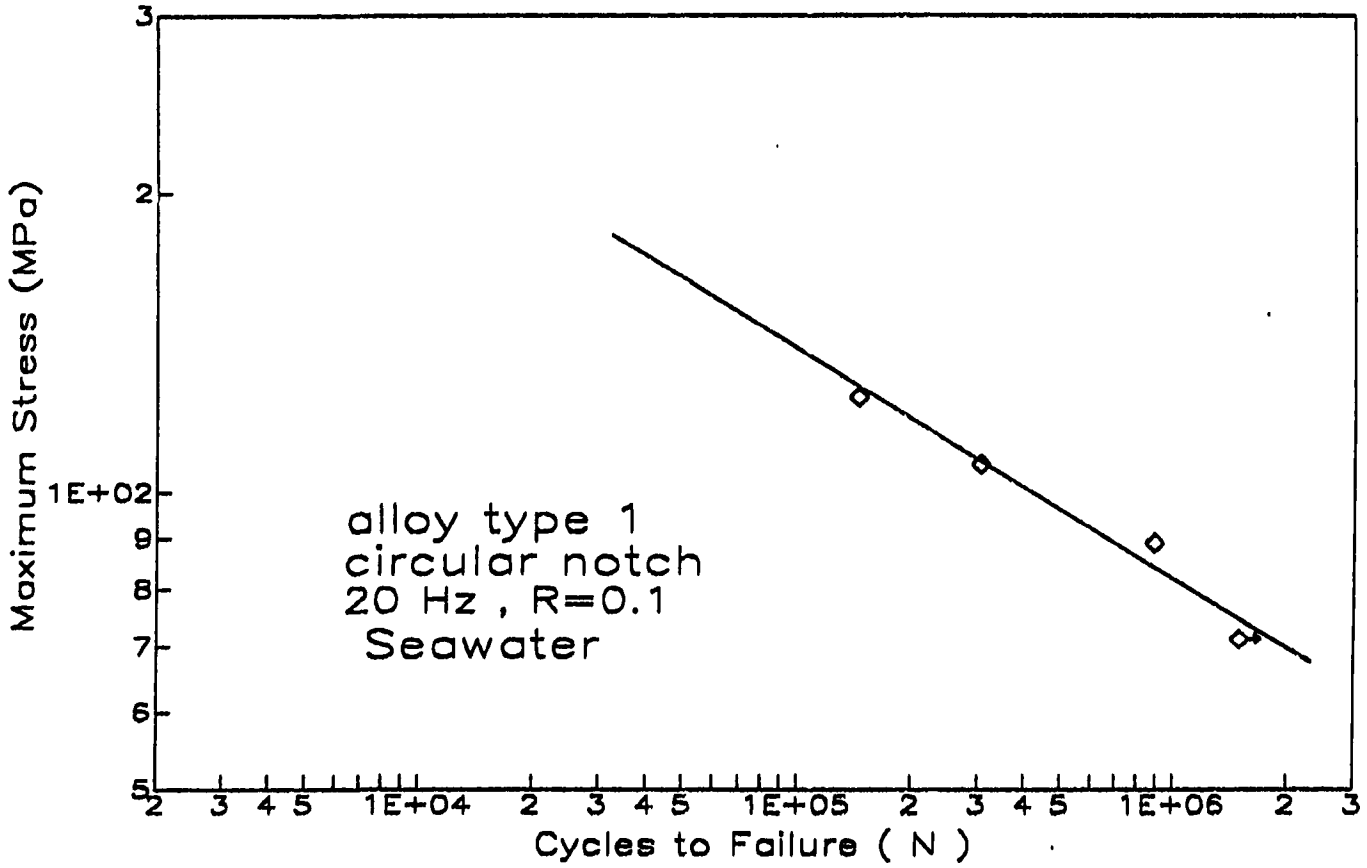

Fig. 5.13 Constant amplitude circular notched specimen experimental results

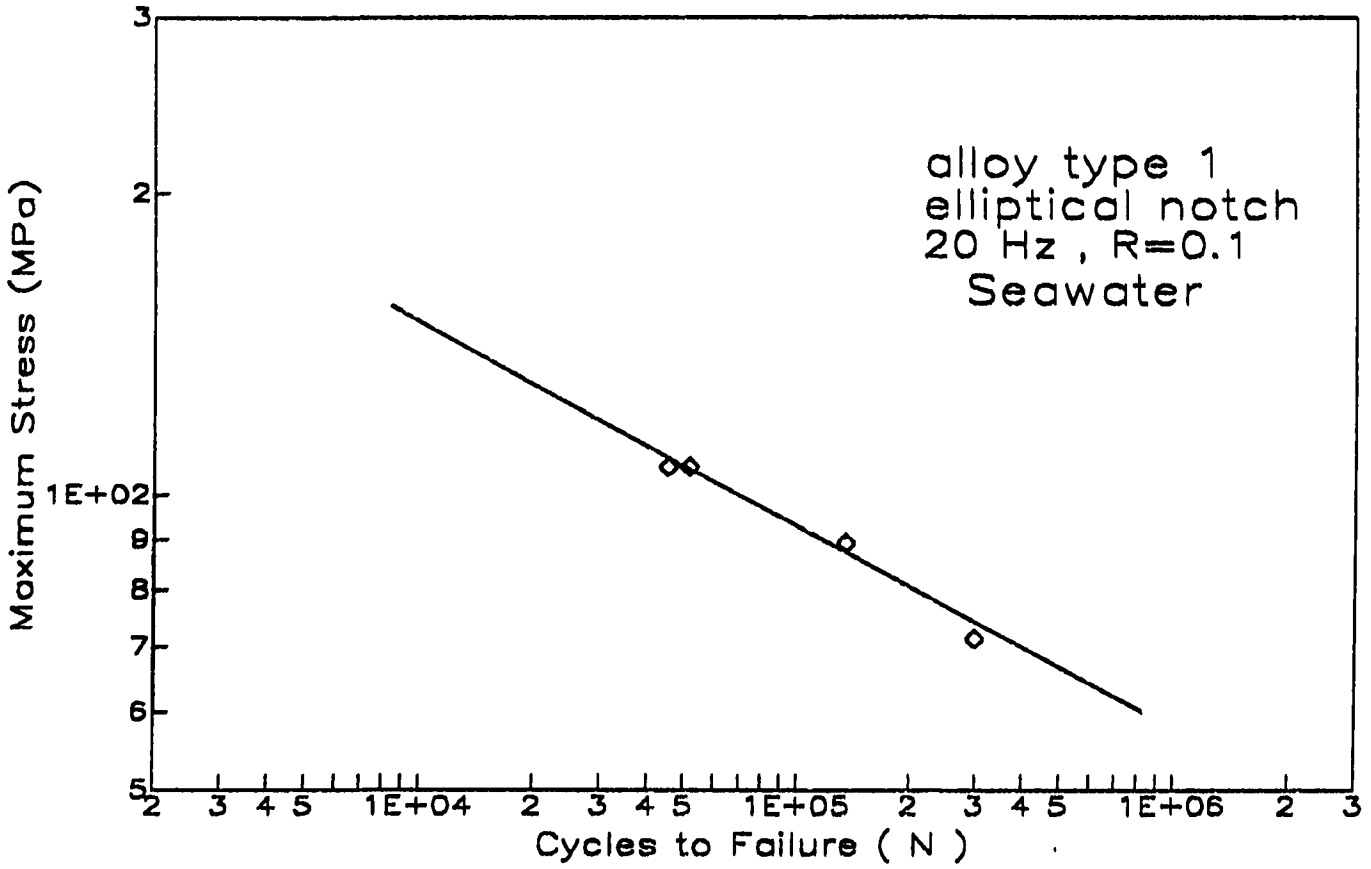

Fig. 5.14 Constant amplitude elliptical notched specimen experimental results

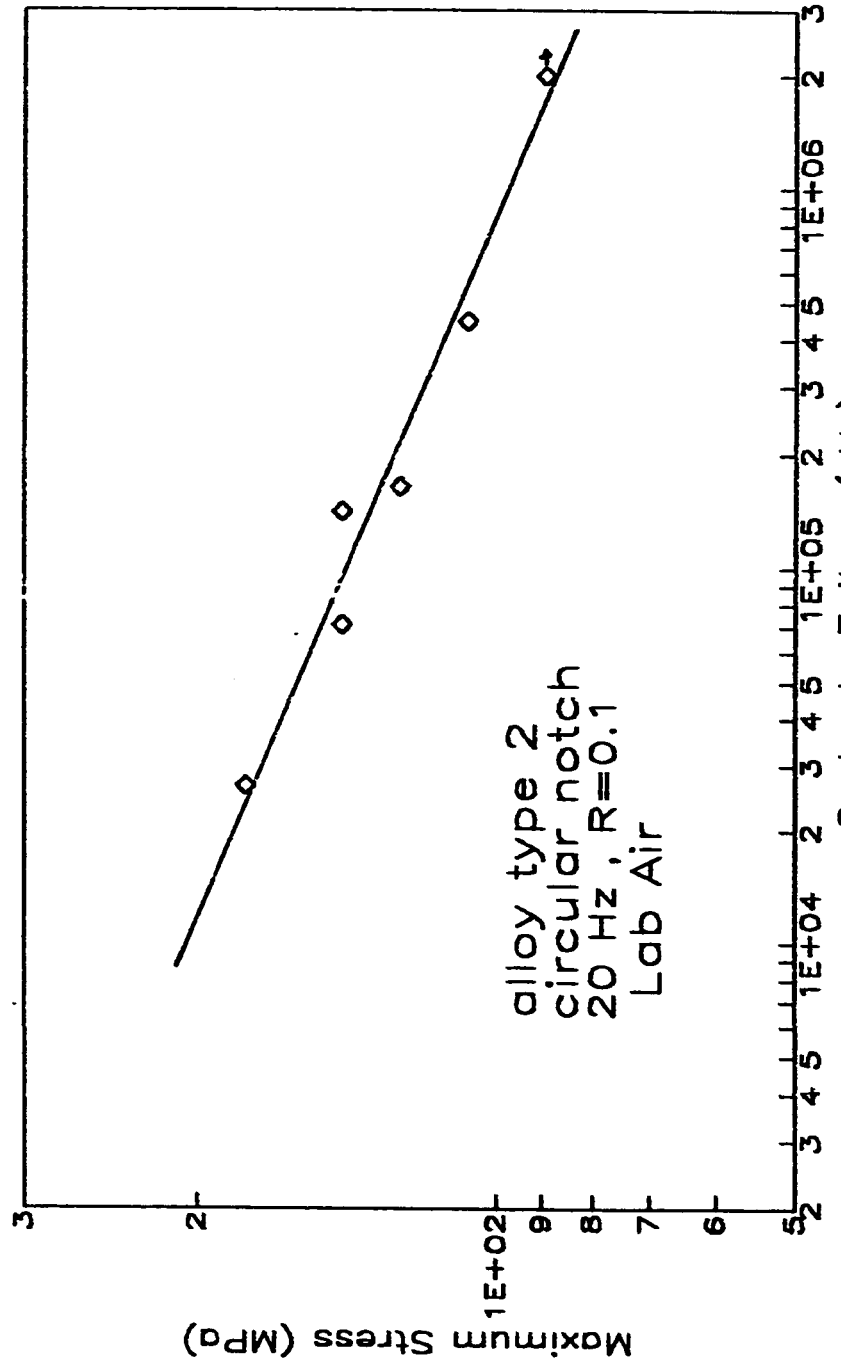

Fig. 5.15 Constant amplitude circular notched specimen experimental results

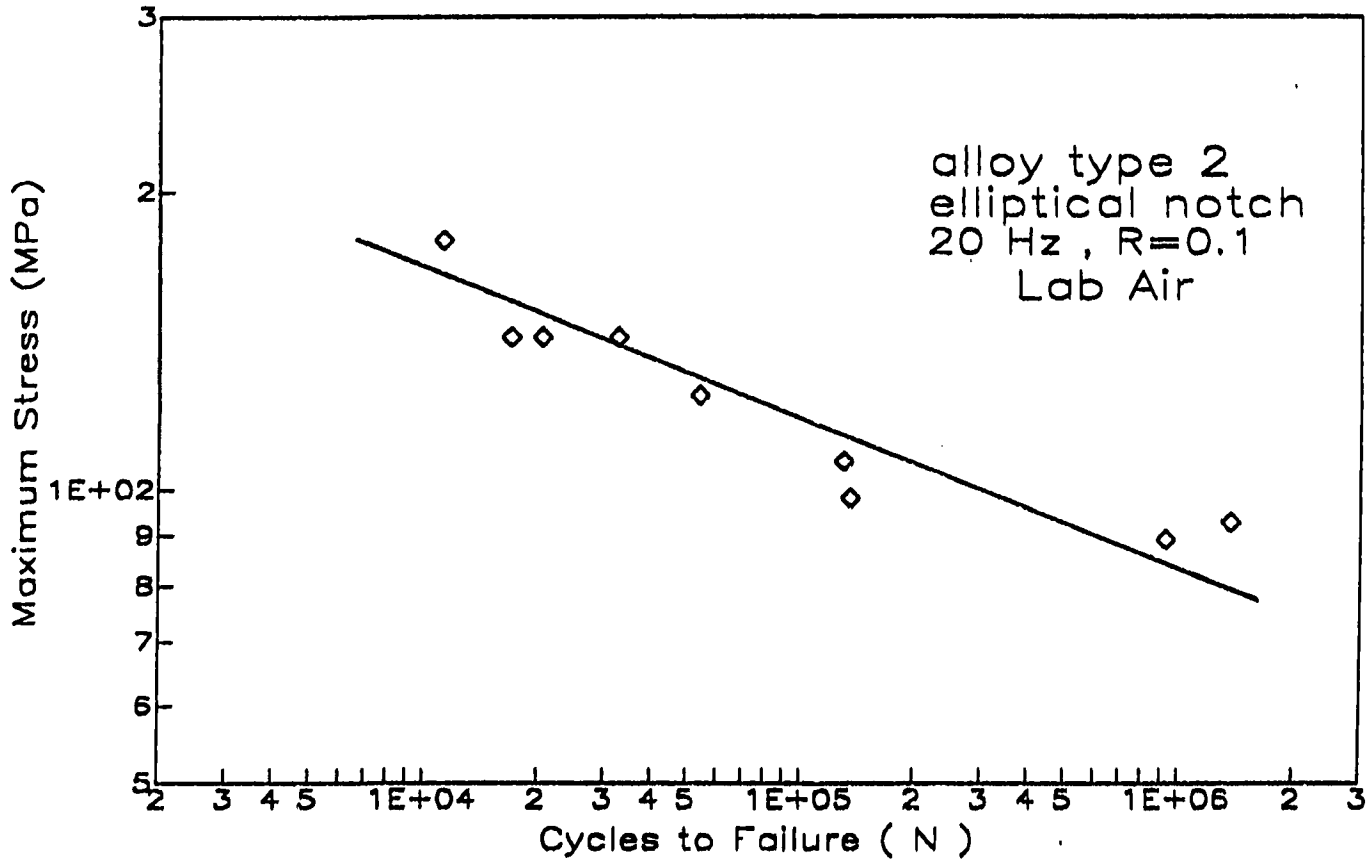

Fig. 5.16 Constant amplitude elliptical notched specimen experimental results

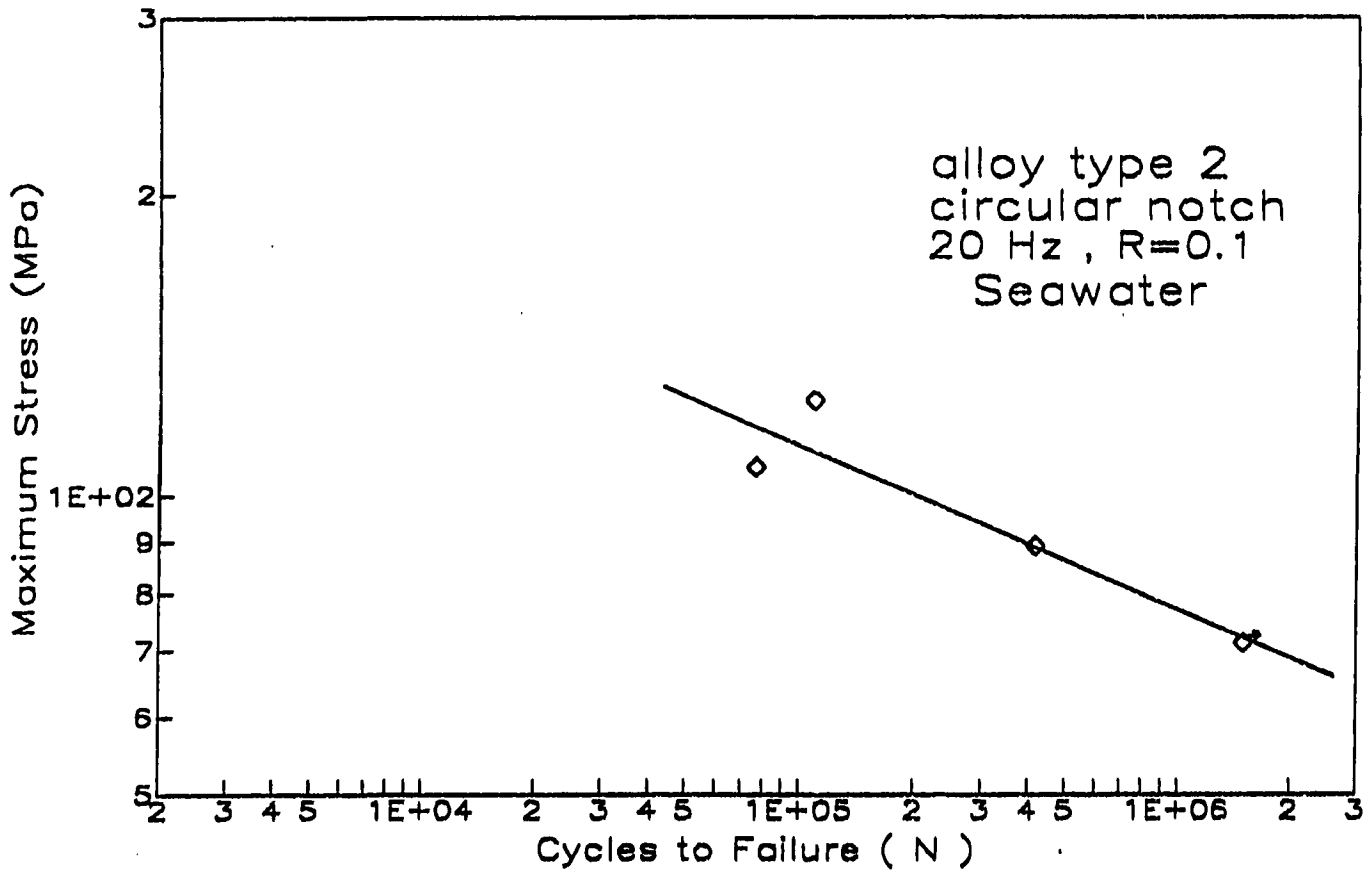

Fig. 5.17 Constant amplitude circular notched specimen experimental results

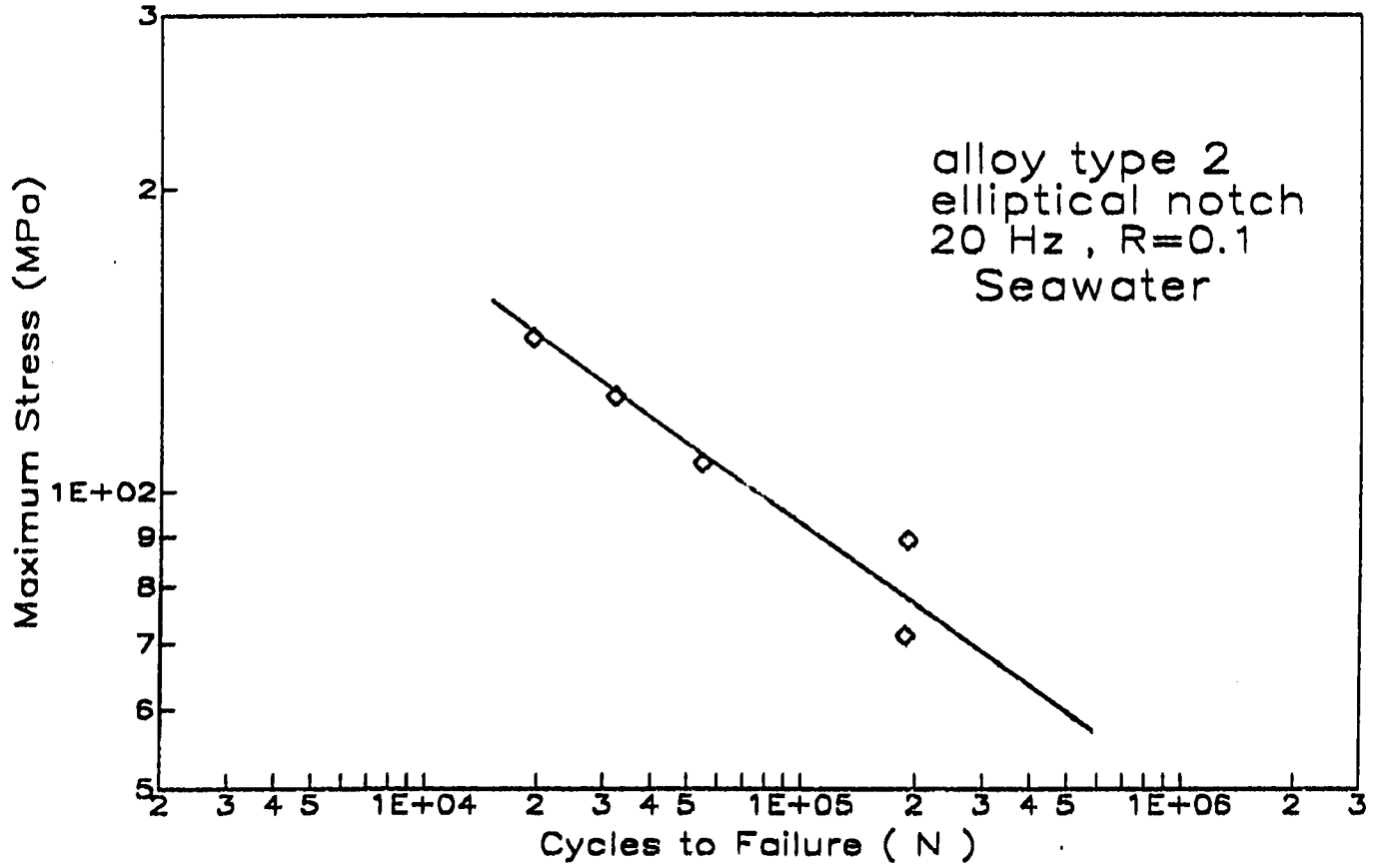

Fig. 5.18 Constant amplitude elliptical notched specimen experimental results

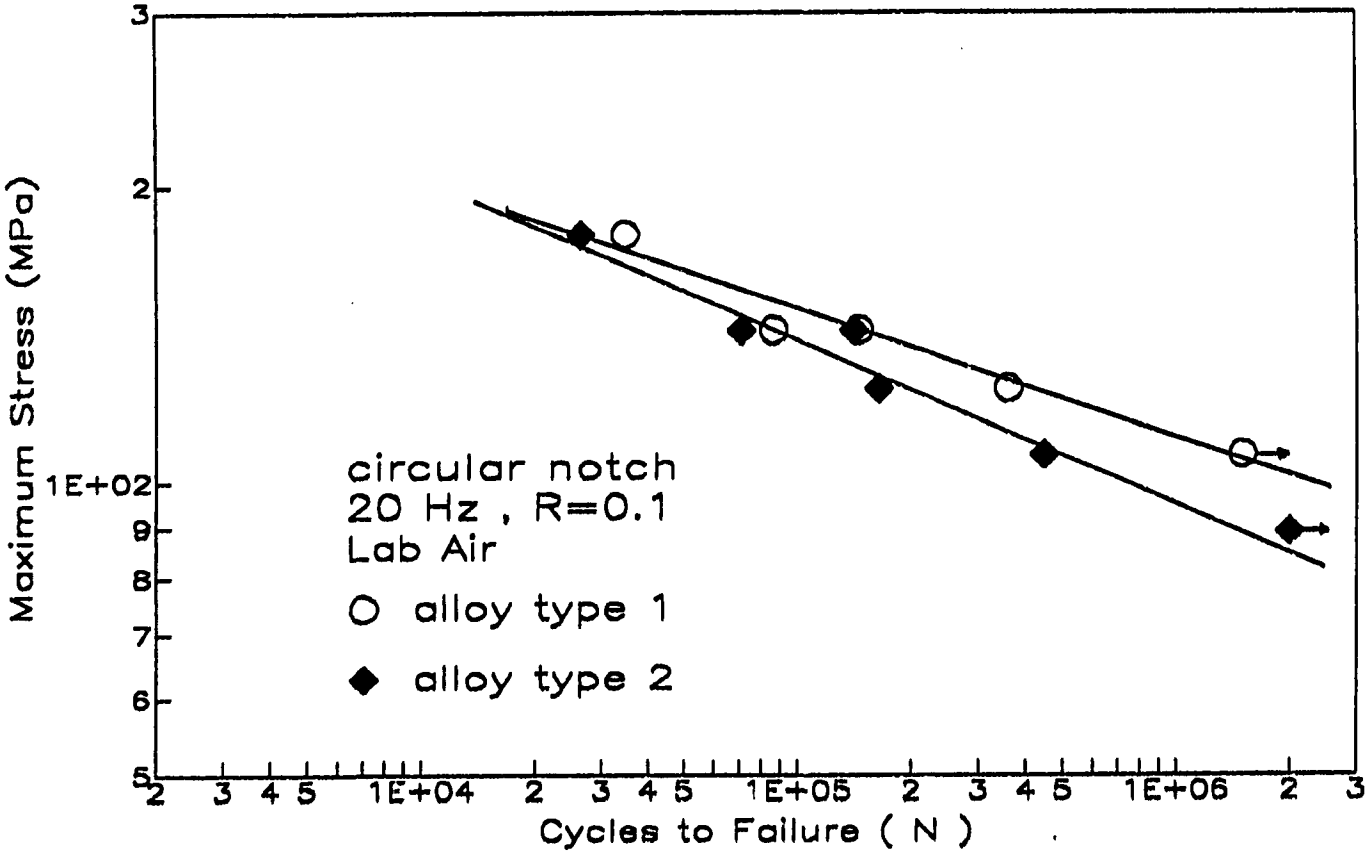

Fig. 6.1 Comparison of circular notched specimens in air

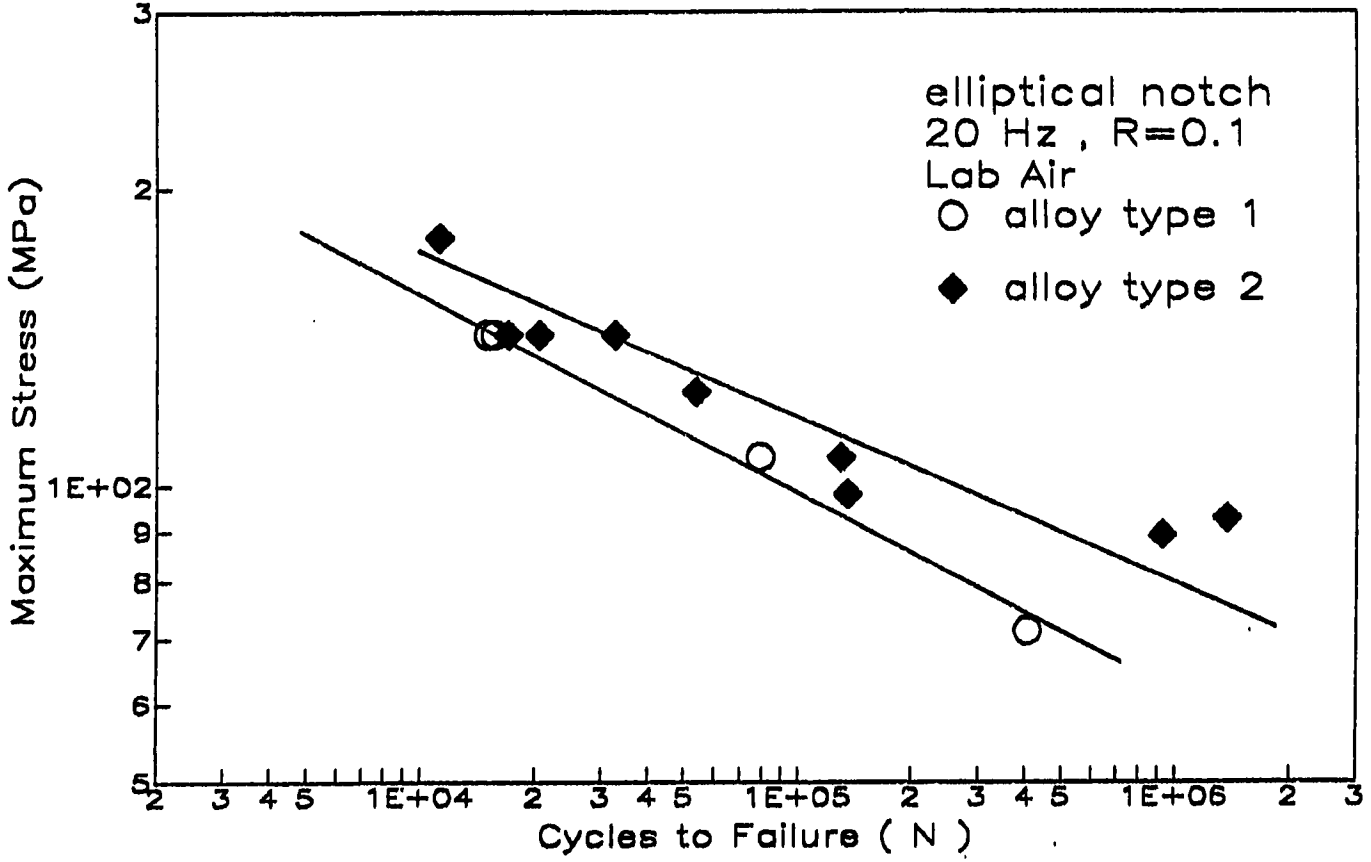

Fig. 6.2 Comparison of elliptical notched specimens in air

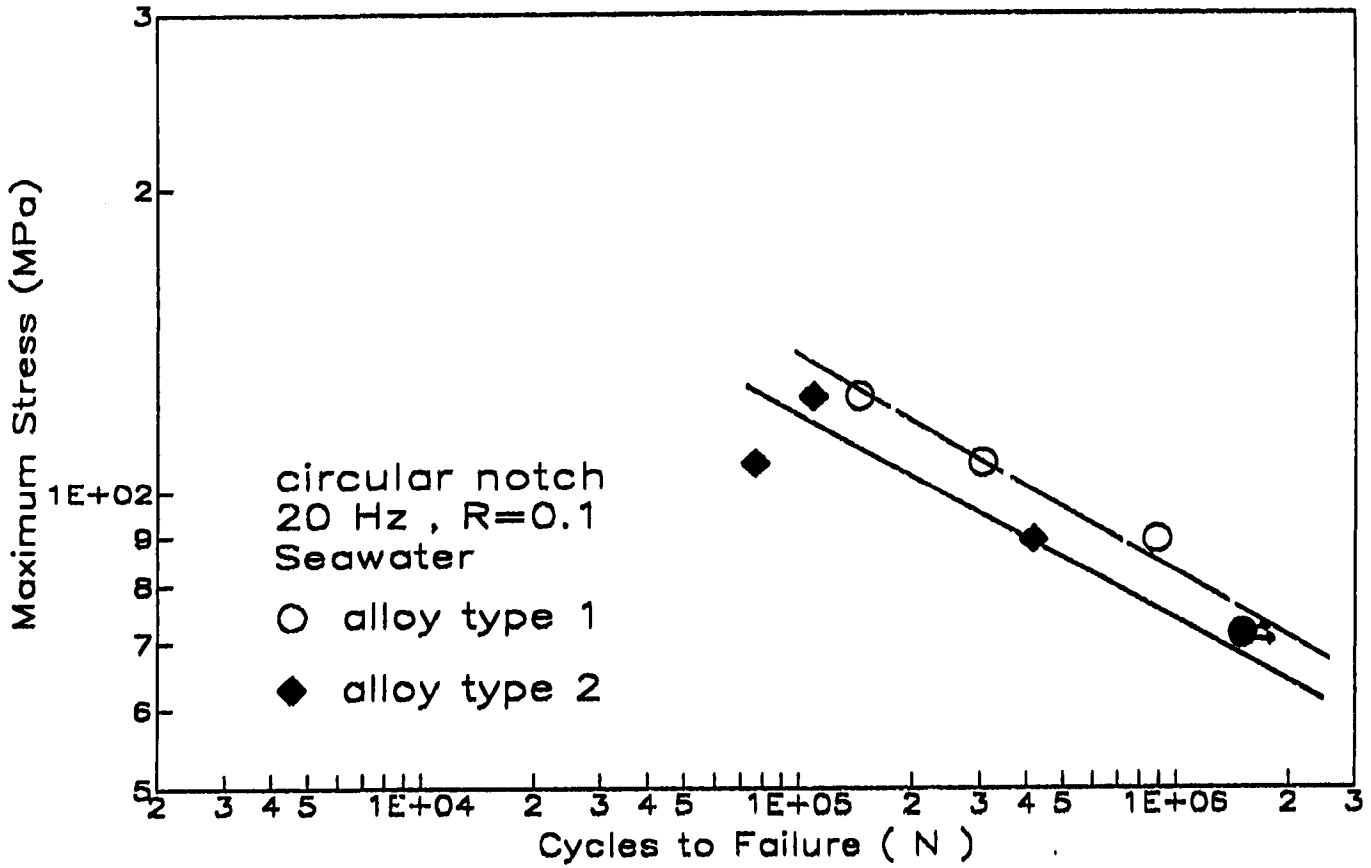

Fig. 6.3 Comparison of circular notched specimens in seawater

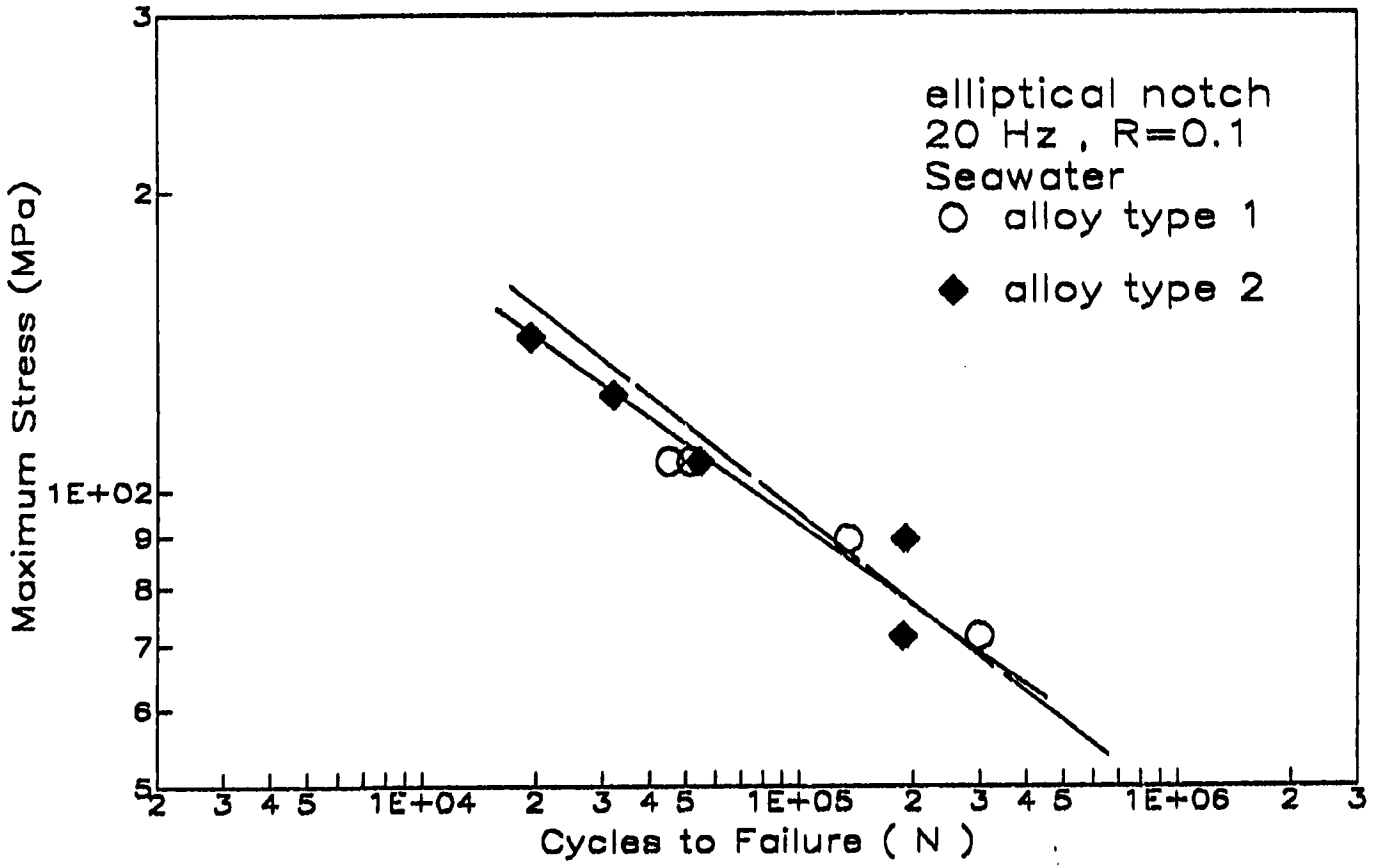

Fig. 6.4 Comparison of elliptical notched specimens in seawater

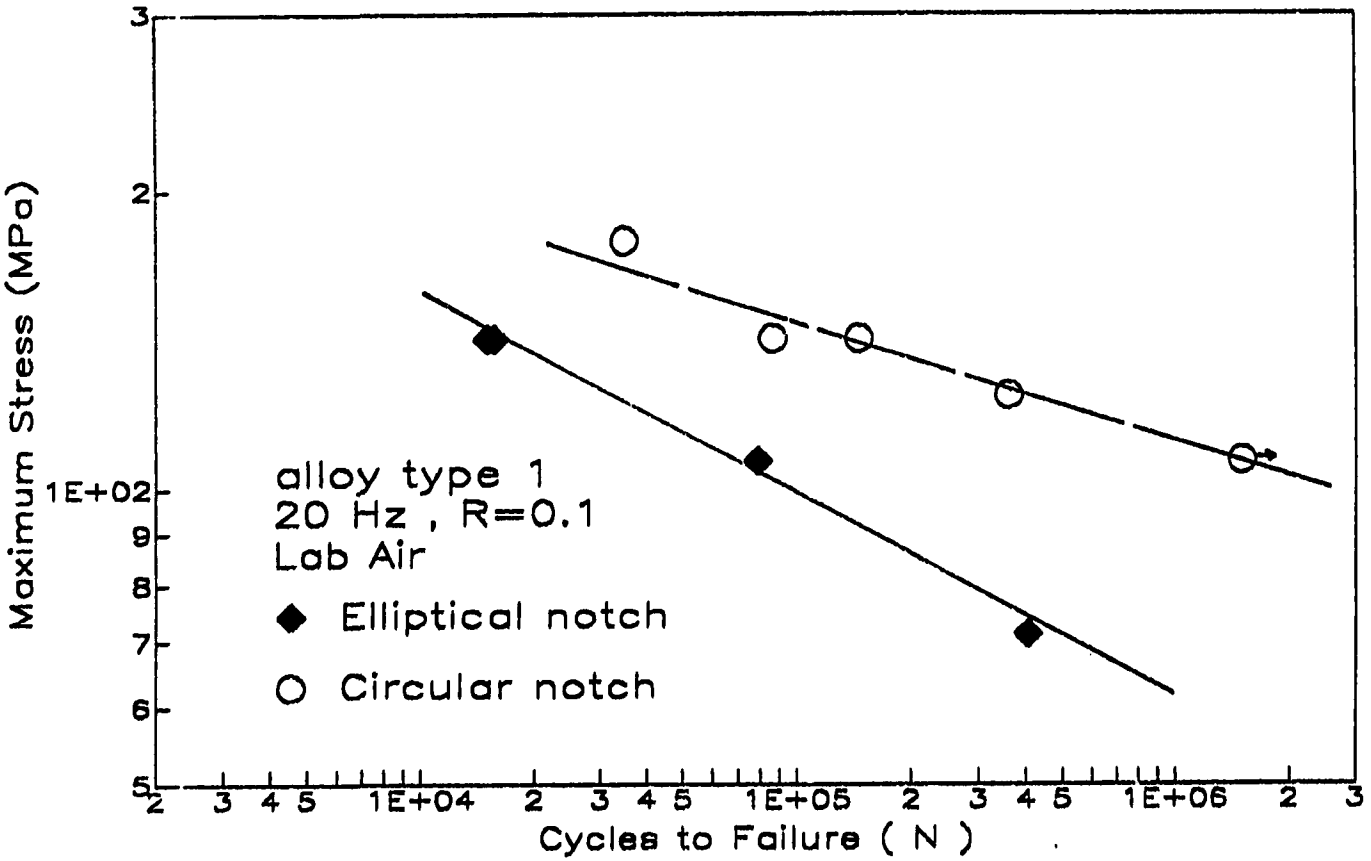

Fig. 6.5 Notch effects on alloy type 1 in air

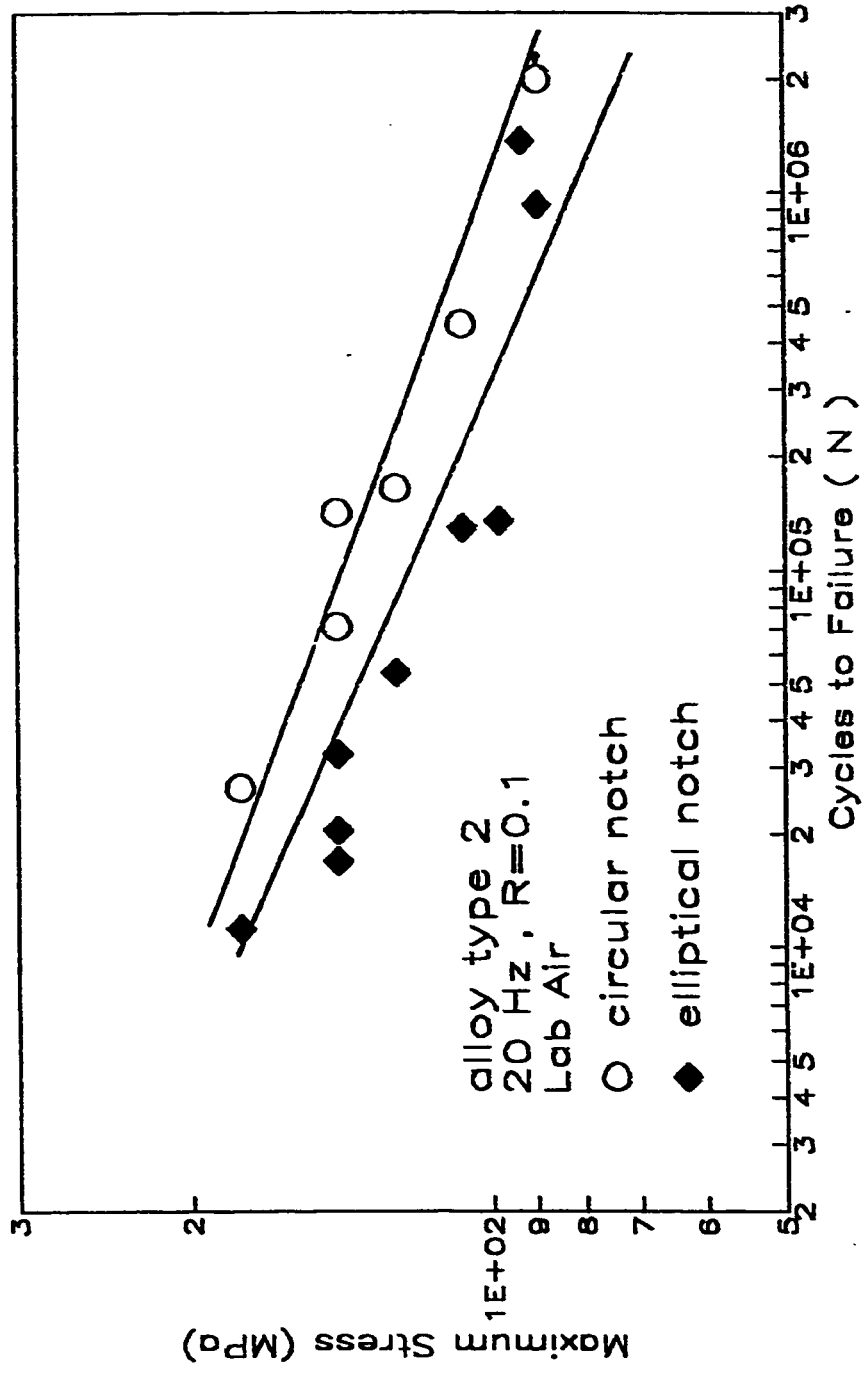

Fig. 6.6 Notch effects on alloy type 2 in air

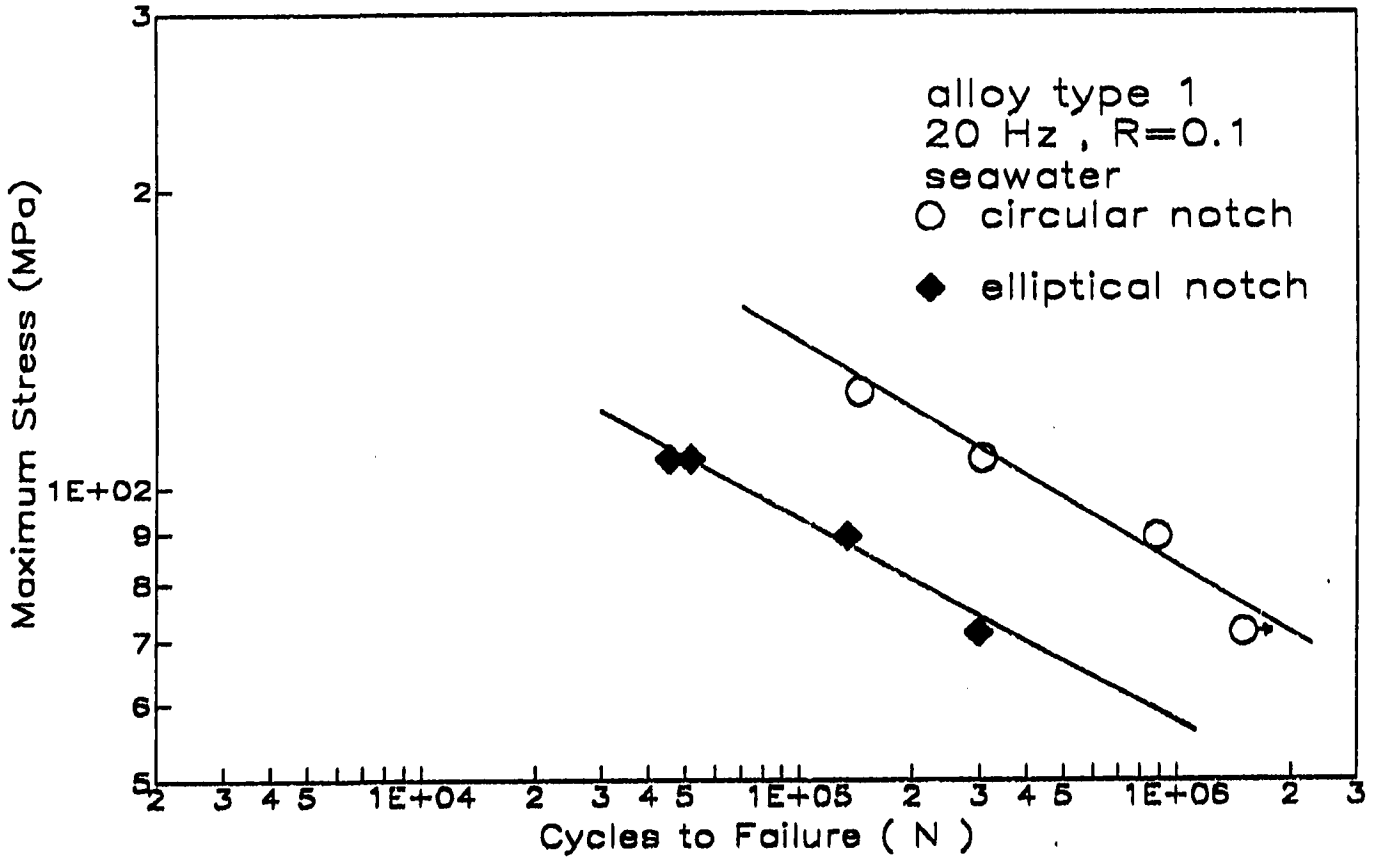

Fig. 6.7 Notch effects on alloy type 1 in seawater

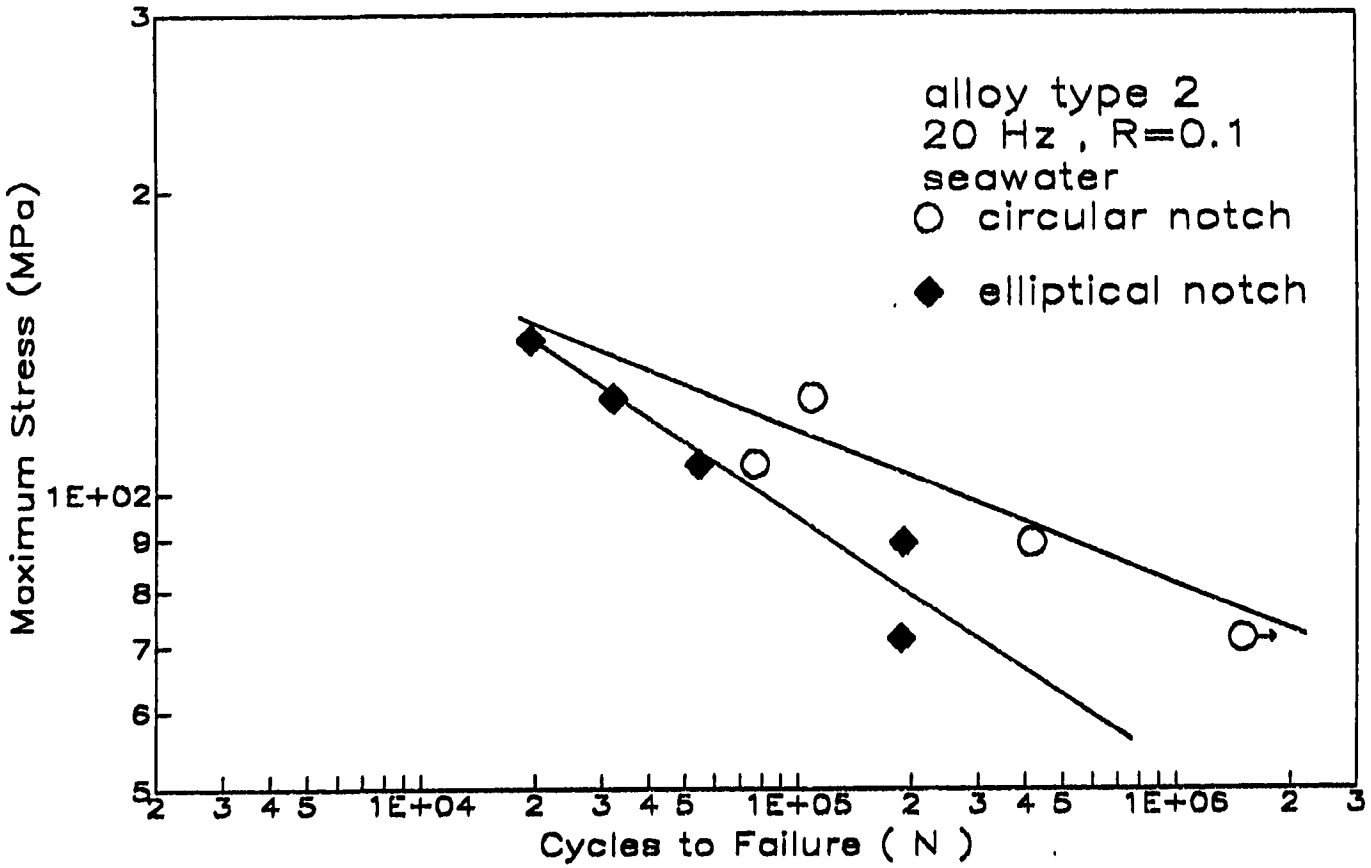

Fig. 6.8 Notch effects on alloy type 2 in seawater

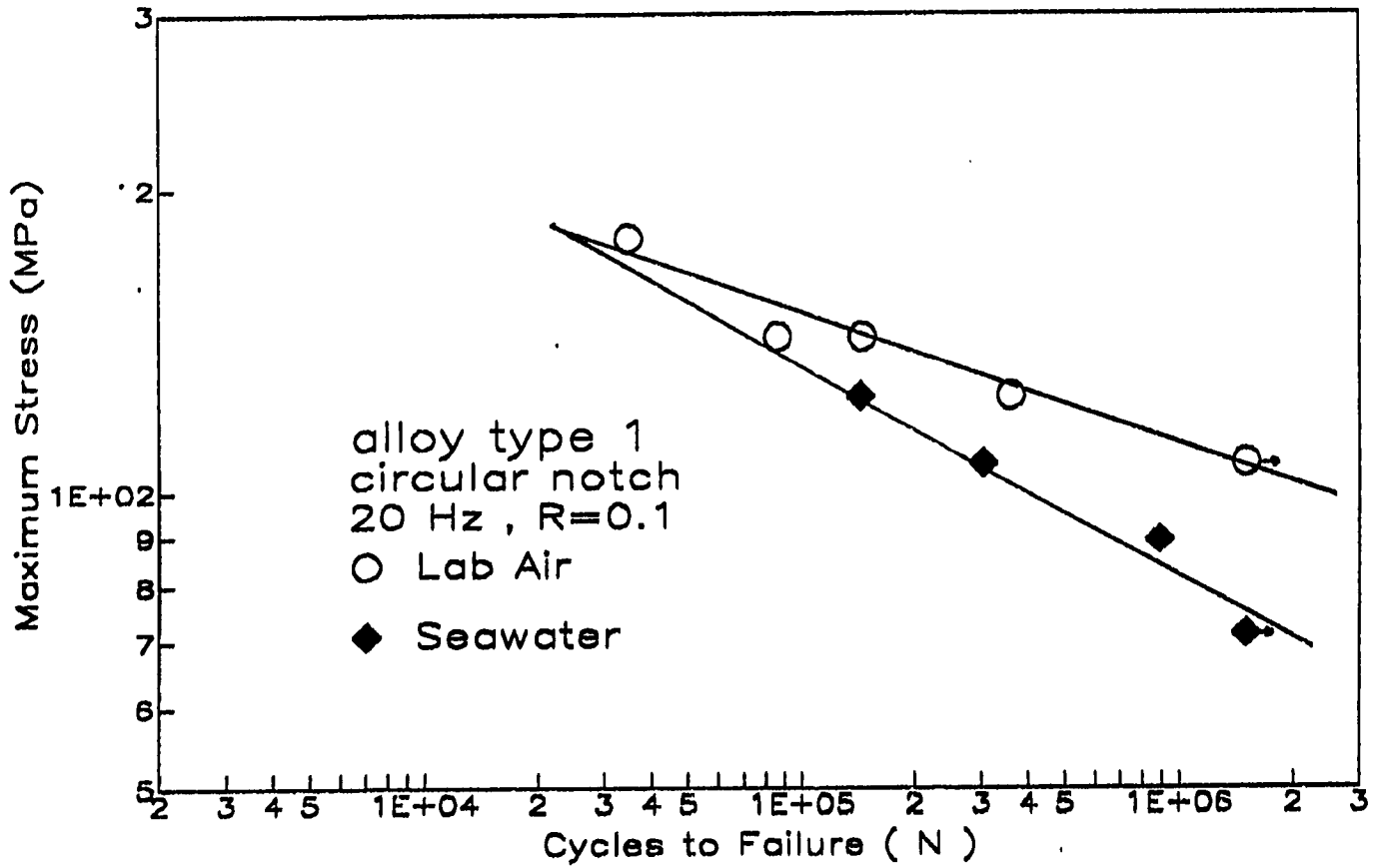

Fig. 6.9 Effects of environment on circular notch

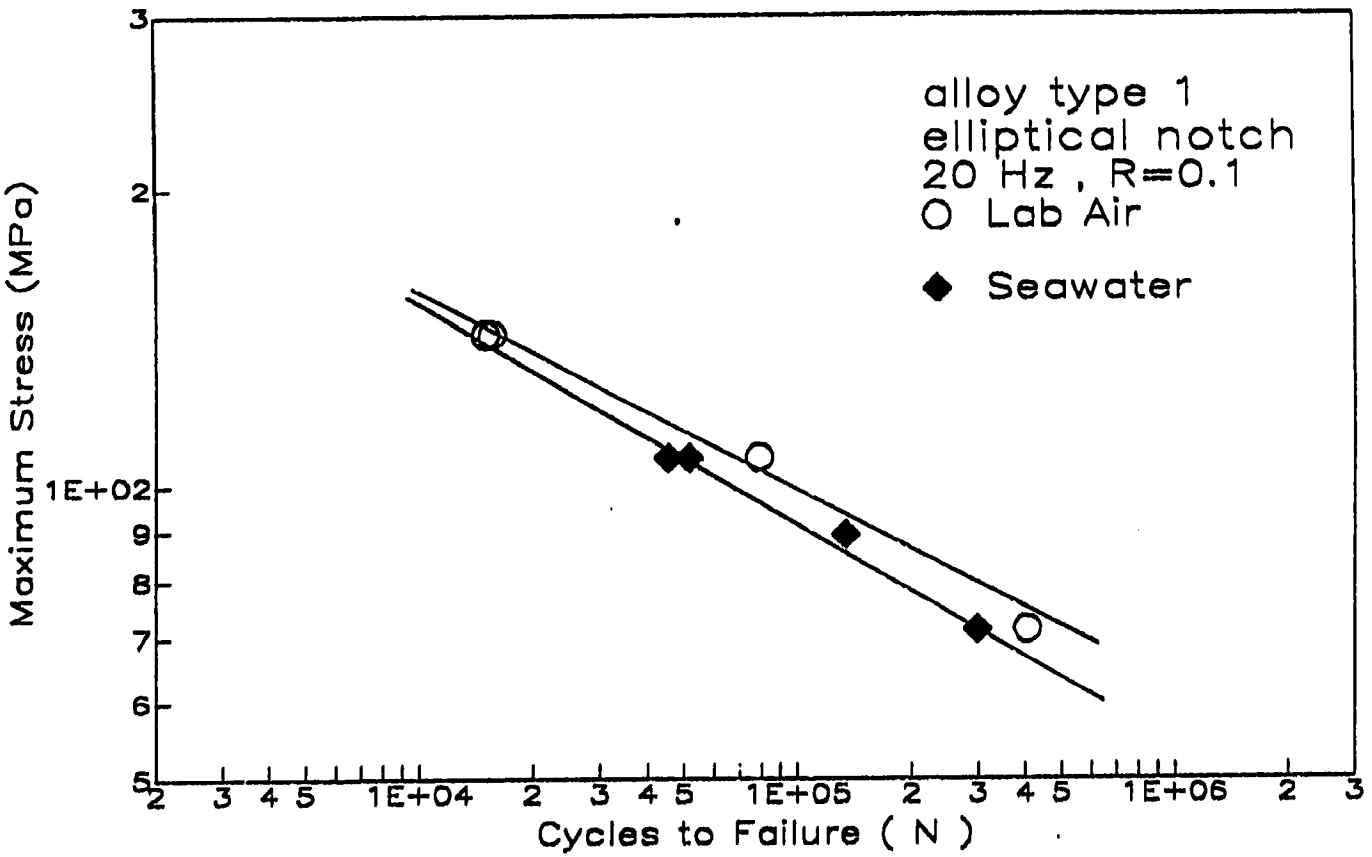

Fig. 6.10 Effects of environment on elliptical notch

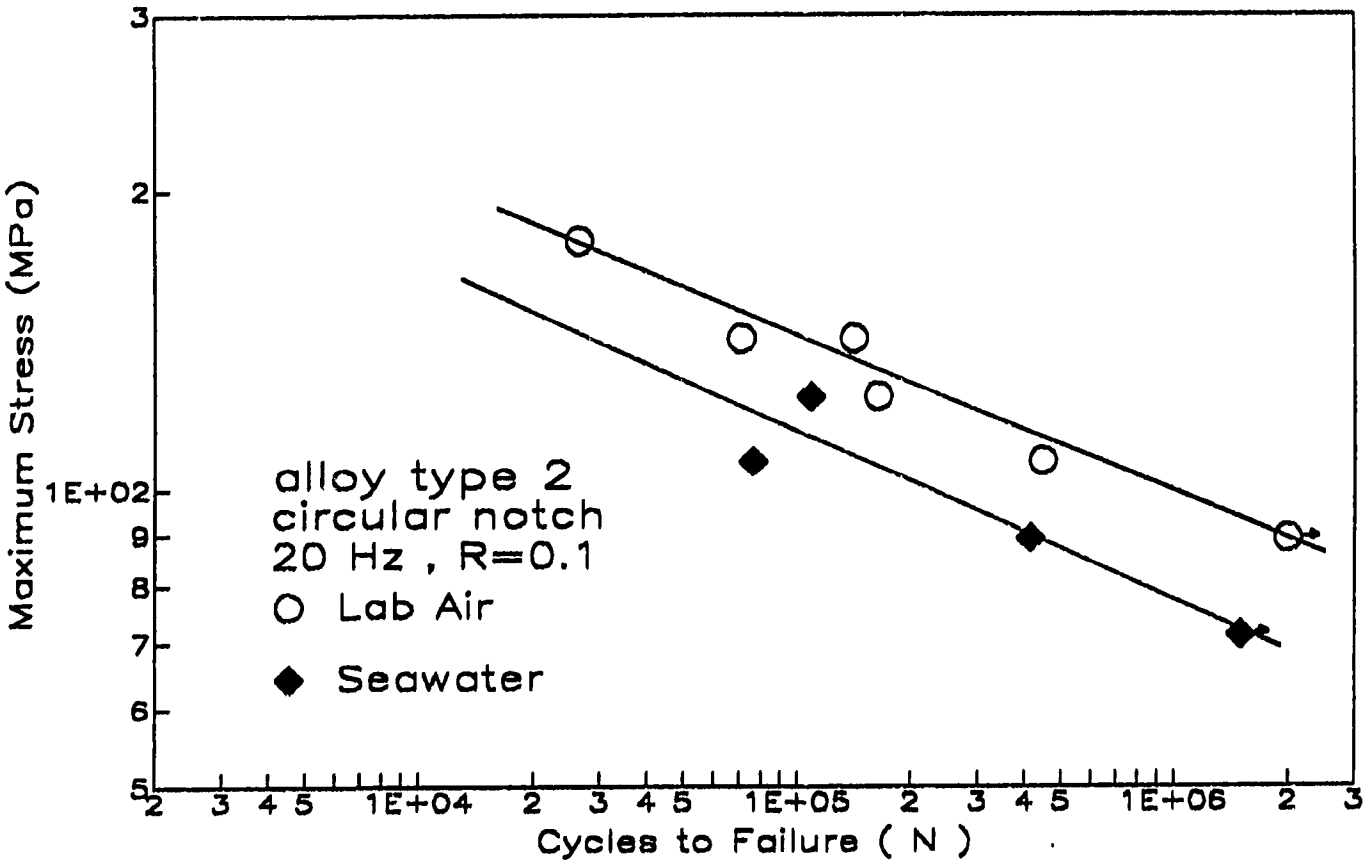

Fig. 6.11 Effects of environment on circular notch

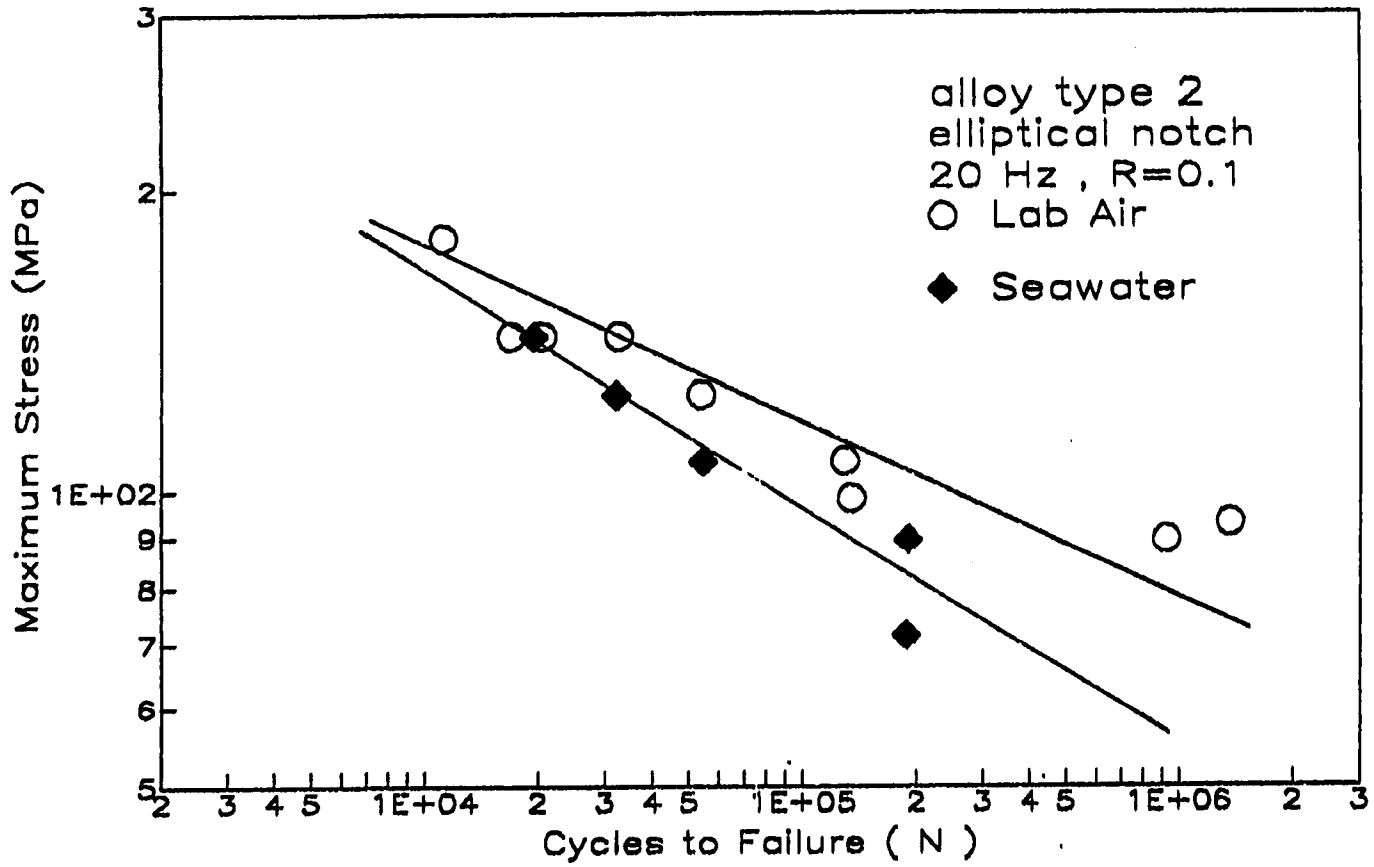

Fig. 6.12 Effects of environment on elliptical notch

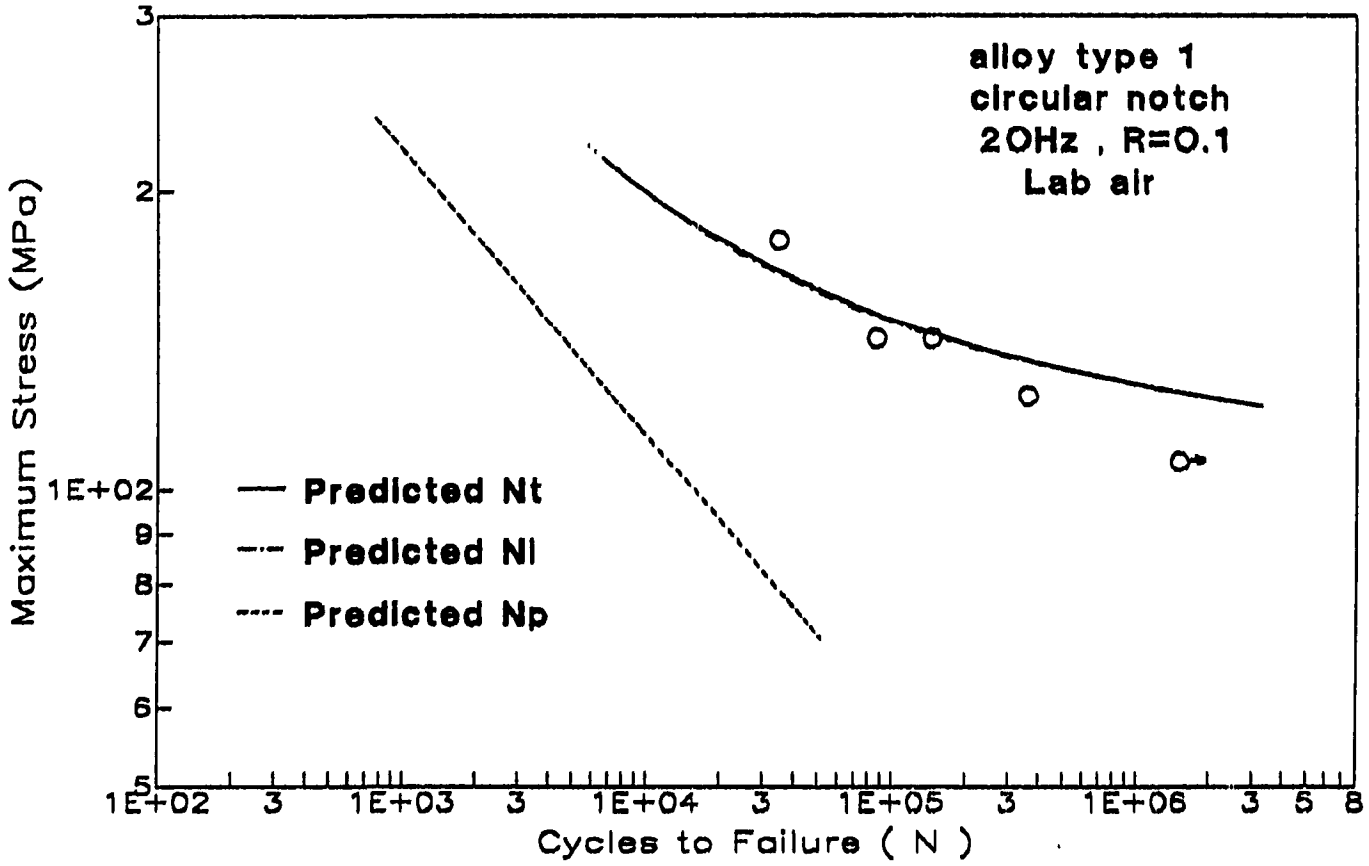

Fig. 6.13 Fatigue life estimates for alloy type 1, circular notch in lab. air

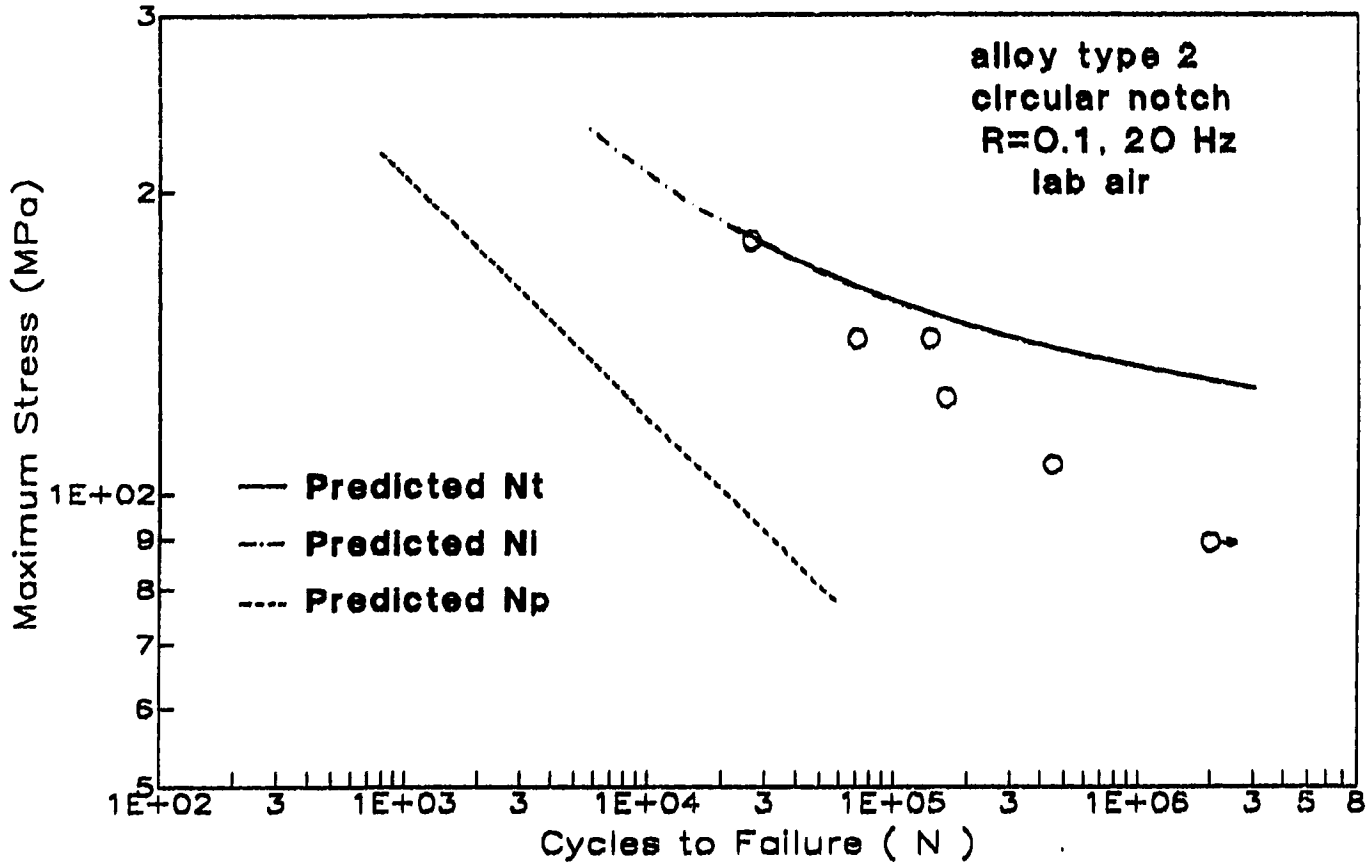

Fig. 6.14 Fatigue life estimates for alloy type 2, circular notch in lab. air

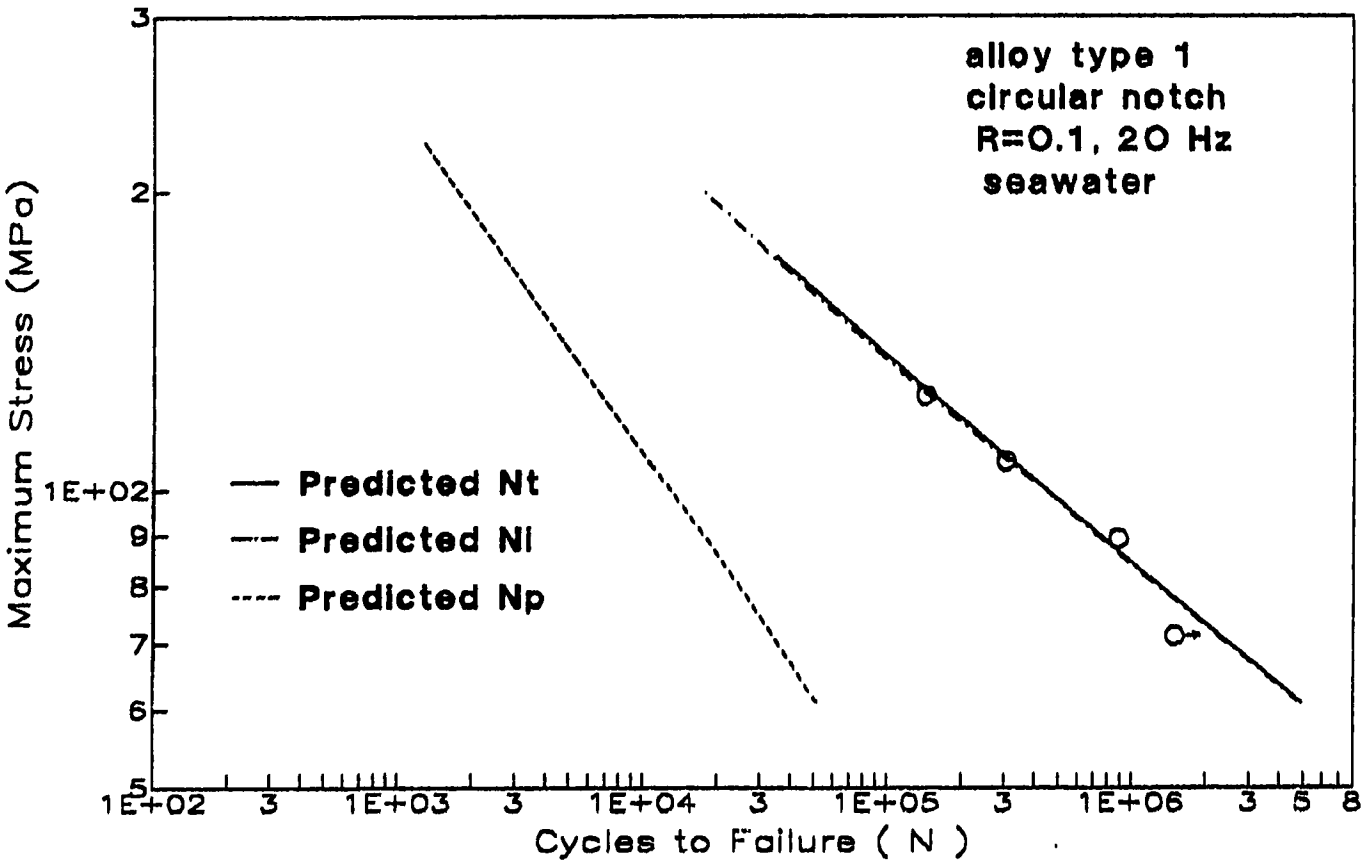

Fig. 6.15 Fatigue life estimates for alloy type 1, circular notch in seawater

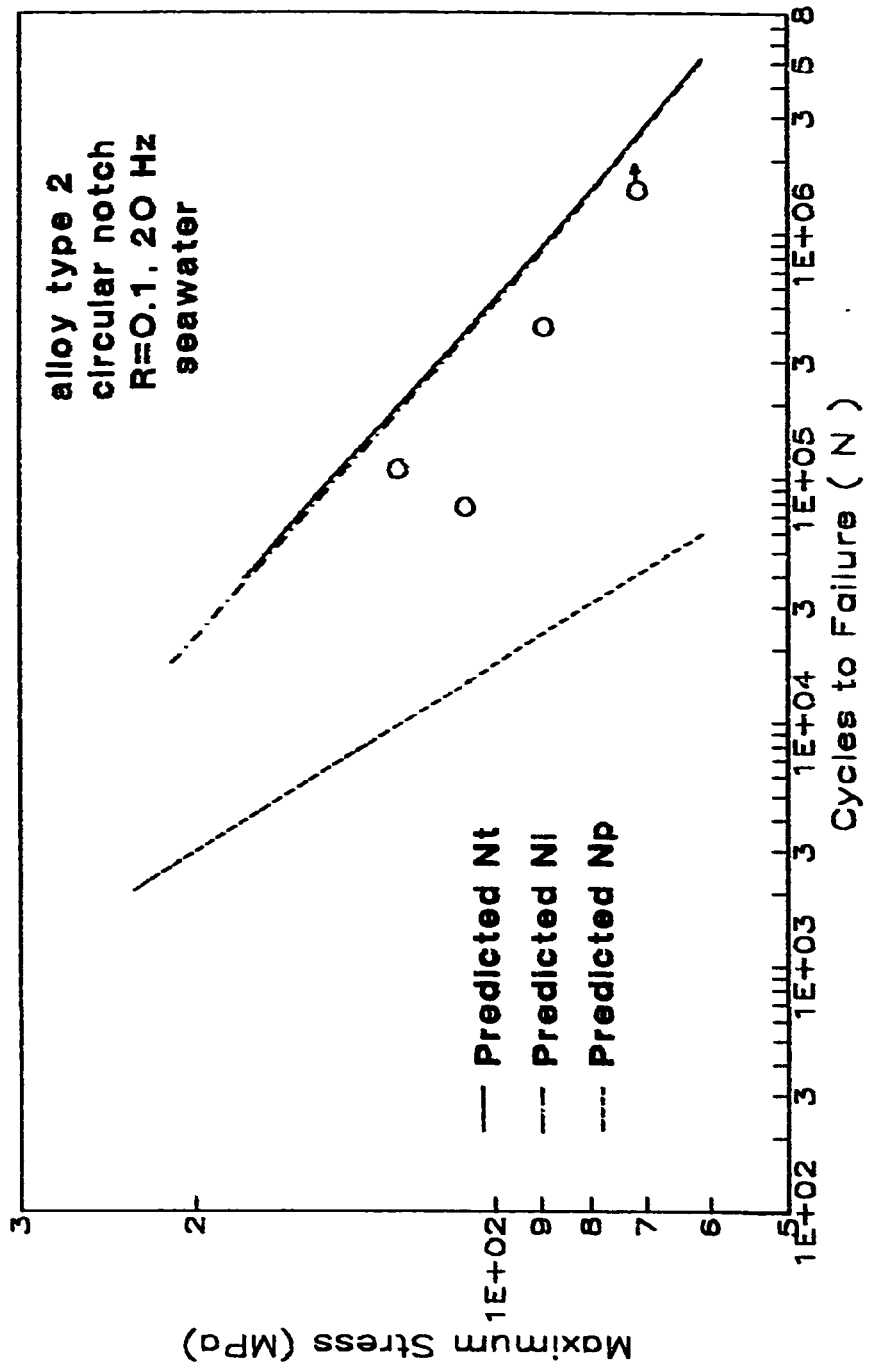

Fig 6.16 Fatigue life estimates for alloy type 2, circular notch in seawater

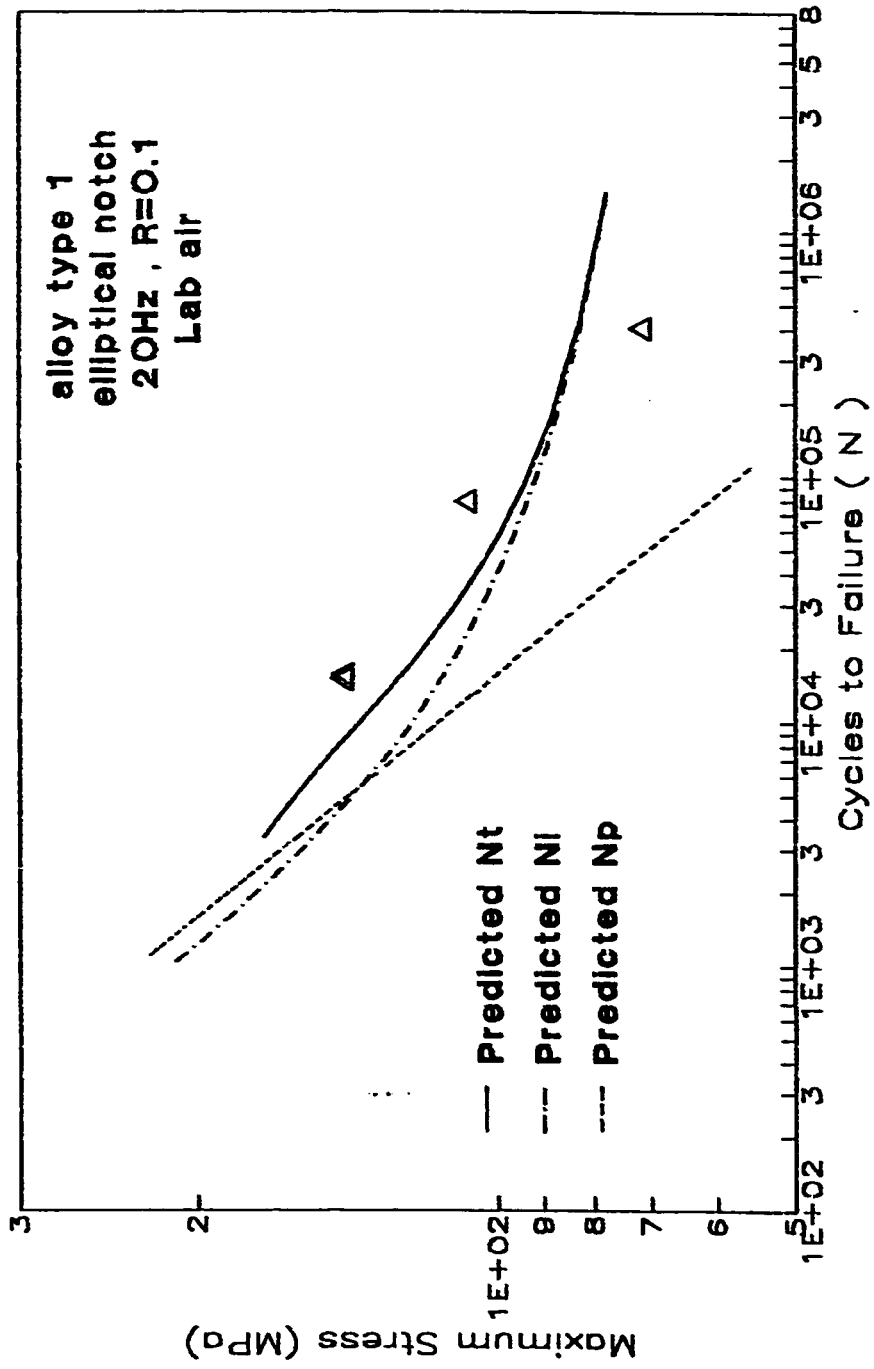

Fig. 6.17 Fatigue life estimates for alloy type 1, elliptical notch in lab. air

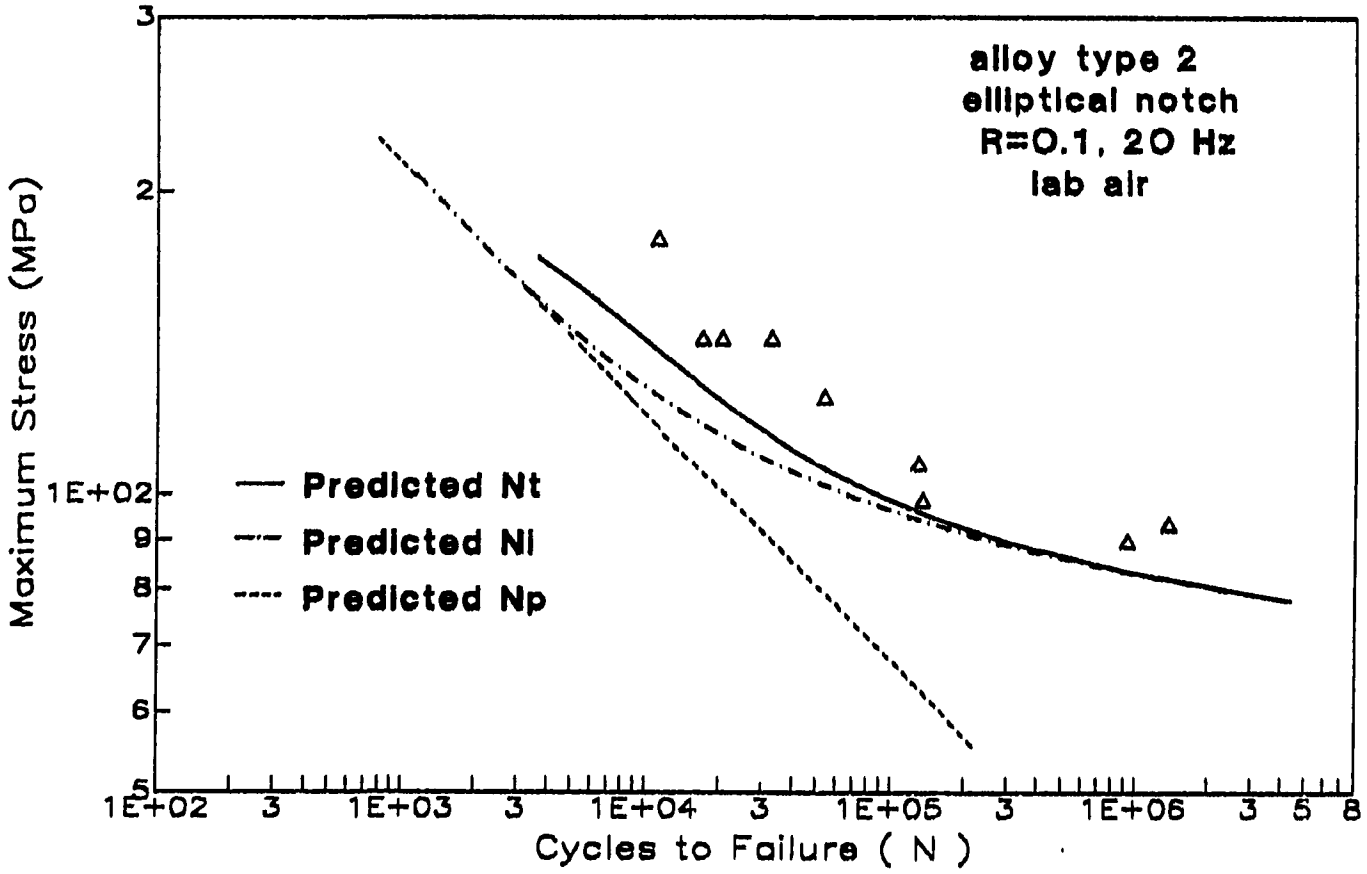

Fig. 6.18 Fatigue life estimates for alloy type 2, elliptical notch in lab. air

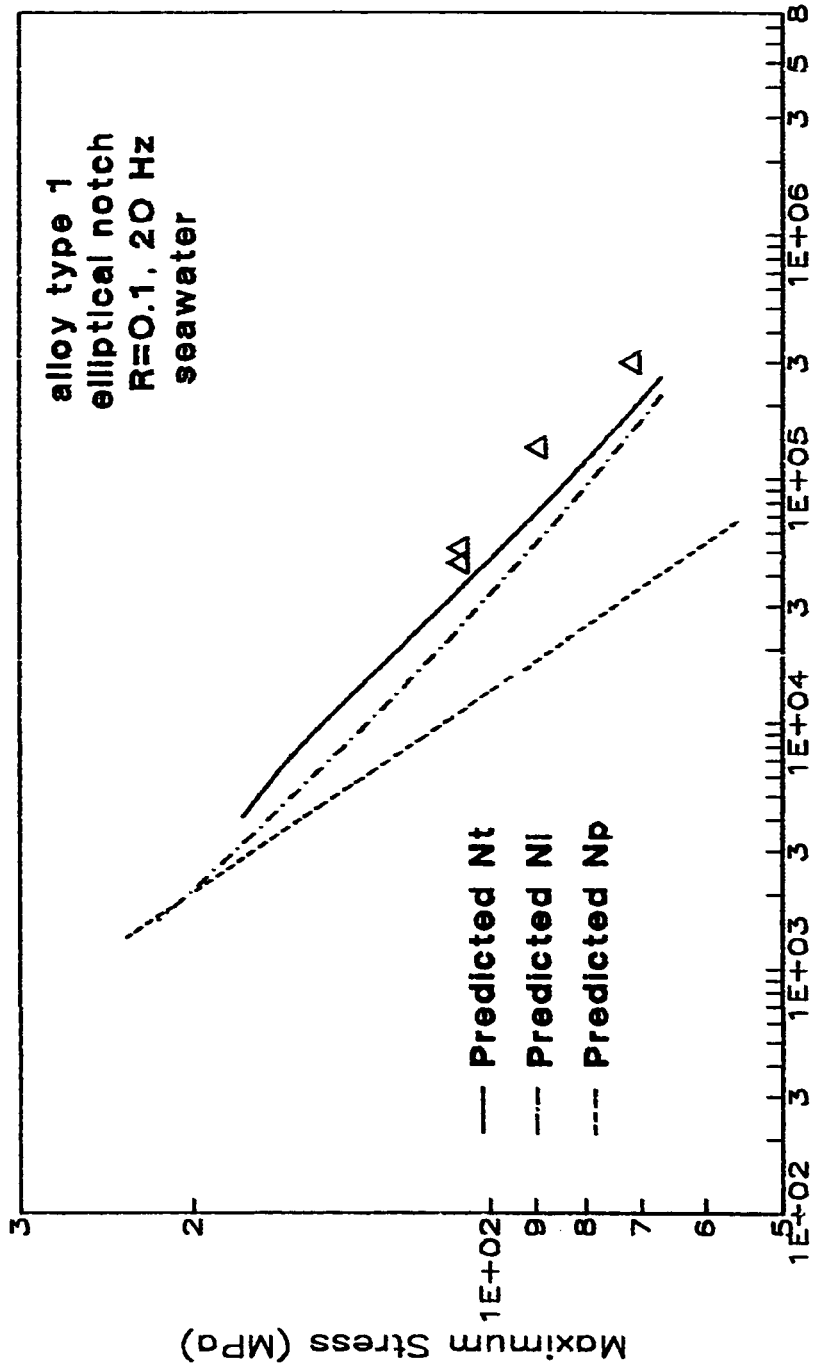

Fig. 6.19 Fatigue life estimates for alloy type 1, elliptical notch in seawater

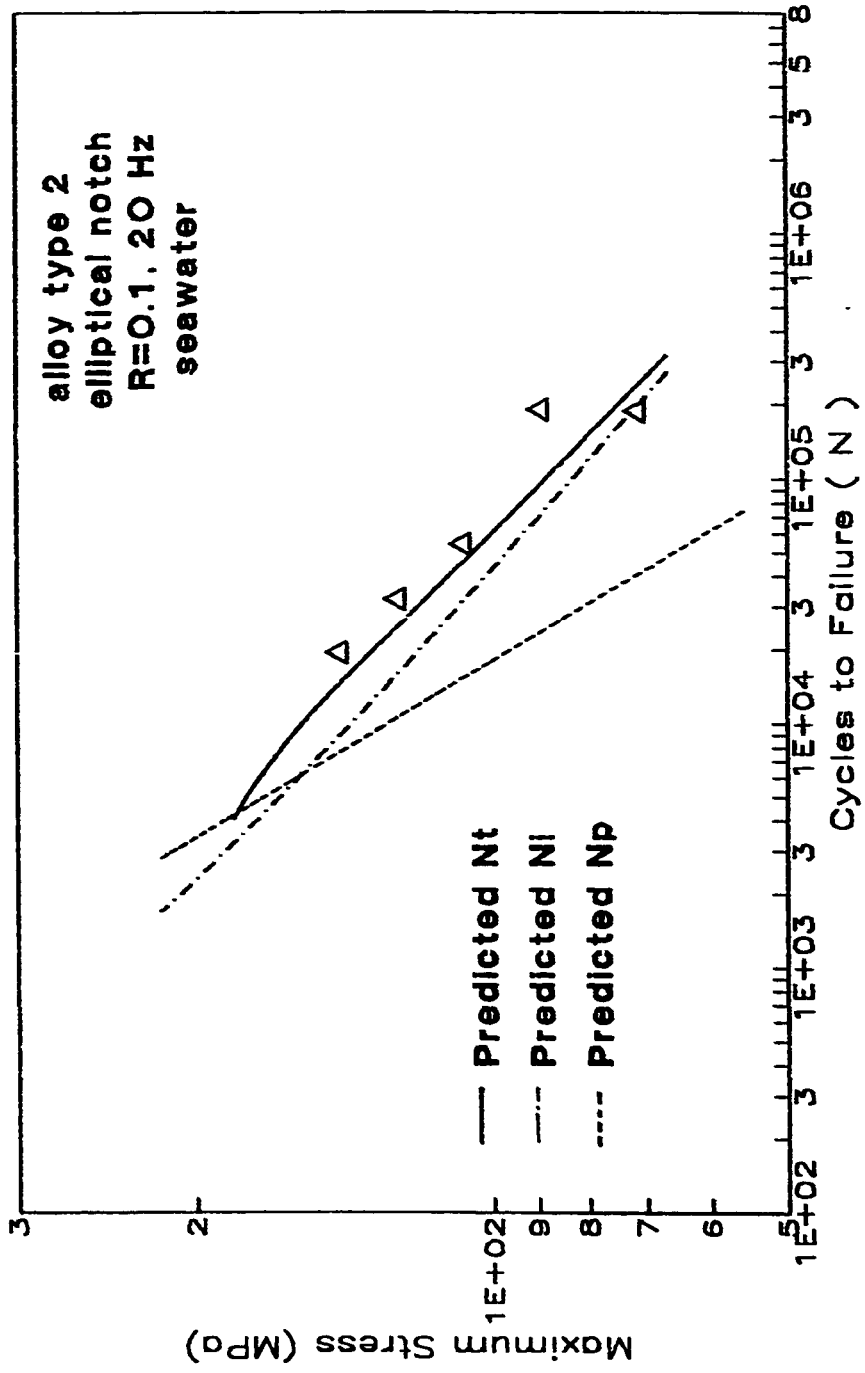

Fig. 6.20 Fatigue life estimates for alloy type 2, elliptical notch in seawater

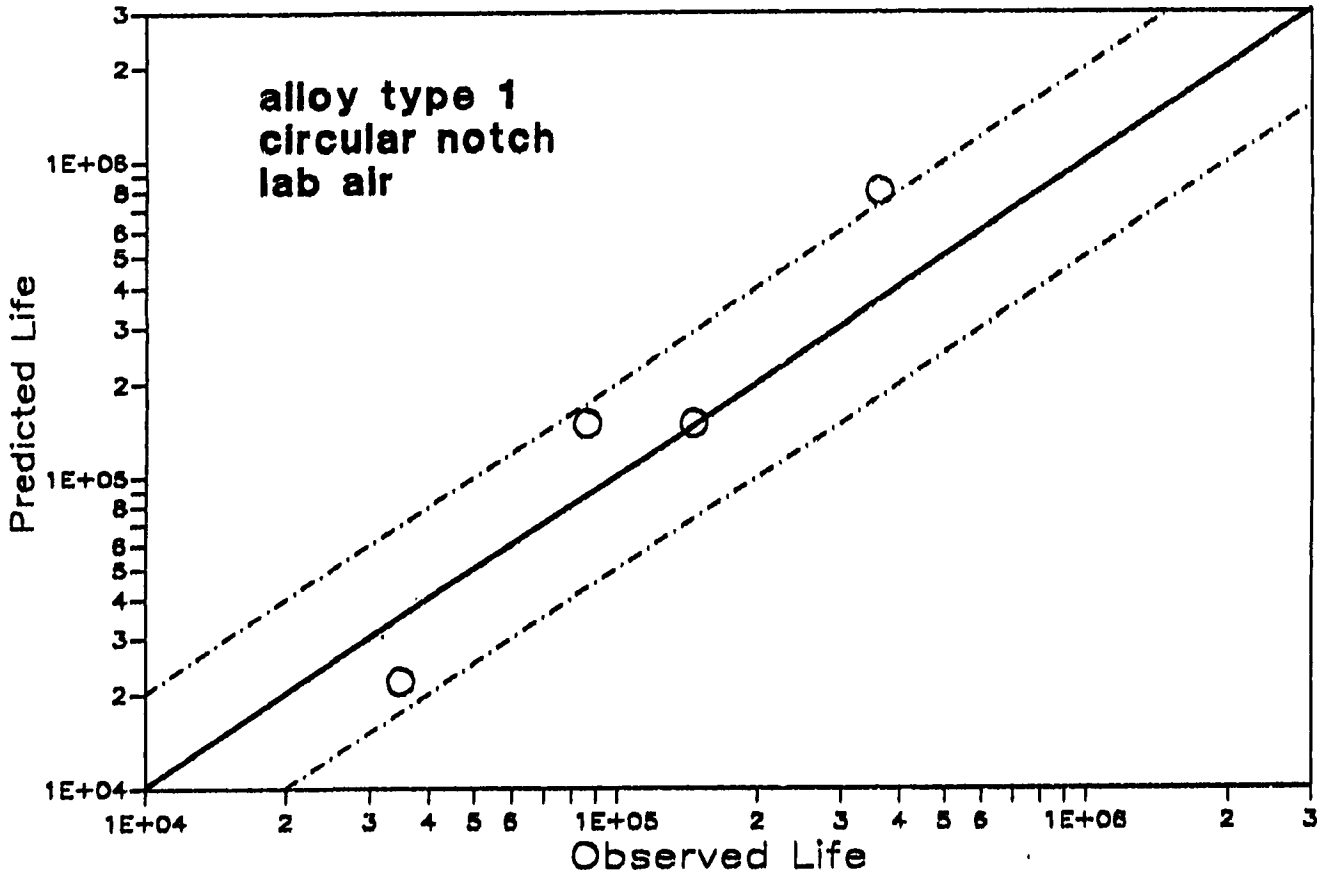

Fig. 6.21 Comparison between experimental and predicted fatigue life

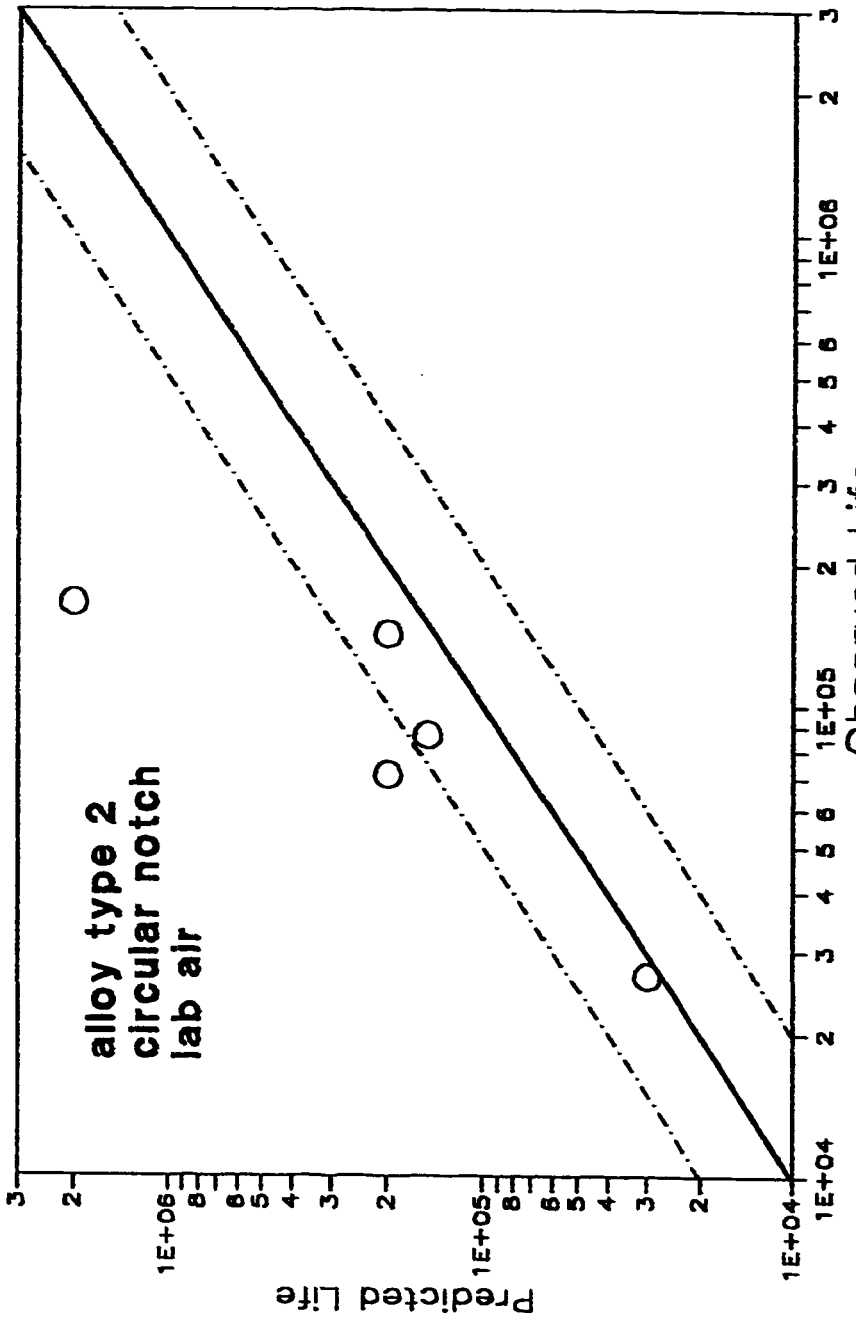

Fig. 6.22 Comparison between experimental and predicted fatigue life

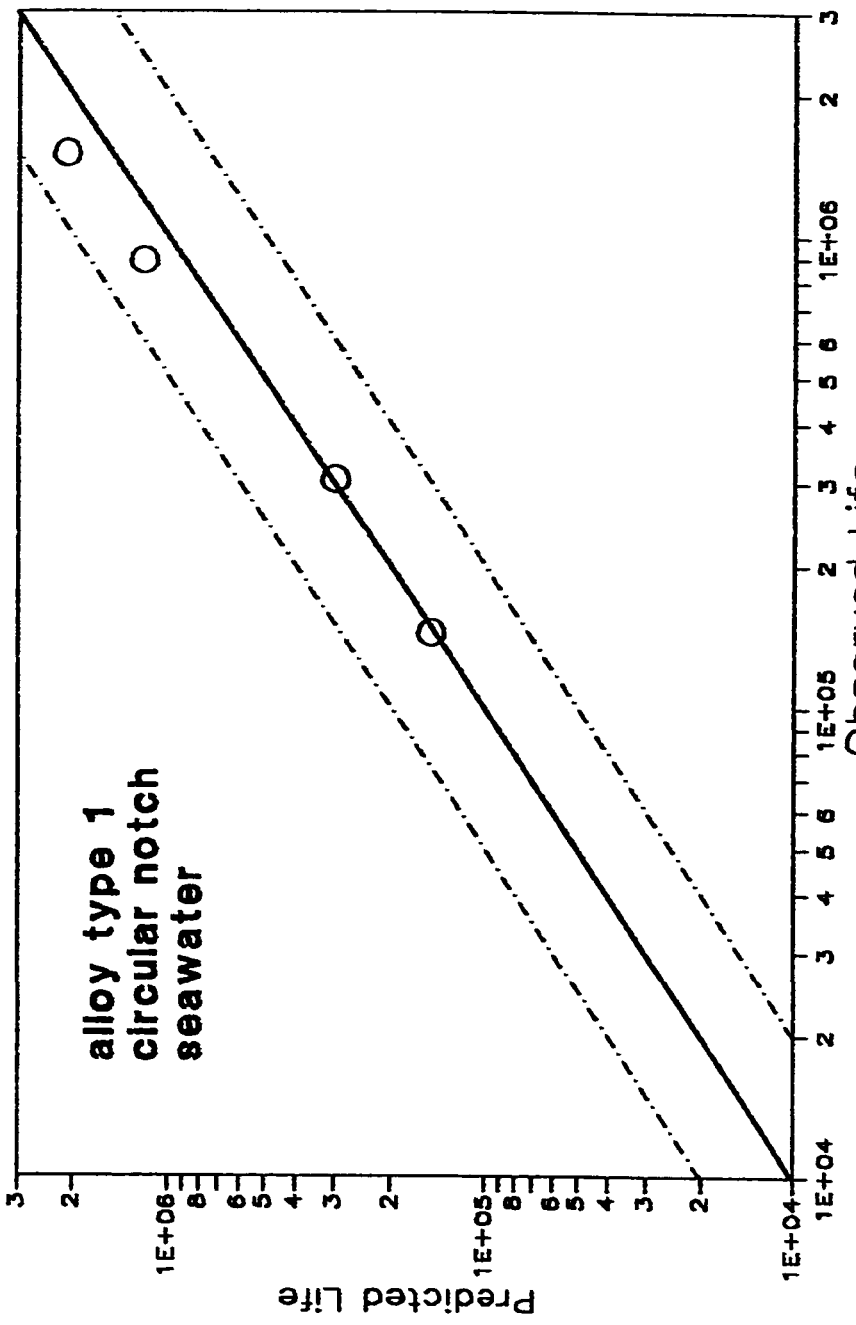

Fig. 6.23 Comparison between experimental and predicted fatigue life

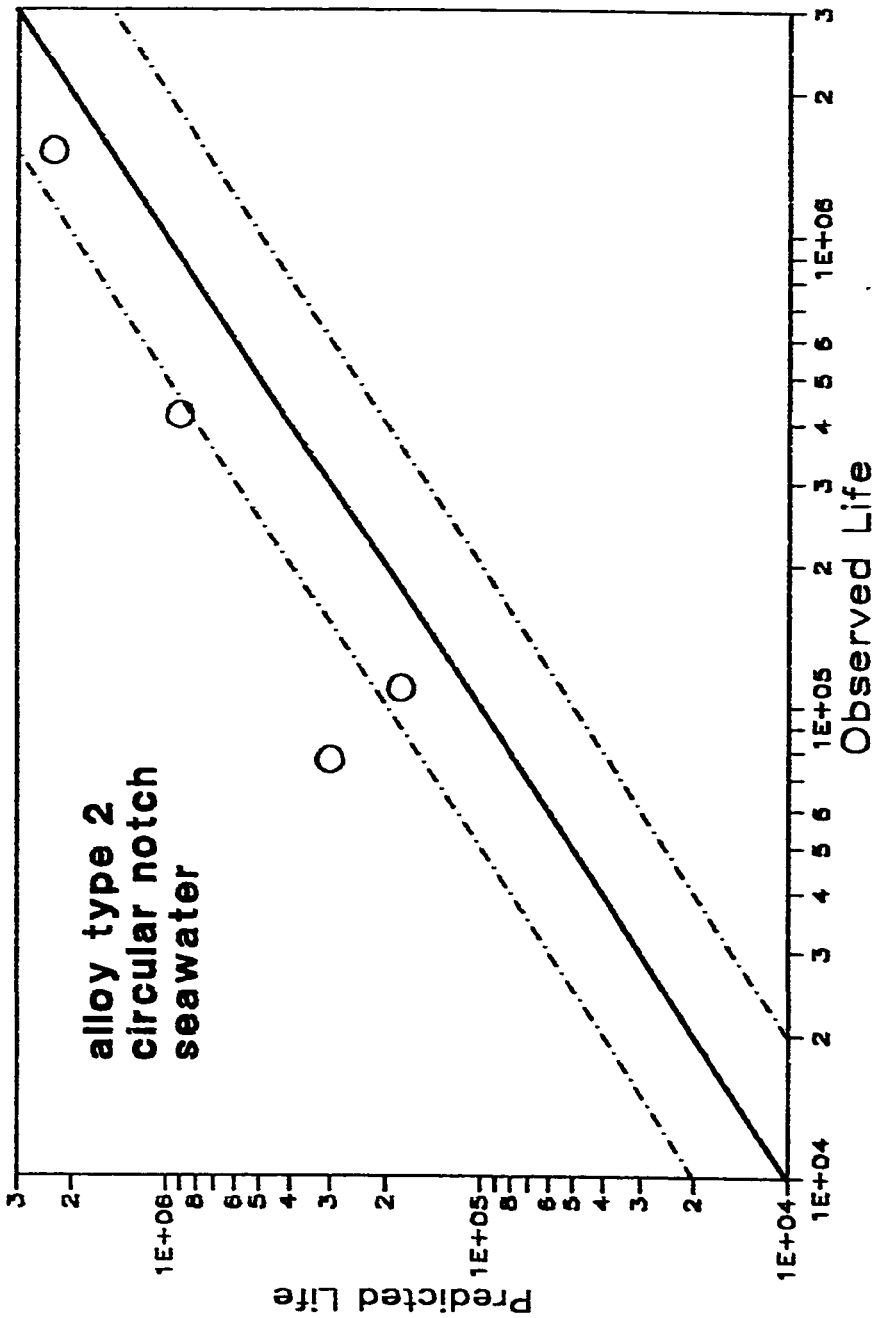

Fig. 6.24 Comparison between experimental and predicted fatigue life

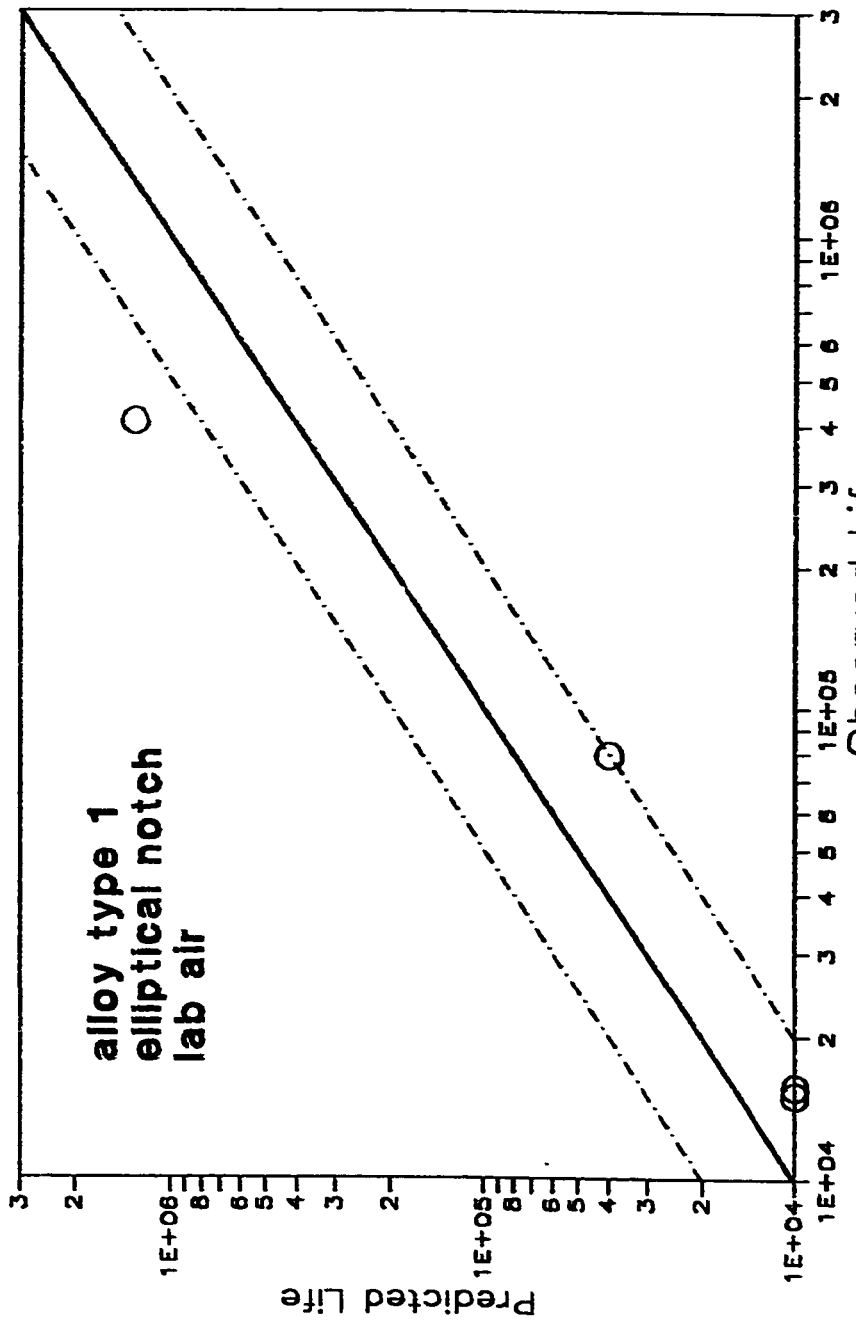

Fig. 6.25 Comparison between experimental and predicted fatigue life

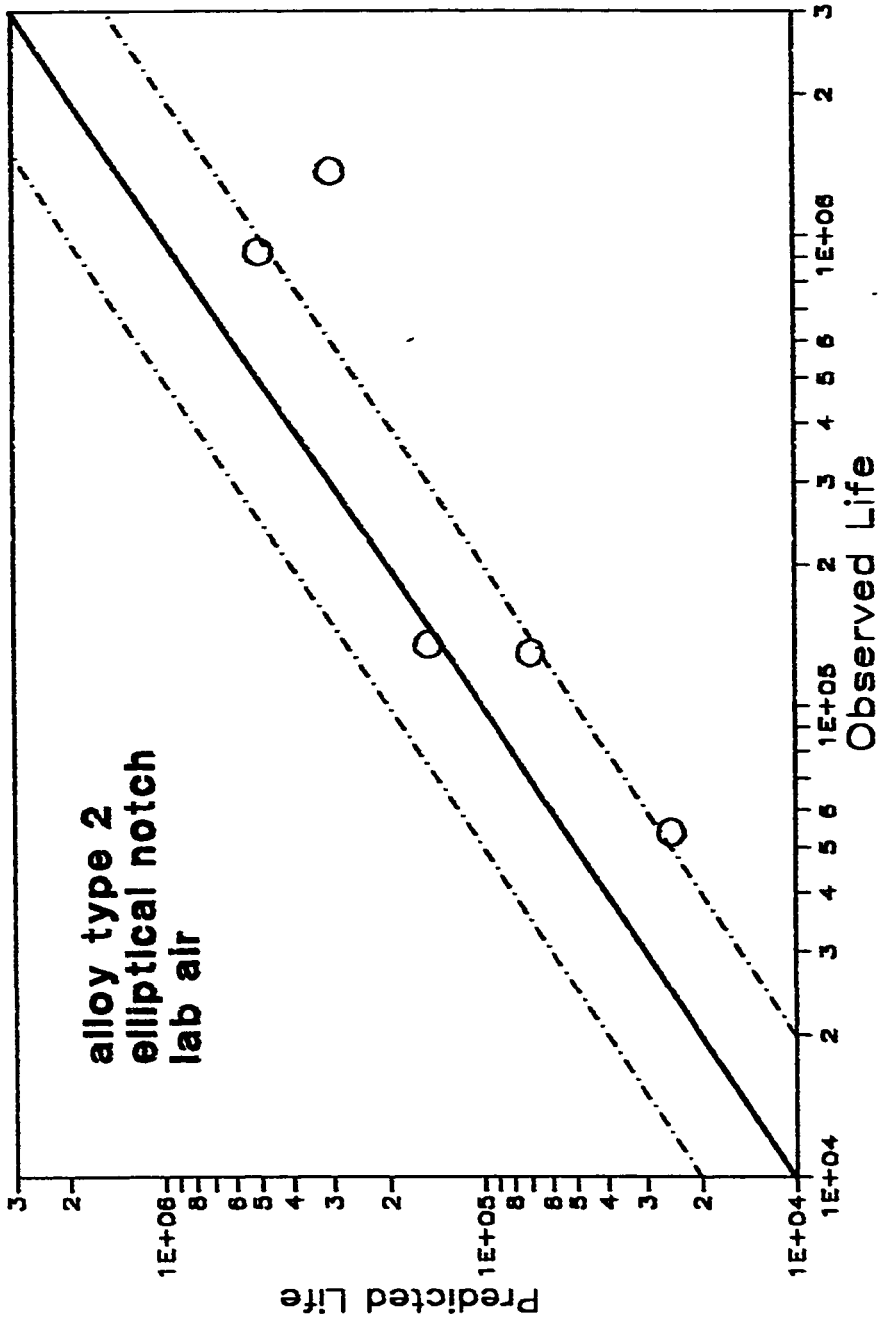

Fig. 6.26 Comparison between experimental and predicted fatigue life

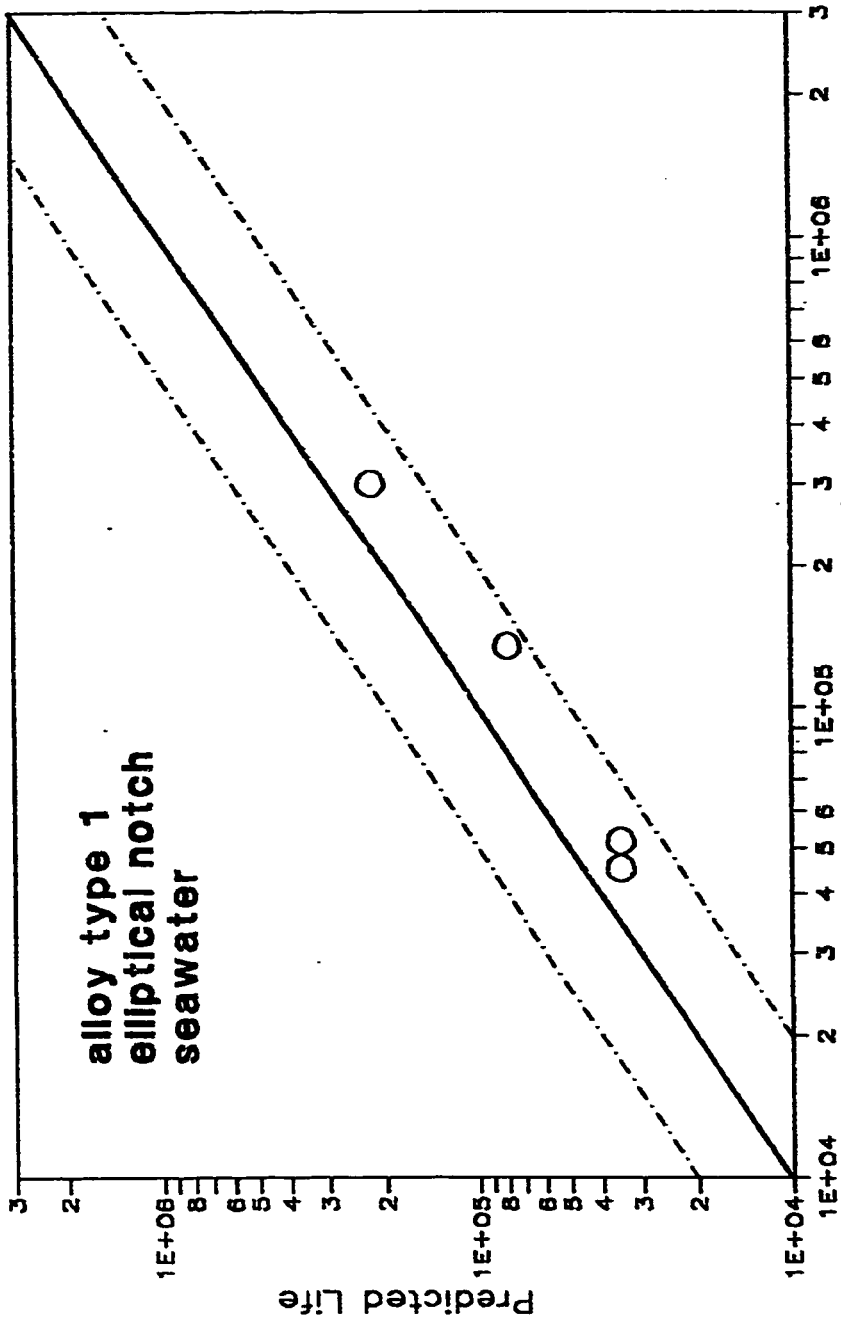

Fig. 6.27 Comparison between experimental and predicted fatigue life

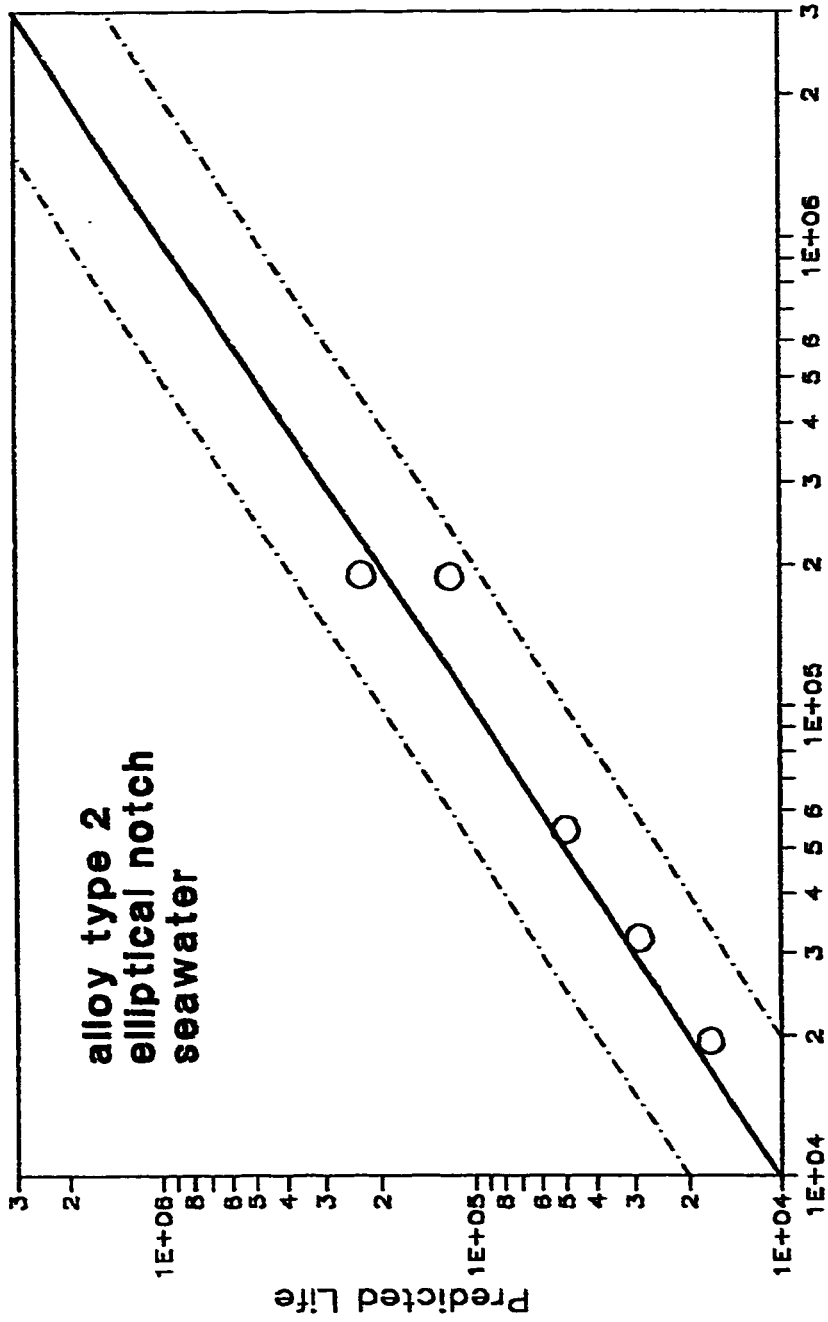

Fig. 6.28 Comparison between experimental and predicted fatigue life

APPENDICES

APPENDIX I

(Fatigue Initiation Life Program)

```
ü'
'
'
'
'********************   Fatigue Life Initiation Program  ***********
'
DIM z(30), s(30), de(30), nf(30), smax(30), nfe(30), smean(30)
CLS
fm$ = "    ###.#     ###.#      ###.#      ########          ########"
fm1$ = " ###.#       ###.#      ###.#     ###.#    ########     ########
fmt6$ = "S.R.(MPa)    M.N.S.     L.S.R.    L.M.S.     N              N"
'*************************************************************************
'                          Mechanical properties
'*************************************************************************
e = 70238: k = 653: n = .179: kt = 4.2: q = 1
fsc = 348: fse = -.044: fdc = .82: fde = -.628
kf = (kt - 1) * q + 1
'
'
s1 = 65
DEF FNf (g) = (g ^ 2) / e + 2 * g * (g / (2 * k)) ^ (1 / n) - (s1 * kf)
num = 30
FOR d = 1 TO num
er1 = .000001: er2 = .01
a = 10: b = 10000
s(d) = s1 + 5
s1 = s(d)
r = .1
smax(d) = s1 / (1 - r)
GOSUB mam
dad:
IF j = -1 THEN 3000
GOTO 3020
3000 PRINT "no solution"
GOTO 3040
3020 g = x
z(d) = g
de(d) = g / e + 2 * (g / (2 * k)) ^ (1 / n)
NEXT d
'**************************
' Solving for The Strain Life Equation
'**************************
DEF FNy (nf) = (fsc - smean1) / e * (2 * nf) ^ fse + fdc * (2 * nf) ^ fc
PRINT "please wait!!"
PRINT fmt6$
FOR p = 1 TO num
smean(p) = (1 + r) / ((1 - r) * 2) * s(p)
smean1 = smean(p)
del! = de(p)
er3 = 9.99999E-15: er4 = 1
aj = 10: bj = 1E+08
GOSUB sadi
fadi:
IF l = -1 THEN 3180
GOTO 3200
3180 PRINT "Cycles to Failure exeeds 1E10"
GOTO 3040
3200 nf(p) = INT(x1)
nfe(p) = .5 * (z(p) / (2 * (fsc - smean1))) ^ (1 / fse)
PRINT USING fm1$; s(p); smax(p); z(p); smean(p); nfe(p); nf(p)
NEXT p
INPUT " do you want to save the output, y/n"; ans$
```

```
IF ans$ = "y" THEN GOTO 200 ELSE GOTO 3040
200 INPUT "Enter name of file  the path as d:\qb45\fatig\"; asd$
asd$ = "d:\qb45\fatig\" + asd$ + ".F42"
OPEN asd$ FOR OUTPUT AS #7
    PRINT #7, "This is the output file "; asd$: PRINT #7, " "
    PRINT #7, "Fatigue strength coefficient= "; fsc; " b = "; fse
    PRINT #7, "Fatigue ductility coefficient= "; fdc; " c = "; fde
    PRINT #7, "K = "; k, " n = "; n, " E = "; e
    PRINT #7, "Kt = "; kt, " q = "; q, "kf = "; kf
    PRINT #7, STRING$(75, "="): PRINT #7, " "
    PRINT #7, fmt6$: PRINT #7, " "
    PRINT #7, STRING$(75, "="): PRINT #7, " "
FOR v = 1 TO num
      PRINT #7, USING fm1$; s(v); smax(v); z(v); smean(v); nfe(v); nf(
      PRINT #7, STRING$(75, "-")
    NEXT
CLOSE #7
3040 END
'**************************
' mam sub
'**************************
mam:
counter = 0
ai = a: bi = b
u = FNf(ai)
v = FNf(bi)
IF (u * v) > 0 THEN 4870
4770 x = .5 * (ai + bi)
counter = counter + 1
w = FNf(x)
IF ABS(w) <= er1 THEN 4860
IF (u * w) < 0 THEN 4830
ai = x: u = w
GOTO 4840
4830 bi = x: v = w
4840 IF ABS(bi - ai) > er2 THEN 4770
4850 j = 1
RETURN dad
4860 j = 0
RETURN dad
4870 j = -1
RETURN dad

sadi:
CONT = 0
a2 = aj: b2 = bj
u1 = FNy(a2)
v1 = FNy(b2)
IF (u1 * v1) > 0 THEN 5070
4970 x1 = .5 * (a2 + b2)
CONT = CONT + 1
w1 = FNy(x1)
IF ABS(w1) <= er3 THEN 5060
IF (u1 * w1) < 0 THEN 5030
a2 = x1: u1 = w1
GOTO 5040
5030 b2 = x1: v1 = w1
5040 IF ABS(b2 - a2) > er4 THEN 4970
5050 l = 1: RETURN fadi
5060 l = 0: RETURN fadi
```

APPENDIX II

(Fatigue Propagation Life Program)

```
'
'
'
'
'*************** Fatigue Crack Propagation Program *****************
'
fmt$ = "    ###.#                          ##.##^^^^        ####.##
fmb$ = " Maximum Stress(MPa)          Af(m)          K at fracture(MP
f$ = "d:\qb45\fcp\fcpxa1.out"
OPEN f$ FOR OUTPUT AS #1
PRINT #1, "This is the output file "; f$: PRINT #1, " "
PRINT #1, STRING$(75, "="): PRINT #1, " "
PRINT #1, fmb$: PRINT #1, " "
PRINT #1, STRING$(75, "="): PRINT #1, " "
pi = 3.1415
CLS : COLOR 0, 14
c = 7.527E-11: m = 3.144: w = .038: ai = .005:
COLOR 0, 14
CLS : PRINT "wait for answer please"
ft = 20
PRINT #1, "C="; c; "m="; m: PRINT #1, " "
PRINT #1, "Fracture Toughness ="; ft: PRINT #1, " "
ds = 65
FOR i = 1 TO 20
cyc = 0: n = 0!: dn = 0!
ds = ds + 5
ac = ai: da = .0001
DO
20  beta = SQR(1 / COS(pi * ac / w))
dk = beta * ds * SQR(pi * ac)
dadn = c * dk ^ m
dn = da / dadn
n = n + dn!: ac = ac + da
cyc = INT(n)
ms = ds / .9
LOOP WHILE dk < ft
PRINT USING fmt$; ms; ac; dk; cyc
PRINT #1, USING fmt$; ms; ac; dk; cyc
PRINT #1, STRING$(75, "-")
NEXT i
CLOSE #1
END
```

APPENDIX III

(Fatigue Crack Growth Data Reduction Program)

```
'
'
'
'
'*****************************************
'    Reduction of Ctack Growth data
'*****************************************
DIM a(50), n(50), aa(10), nn(10), bb(3), dadn(50), delk(50), areg(50),
fmt1$ = "Obs.   cyc      a(mes)     a(reg)    m.mc.    delk     da/dN
fmt2$ = " "
fmt3$ = "Obs.    cyc      a(mes)       a(reg)   Cor.Cof.   delk(N m^1/2)
fmt4$ = " ##    ######  ##.###^^^^   ##.###^^^^   #.###    ###.##^^^^
fmt5$ = " ##    ######  ##.###^^^^"
fmt6$ = "*##    ######  ##.###^^^^   ##.###^^^^   #.###    ###.##^^^^
CLS : COLOR 14, 0
'*****************************************
'    Specimen Dimensions and  Load ( change your values before runing)
'*****************************************
'--------------- Precracking crack length in mm ---------------------
        am = 6.5: B = 2: w = 38
'----------------- Maximum load and minimum load in N ---------------
        pmax = 7000:   pmin = 700
'----------------- yield strength of materials in MPa ---------------
        ys = 214
'------------------------------------------------------------------------
B = B / 1000: w = w / 1000:
r = pmin / pmax
pi = 3.1416
pp = pmax - pmin
'*************************************
'     Reading ( a Vs. N ) Data
'*************************************
INPUT "name of data file with its path"; datafile$
OPEN datafile$ FOR INPUT AS #3
INPUT #3, npts
        FOR i = 1 TO npts
            INPUT #3, a(i), n(i)
            a(i) = (a(i) + am) / 1000
        NEXT
CLOSE #3
PRINT STRING$(75, "-")
PRINT fmt1$
PRINT STRING$(75, "-")
FOR u = 1 TO 3
PRINT USING fmt5$; u; n(u); a(u)
NEXT
'************************
'   Regression Analysis
'************************
npts = npts - 6
k = 0
FOR i = 1 TO npts
l = 0
k = k + 1
k1 = k + 6
FOR j = k TO k1
l = l + 1
aa(l) = a(j)
nn(l) = n(j)
NEXT
c1 = .5 * (nn(1) + nn(7))
c2 = .5 * (nn(7) - nn(1))
```

```
sx = 0: sx2 = 0: sx3 = 0: sx4 = 0: sy = 0: syx = 0: syx2 = 0: qq = 0
FOR z = 1 TO 7
x = (nn(z) - c1) / c2

sx = 0: sx2 = 0: sx3 = 0: sx4 = 0: sy = 0: syx = 0: syx2 = 0: qq = 0
FOR z = 1 TO 7
x = (nn(z) - c1) / c2
yy = aa(z)
sx = sx + x
sx2 = sx2 + x ^ 2
sx3 = sx3 + x ^ 3
sx4 = sx4 + x ^ 4
sy = sy + yy
syx = syx + x * yy
syx2 = syx2 + yy * x ^ 2
NEXT
den = 7 * (sx2 * sx4 - sx3 ^ 2) - sx * (sx * sx4 - sx2 * sx3) + sx2 * (
t2 = sy * (sx2 * sx4 - sx3 ^ 2) - syx * (sx * sx4 - sx2 * sx3) + syx2 *
bb(1) = t2 / den
t3 = 7 * (syx * sx4 - syx2 * sx3) - sx * (sy * sx4 - syx2 * sx2) + sx2
bb(2) = t3 / den
t4 = 7 * (sx2 * syx2 - sx3 * syx) - sx * (sx * syx2 - sx3 * sy) + sx2 *
bb(3) = t4 / den
yb = sy / 7
rss = 0
tss = 0
FOR j = 1 TO 7
x = (nn(j) - c1) / c2
yhat = bb(1) + bb(2) * x + bb(3) * x ^ 2
rss = rss + (aa(j) - yhat) ^ 2
tss = tss + (aa(j) - yb) ^ 2
NEXT
r2 = 1 - rss / tss
corcof(i) = r2
dadn(i) = bb(2) / c2 + 2 * bb(3) * (nn(4) - c1) / c2 ^ 2
x = (nn(4) - c1) / c2
ar = bb(1) + bb(2) * x + bb(3) * x ^ 2
areg(i) = ar
'************************
'   delta K Calculation for Center Crack
'************************
snet = 0
qq = i + 3
t = pi * ar / w
sec = (1 / (COS(t)))
hft1 = SQR((t * sec / w))
snet = pmax / (B * (w - 2 * ar))
snet = snet / 1000000
s(i) = snet
delk(i) = (hft1 * pp) / B

'************************
' Printing to the Screen
'************************
IF snet < ys THEN
PRINT USING " ##     #######     ##.###^^^^  ##.###^^^^    .###    ##.##^^
ELSE
PRINT USING "*##     #######     ##.###^^^^  ##.###^^^^    .###    ##.##^^
END IF
NEXT
j = npts + 4
k = npts + 6
```

```
FOR i = j TO k
PRINT USING fmt5$; i; n(i); a(i)
NEXT
INPUT " do you want to save the output, y/n"; ans$
IF ans$ = "y" THEN GOTO 200 ELSE GOTO 300
CLS
200 INPUT "Enter name of file with the Path"; asd$
OPEN asd$ FOR OUTPUT AS #7
    PRINT #7, "This is the output file "; asd$: PRINT #7, " "
    PRINT #7, "for the data from  "; datafile$: PRINT #7, " "
    PRINT #7, STRING$(75, "="): PRINT #7, " "
    PRINT #7, fmt3$: PRINT #7, " "
    PRINT #7, STRING$(75, "="): PRINT #7, " "
  FOR v = 1 TO 3
  PRINT #7, USING fmt5$; v; n(v); a(v)
  PRINT #7, STRING$(75, "-")
  NEXT
    FOR m = 1 TO npts
    mm = m + 3
      IF s(m) < ys THEN
      PRINT #7, USING fmt4$; mm; n(mm); a(mm); areg(m); corcof(m); del
      PRINT #7, STRING$(75, "-")
      ELSE
      PRINT #7, USING fmt6$; mm; n(mm); a(mm); areg(m); corcof(m); del
      PRINT #7, STRING$(75, "-")
      END IF
    NEXT
        j = npts + 4: k = npts + 6
        FOR km = j TO k
        PRINT STRING$(75, "-")
        PRINT #7, USING fmt5$; km; n(km); a(km)
        PRINT #7, STRING$(75, "-")
        NEXT
CLOSE #7
300 END
```